FINAL REPORT: NAGW-256

A Jupiter Data Analysis Program (JDAP) Research Grant on Wave Accessibility and Attributes

Wynne Calvert

Department of Physics and Astronomy
The University of Iowa
Iowa City, Iowa 52242
(319)335-1920

Summary. Eleven papers were produced under this grant, on the source location and triggering of the jovian decametric radio emissions, and on the comparable behavior of the Earth's auroral kilometric radiation. Recent highlights include the theoretical result that such emissions can cause discrete auroral arcs, and the experimental result that the jovian S-burst emissions exhibit the longitudinal oscillation modes which would be expected of natural radio lasing.

INTRODUCTION

For more than thirty years the intense decametric radio emissons from Jupiter (DAM) and the corresponding auroral kilometric radiation from the Earth (AKR) have remained major radio science mysteries. Part of the problem, aside from their inherent complexity, has been the difficulty of measuring their source location and emission properties from limited observations. Under this grant progress has been made on this problem by locating the source directly, by an analysis of the faraday rotation observed with Voyager as the wave path crossed the Io plasma torus, and indirectly by comparing the peak frequencies of the decametric emission with that at the foot of the Io flux tube. Progress was also made on the general question of how the emissions originate by finding properties of both the AKR and the DAM which would imply emission by natural radio lasing.

Eleven papers were produced, and except for the two most recent ones which are still undergoing editorial review, they are included as appendices to this report. In the following sections, the content of these papers will be summarized.

SOURCE LOCATION

W. Calvert, The source location of certain jovian decametric radio emissions, J. Geophys. Res., 88, 6165-6170, 1983.

F. Genova and W. Calvert, The source location of jovian millisecond radio bursts with respect to Jupiter's magnetic field, J. Geophys. Res., in press, 1987.

M. G. Aubier, W. Calvert, and F. Genova, Source location of Jupiter's Io-dependent radio emissions, Proc. 2nd Int'l. Workshop on Planetary Radio Emissions (Graz, Austria, Sept. 1987), H. O. Rucker and S. J. Bauer, eds., submitted, 1987.

In these papers the source location of the jovian decametric radio emissions is measured by two different observational techniques. In the first paper, use is made of the faraday rotation which occurs in the Io plasma torus in order to determine the wave arrival directions during Voyager 1's flyby of Jupiter, with the result that the emissions must originate from near the cyclotron frequency on high-latitude field lines. In the other two papers, separately for the S-bursts and L-bursts which Jupiter produces, use is made of the almost certain emission at cyclotron frequency, as verified by the first paper, in order to restrict the range of GML longitudes at which emission should be possible, according to models of the jovian magnetic field. In these papers, along with others published by Genova and Aubier, it is shown that the emission region must be displaced by up to 70° behind the Io flux tube as it moves across the surface of Jupiter, and that this displacement is too large to be accounted for by either errors in the current magnetic models or the proposed Io-controlled emission theories.

TRIGGERED JOVIAN RADIO EMISSIONS

W. Calvert, Triggered jovian radio emissions, Geophys. Res. Lett., 12, 179-182, 1985.

W. Calvert, Affirmation of triggered jovian radio emissions and their attribution to corrotating radio lasers, Geophys. Res. Lett., 12, 625-626, 1985.

In these two papers, the discovery of triggered jovian hectometric radio emissions, which are presumably just low-frequency extensions of the decametric emissions usually detected at the Earth, was announced and debated with M. D. Desch and M. L. Kaiser. The significance of this remarkable phenomenon is that it immediately implies that the sources must be oscillating lasers, rather than just open-loop amplification acting alone.

CORRESPONDING AKR STUDIES

W. M. Farrell, W. Calvert, and D. A. Gurnett, AKR signal increases caused by triggering, Geophys. Res. Lett., 13, 370-372, 1986.

M. M. Baumback, D. A. Gurnett, W. Calvert, and S. D. Shawhan, Satellite interferometric measurements of auroral kilometric radiation, Geophys. Res. Lett., 13, 1105-1108, 1986.

M. M. Baumback and W. Calvert, The minimum bandwidths of auroral kilometric radiation, Geophys. Res., Lett., 14, 119-122, 1987.

In these three papers with graduate students at the University of Iowa, the comparable triggering of the AKR at the earth is verified statistically, and the spectral coherence and monochromaticity of the AKR emissions, which can only be accounted for by radio lasing, are conclusively demonstrated. These corresponding studies of the AKR at the earth are important to the studies of the jovian emissions because they verify that basically the same mechanism is involved, and that we can therefore apply much of what we learn at the earth to the jovian radio emission problem.

LASING AT JUPITER

W. Calvert, Y. Leblanc, and G. R. A. Ellis, Natural radio lasing at Jupiter, Astrophys. J., submitted, 1987.

W. Calvert, Planetary radio lasing, Proc. 2nd Int'l Workshop on Planetary Radio Emissions (Graz, Austria, Sept. 1987), H. O. Rucker and S. J. Bauer, eds., submitted, 1987.

In these two papers, a strong case is made for the generation of the jovian radio S-bursts by natural radio lasing, including the recent discovery of the expected longitudinal laser modes in the S-burst spectra, corresponding to different half-integral numbers of wavelengths between the effective laser mirrors. As with the corresponding discovery of these longitudinal laser modes in the spectra of the AKR, this conclusively confirms the laser concept and permits measuring the source size from the spectral spacings between the modes.

AURORAL PRECIPITATION

W. Calvert, Auroral precipitation caused by auroral kilometric radiation, J. Geophys. Res., 92, 8792-8794, 1987.

Although its application to Jupiter is not yet certain, in this paper it is pointed out that the AKR can account for the auroral electron precipitation at the earth, by the pitch-angle scattering of energetic electrons into the loss cone. Although difficult to accept in the light of current auroral theories, which all attribute the electron precipitation to localized acceleration, this new theory for the aurora accounts for the occurrence of auroral arcs and their widths, as well as possible other aspects of the auroral electron precipitation patterns. If it proves correct, this new concept should revolutionize auroral research.

CONCLUSIONS

The principal conclusion of this work is that radio lasing must be responsible for at least part of the planetary cyclotron radio emissions from both the earth and Jupiter. Moreover, at the earth it was concluded that this may have far-reaching consequences to the generation of the aurora, by the unavoidable electron pitch-angle scattering which such emission must cause. It was also concluded that there is a fundamental discrepancy of up to 70° in CML longitude between the apparent source location of the decametric emissions from Jupiter and the position of the Io flux tube, which is thus far irreconcilable with current Io-controlled emission theories.

JOURNAL OF GEOPHYSICAL RESEARCH, VOL. 88, NO. A8, PAGES 6165–6170, AUGUST 1, 1983

The Source Location of Certain Jovian Decametric Radio Emissions

W. CALVERT

Department of Physics and Astronomy, The University of Iowa, Iowa City, Iowa 52242

New evidence supporting the widely accepted concept that certain of the Jovian decametric radio waves originate as northern hemisphere extraordinary mode cyclotron emissions (possibly from the Io flux tube) has been found in the Voyager radio observations. Shortly after the closest approach to Jupiter, the wave signals received by Voyager 1 near 10 MHz exhibited cusps in the fringe pattern which is attributed to Faraday rotation in the Io plasma torus. The diminished Faraday rotation indicated by these cusps implies that the wave path had become perpendicular to the magnetic field in the torus. At nearly the same time, the wave polarization near 1 MHz (where Faraday rotation is absent) exhibited a sudden reversal of its rotation sense, indicating that the wave path for those frequencies had also become perpendicular to the magnetic field at the spacecraft. For these two events it was possible to project the wave paths back toward Jupiter and determine to some extent where the waves originated. It was found that the waves came from the northern hemisphere, at progressively lower altitudes with increasing frequency, and if the source is assumed to be associated with an $L = 6$ field line, the emission seems to have occurred near the source cyclotron frequency somewhere in the local midnight sector. This suggests that the source could be at the Io flux tube, since Io was then also near local midnight. Since the polarization rotation sense was apparently right handed with respect to the source magnetic field, the emitted wave mode must have been extraordinary. Furthermore, in order for the torus to produce a detectable Faraday rotation, the emitted wave polarization must have been substantially noncircular, and that would require a low plasma density near the source, much like that which occurs with auroral kilometric radiation at the earth.

INTRODUCTION

It is widely believed that many of the Jovian decametric radio waves originate as extraordinary mode cyclotron emissions from the northern hemisphere [see *Carr and Desch*, 1976], and the new evidence presented below will support that concept. Heretofore, the principal evidence for such a source model has been that the emissions tended to exhibit a right-handed wave polarization and that they often extended up to frequencies well above the peak cyclotron frequency in the southern hemisphere. Direct observations of the source location have been lacking, primarily because of the limited angular resolving power of radio observations from the earth and the omnidirectional antennas used on Voyager. However, special events have now been found in the Voyager 1 radio observations which accurately revealed the source direction. These events resulted from the behavior of the wave polarization, and the Faraday rotation of that polarization, for wave directions nearly perpendicular to the magnetic field. For such events it was possible to project the wave paths back toward Jupiter and learn about their origin.

Since the events depend upon Faraday rotation in the Io plasma torus, that will be discussed first, followed by a description of the Voyager 1 observations. The nature of the direction sensitive events will then be described and the wave path projections carried out. Finally, the implications of these projections will be discussed and the conclusions summarized.

FARADAY ROTATION

Faraday rotation occurs when the polarization of a wave differs from the characteristic polarizations for propagation in a plasma. These characteristic polarizations, which are usually called ordinary and extraordinary, both become almost circular with opposite rotation senses whenever the frequency is high, the plasma density is low, and the magnetic field is weak (see below). Under such circumstances, the right-handed extraordinary wave travels faster than the left-handed ordinary wave, and thus the composite wave undergoes a right-handed rotation of its polarization ellipse axis by an angle equal to half the phase difference which develops as the waves propagate. In this context, the right and left rotation senses are determined with respect to the magnetic field component in the propagation direction (the so-called plasma wave convention), rather than with respect to the propagation direction itself (the astronomical convention). In the discussions below, care will be taken to distinguish these two conventions for specifying the polarization rotation sense.

Io torus. The torus of enhanced plasma density encircling Jupiter and presumably caused by its moon Io [*Brown*, 1976; *Broadfoot et al.*, 1979; *Warwick et al.*, 1979*a*; *Birmingham et al.*, 1981; *Bagenal et al.*, 1980; *Bagenal and Sullivan*, 1981; *Levy et al.*, 1981] is a suitable medium for Faraday rotation at decametric wave frequencies. This Io plasma torus is presumably symmetrical about the centrifugal equator, approximately 6 R_J (Jovian radii) from the planetary center, and it exhibits plasma densities as high as 2000 cm^{-3}. The cyclotron frequency f_H is roughly 46 kHz inside the torus, and the plasma frequencies f_N are typically 400 kHz or less.

Polarization. According to *Budden's* [1961] equation 5.12, the characteristic polarizations in a magnetoplasma can be described by the imaginary quantity ρ, which is the complex ratio of the electric field components in the wave front and is given by

$$\rho = j[\beta/2 \pm (1 + \beta^2/4)^{1/2}] \quad (1)$$

where j is the square root of minus one. For a wave frequency f much higher than the plasma frequency f_N,

$$\beta = f_H \sin^2 \theta / f \cos \theta \quad (2)$$

where f_H is the cyclotron frequency and θ is the angle between the wave normal direction and the magnetic field. For acute

Paper number 3A0654.
0148-0227/83/003A-0654$05.00

wave angles ($\theta < 90°$) the positive sign in (1) pertains to the extraordinary wave mode, and the negative sign refers to the ordinary. For $\beta = 0$, which occurs either for parallel propagation or for very low cyclotron frequencies, the values of ρ are $+j$ and $-j$, indicating right and left circular polarizations, respectively (plasma convention). In the latter case the region of nearly circular polarization can extend to quite large propagation angles, leaving only a thin wedge orthogonal to the magnetic field where the polarization is substantially noncircular. For example, in the Io torus at 10 MHz, both polarizations are circular to within 10% ($0.9 < |\rho| < 1.1$) for all wave directions except those within 1.3° of the magnetic perpendicular ($88.7° < \theta < 91.3°$).

Phase shift. The differential phase shift which determines the Faraday rotation angle (in radians) is given by

$$\Delta\phi = 2\pi f(n_0 - n_x)\Delta z/c \tag{3}$$

where n_0 and n_x are the wave refractive indices, c is the speed of light, and Δz is the path distance over which the rotation occurs. For the refractive index,

$$n = 1 - {f_N}^2/2f(f + j\rho f_H \cos\theta) \tag{4}$$

which is an approximation of *Budden*'s [1961] equation 5.35 that is valid as long as f_N is sufficiently small,

$$n_0 - n_x = \frac{{f_N}^2 f_H}{f({f^2} - {f_H}^2)}\left\{\cos^2\theta + \frac{{f_H}^2 \sin^4\theta}{4f^2}\right\}^{1/2} \tag{5}$$

Except for the narrow range of noncircular polarization, where $\cos\theta/\sin^2\theta$ becomes less than $f_H/2f$, the phase shift is thus approximately proportional to the cosine of the wave angle.

Rotation angle. Outside the noncircular range, and for f_H much less than f, the Faraday rotation angle (half of the phase shift $\Delta\phi$) is then approximately

$$\psi = \frac{159°}{f^2}\int N\,dz\,[f_H/0.046]\cos\theta \tag{6}$$

where the frequencies are now measured in megahertz, the plasma density N is measured in cm^{-3}, and the distance dz is measured in Jovian radii ($R_J = 71{,}398$ km). The factor $f_H/0.046$ in the integrand allows for a magnetic field variation from its average value within the torus, which can affect precise density comparisons. The angle ψ in (6) is the angle by which the axis of the wave's polarization ellipse will rotate as that wave traverses the torus. Since the radially integrated densities of the torus are typically 2000 R_J/cm^3 within 0.5 R_J of the centrifugal equator (deduced from *Bagenal and Sullivan*'s [1981] Figure 12), this rotation could be as large as 10 revolutions at 10 MHz, decreased appropriately by the cosine factor.

Limit polarization. For Faraday rotation to occur (or at least for it to produce an observable effect in this case), the initial wave polarization must differ from the characteristic plasma polarizations. This would imply that the Jovian emissions must have attained a noncircular limit polarization somewhere near the source, where β was still relatively large. This limit polarization, previously discussed in regard to the Jovian emissions by *Goertz* [1974], is established at the point where the rate of phase change (e.g., the $\Delta\phi/\Delta z$ from (3)) becomes negligible on the scale at which the polarization itself is changing [see *Budden*, 1961, chapter 19]. For the extraordinary wave mode, which is presumably generated near where $f = f_H$, a noncircular limit polarization would require a low source plasma density (represented by the ${f_N}^2$ in (5)) and a large emission angle (represented by the θ in (2)). For instance, in the case presented below, the deduced emission angle was 68°, and that would be consistent with a limit polarization of $\rho = 2.7j$, provided the source plasma density were sufficiently small. Although the actual axis radio of the polarization ellipse (which equals the magnitude of ρ) might be somewhat less than 2.7, such axis ratios should be sufficient to produce observable fringes in the planetary radio astronomy data.

OBSERVATIONS

The pertinent decametric radio observations were obtained with Voyager 1 shortly after its closest approach to Jupiter, using the planetary radio astronomy (PRA) instrument [*Warwick et al.*, 1977, 1979*a*]. The spacecraft had just completed its excursion through the dusk sector, during which it had traversed its southernmost latitudes of the encounter and whipped by Io. It was then returning northward across the equator near local Jovian midnight. Under such conditions, the wave paths from the Jovian northern hemisphere had to pass more or less directly through the Io torus to reach Voyager 1. Voyager 1, in fact, was still within the outer portion of the torus, at a distance of around 8 R_J, during the pertinent observations. The Jovian north magnetic pole was near superior conjunction at the time, inclined away from Voyager 1, whereas the moon Io was near inferior conjunction, almost directly between Voyager and Jupiter.

PRA data. The PRA instrument is essentially a dual-channel, swept frequency radio receiver which covers the spectrum from 20 kHz to 40 MHz in two bands, separated at roughly 1.3 MHz. The data in these two bands, recorded between 1500 and 2400 spacecraft event time (SCET) on March 5, 1979, are shown in Figures 1 and 2, as black and white shadings. In each case the frequency increases downward and the time increases toward the right. The two PRA channels respond to the quadrature sum and difference signals from a pair of orthogonal monopoles extending backward away from the rear of the Voyager telemetry dish. At low frequencies these two monopoles each act somewhat like Hertzian dipoles, and the two channels, designated R and L, would then respond to right and left circularly polarized waves arriving normal to the antenna plane (astronomical convention). At other angles, and also at the higher frequencies, the effective polarizations for these two channels can be quite different from circular. Furthermore, when the waves arrive from the opposite side of the antenna plane, as was the case during much of the observing period, the role of the R and L channels will be reversed.

Figure 1*a* shows the R channel signals as darker shadings. Figure 1*b* shows the difference between the L and R channels, where white indicates that the R channel signal was strongest, and black indicates the reverse. Grey indicates that there was insufficient signal strength for this determination. Figure 2 shows the difference signals for the same period at the lower frequencies, similarly coded. For the most part, a white signal in Figure 2 or at the top of Figure 1*b* indicates that the received signal was predominantly left-hand polarized (astronomical convention), and black indicates the reverse.

Fringes. The wave signals in Figure 1 exhibit a sometimes bewildering variety of patterns, including the curved, more or less vertical arcs in Figure 1*a* at 2100 SCET, which have attracted so much interest but which will be ignored in the current analysis. Superimposed on the arc pattern is a roughly horizon-

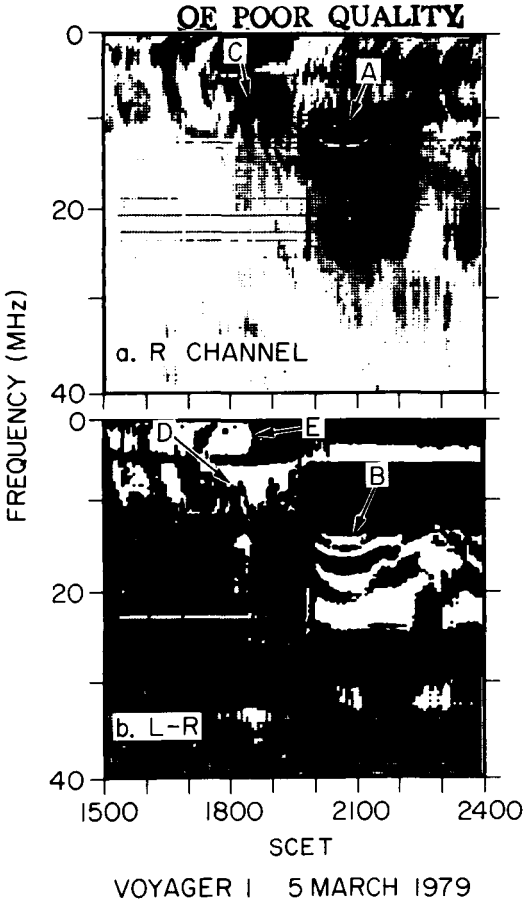

Fig. 1. Jovian decametic radio emissions observed with Voyager 1, showing (A and B) the fringe patterns produced by Faraday rotation in the Io plasma torus, (C and D) the cusps in those patterns indicating when the wave path was perpendicular to the magnetic field in the torus, and (E) a polarization sense reversal which occurred when the wave path was perpendicular to the magnetic field at the spacecraft. Figure 1*b* shows the difference between the two PRA channels, whereas Figure 1*a* shows the R channel signals alone. These cusp and reversal features permit projecting the wave directions back toward Jupiter, as was done in Figure 3, to learn about the source location.

tal fringe pattern, designated A and consisting of regularly spaced nulls in the R channel signals extending from 10 to 13 MHz. This fringe pattern is attributed to Faraday rotation in the Io plasma torus. The similar fringe pattern, at B in Figure 1*b*, is attributed to the same torus Faraday rotation, and that pattern persisted for much of the following day, undulating up and down at twice the planetary rotation rate. These undulations, of course, reflect the varying density and angle encountered by the wave as it traversed the torus with different magnetic latitudes.

The R channel nulls in Figure 1 were found to be spaced inversely proportional to the square of the frequency, as would be required by (6). Moreover, for the source location determined below, the integrated torus electron density deduced from the fringe spacings was found to decrease from 4300 R_J/cm^3 at 1900 SCET to 470 R_J/cm^3 at 2215 SCET, to an estimated accuracy of about 30%. This decrease represents the expected decrease of the torus density with centrifugal latitude, since the wave path intercept with the torus (always assumed to occur at $L = 6$) moved northward from the centrifugal equator by about 1.5 R_J during that interval. The observed decrease was monotonic, despite the prominent maximum in the amount of Faraday rotation in Figure 1 at 2100 SCET, which was apparently caused by the competing density and cosine factors in (6), rather than by an actual density peak. The integrated densities were also compared with the existing torus models [*Birmingham et al.*, 1981, Figure 3; *Bagenal and Sullivan*, 1981, Figure 12; *Tokar et al.*, 1982, Figure 3] and found to agree with them just about as well as they agree with one another. That is, all the measurements agreed with all the models to better than a factor of 1.6, within 0.8 R_J of the centrifugal equator, increasing to a factor of 3 at 1.5 R_J. The fringes thus seem to fit reasonably well the frequency, density, and wave angle dependencies of (6), and they indicate a monotonic latitudinal torus density decrease of about an order of magnitude, between the centrifugal equator and 1.5 R_J above the centrifugal equator. This is excellent evidence that the fringes were caused by Faraday rotation in the torus.

Previous interpretation. Despite their apparent agreement with (6), fringe patterns like those in Figure 1 have been interpreted differently by the PRA team [*Warwick et al.*, 1979*b*]. Since Faraday rotation in the Io torus would only rotate the wave's electric polarization ellipse and leave its rotation sense unchanged, they reasoned that such an effect could not produce the apparent polarization sense reversals observed by their instrument. Furthermore, presumably assuming that the PRA antennas behaved like quadrature-phased short crossed dipoles, they reasoned that a torus Faraday rotation should have always produced identical fringes in the two PRA channels, rather than the interlaced R and L fringes which they had found.

The overlooked factor seems to be the radiation phase shifts of the unbalanced monopole antennas actually used on Voyager, whose electrical centers are not colocated. Such phase shifts, which depend on both the frequency and the Voyager orientation, can sometimes be a sizable fraction of the wave cycle, and that would certainly be sufficient to change the antenna polarization, by effectively altering the carefully adjusted quadrature phasing of the receiver. For example, when the two antennas are excited at their halfwave resonances (which occur together at around 15 MHz), their electrical centers would lie near their respective midpoints, which are spaced $\sqrt{2}/4$ wavelengths apart. Along a line through these midpoints, then, there would be an additional phase shift for the more distant antenna of 127°; and for a direction out of the antenna plane at an angle of 45° to that line, the phase shift would be 90°. For such a view direction, the two PRA channels would respond to crossed linear polarizations, since the spatial phase shift would exactly cancel that of the receiver. Provided the incoming wave polarization were sufficiently noncircular, the torus Faraday rotation would then be able to produce both interlaced fringes and apparent polarization sense reversals in the PRA data. A detailed study of the event analyzed by *Warwick et al.* [1979*b*], using the actual Voyager orientation, has confirmed this concept and shown that the emitted polarization ellipse (for the Io B source at 12–16 MHz) sometimes exhibits an axis ratio exceeding 3 : 1 [*Calvert*, 1982*b*].

Analysis

The features in Figures 1 and 2 which indicate the source directions are designated C through F. They consist of cusps in the Faraday fringe pattern (C and D) and reversals of the apparent polarization sense (E and F), as will now be described.

Cusps. The Faraday fringes at A in Figure 1 appear to converge toward the left, and this is attributed to a decreasing value for the cosine factor in (6), although the varying integrated torus density encountered by the wave may have also played a role. The converging pattern appears to form a cusp at

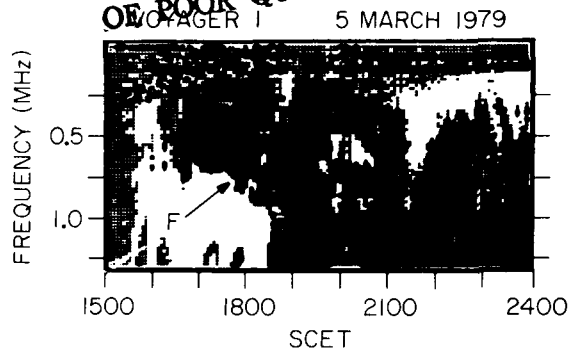

Fig. 2. PRA difference signals for the same period as Figure 1 showing (F) the polarization sense reversal at lower frequencies. For most of this record, and for the low-frequency (top) portion of Figure 1*b*, the white shading indicates a left-handed rotation sense with respect to the propagation direction (astronomical convention). Since the wave angle changed from obtuse to acute during the reversal, the wave polarization was right handed with respect to the magnetic field component (plasma convention) and hence that of the extraordinary wave mode.

C, centered at 1820 SCET and 13 MHz, indicating that the cosine factor had then become quite small and hence that the wave path was perpendicular to the magnetic field in the torus. A hint of the same cusp also appears at D in Figure 1*b* at 1805 SCET and 9 MHz, although it consists only of a pair of brief white signals flanking a black area. That cusp, at a somewhat earlier time and lower frequency, would suggest a source at a slightly greater altitude, as will also be shown below. This, however, could have been fortuitous, since it is not known why the cusps appeared differently on the two records.

Such cusps, competing with a great variety of other patterns, were initially hard to spot in the Voyager data, and these are the only two which have yet been found. This apparent uniqueness of the feature is attributed to the unique geometry which occurred only near closest approach, during which the spacecraft was sufficiently close to the planet and south of the magnetic equator for a wave path from the northern hemisphere to become perpendicular to the torus magnetic field.

Reversals. Once the significance of the fringe cusps was recognized, a second feature was found which also indicated when the wave path was perpendicular to the magnetic field. This feature, designated E in Figure 1 and F in Figure 2, was a reversal of the polarization rotation sense (in the astronomical convention) from left handed (white) to right handed (black). In Figure 1 this reversal occurred at progressively increasing frequencies, from 0.75 MHz at 1750 SCET to 1.0 MHz at 1830 SCET. These times overlap those for the fringe cusps, and this is attributed to a different source direction at the lower frequencies and the slightly different magnetic field directions in the torus and at the spacecraft.

The explanation for these polarization reversals is as follows: At these lower frequencies the limit polarization for the escaping waves is apparently almost circular, since they exhibit no Faraday rotation. When these waves encounter the torus, they excite only one of the two characteristic polarizations, and the waves then travel the remainder of the distance to Voyager 1 as a pure characteristic mode. Consequently, when such waves traverse the magnetic perpendicular, their polarization sense (in the astronomical convention) should reverse, since the component of the magnetic field in the wave direction changes sign. During this reversal the E plane [see *Allis et al.*, 1963, chapter 4] flips over and the polarization ellipse in the wave front abruptly collapses and reforms itself with the opposite rotation sense. In other words, the polarization sense reversals at E and F in the figures are attributed to those of a characteristic wave mode as it traversed the magnetic perpendicular near the spacecraft.

Other apparent polarization reversals, like that at the right in Figure 2, occur in the Voyager PRA data. Clearly, there is no guarantee that all such reversals should fit the same interpretation, since much the same behavior could also have resulted from the superposition of two oppositely polarized signals of varying strength. Besides their unique position near the cusps, the reversals at E and F appear to be different from most of the others which occur in the same frequency interval, in that they cut across otherwise continuous features of the data, and from the separate signal records (not shown), it appears that the R channel signals weakened across the boundary as the L channel signals strengthened.

Wave path projections. The projections for the polarization sense reversals were quite straightforward, being prependicular to the magnetic field at the known position of the Voyager 1. For the Faraday cusps the projection was carried out by assuming various effective source heights along the north magnetic polar axis and calculating the resulting wave angle with respect to the magnetic field at 6 R_J inside the torus. This angle being 90° at the measured times when the cusps occurred then gave the effective polar heights to which the projections were drawn. This procedure also gave an idea of the sensitivity of this technique to timing errors, indicating that a half-hour uncertainty in the cusp time would result in a 0.3 R_J uncertainty in the source altitude.

A simple dipolar magnetic field model was used for the projections, since that should be adequate at the distances of Voyager 1 and the torus. The magnetic field direction was then determined from its dip angle I with respect to the local horizontal, given by

$$\tan I = 2 \tan \lambda_m \tag{7}$$

where λ_m is the magnetic latitude. The pertinent wave paths, which are assumed to lie nearly in the magnetic meridian through Voyager 1 (e.g., within the 7° angle subtended by Jupiter's radius), are shown in Figure 3. This figure is essentially a side view of the propagation situation from somewhere near dusk, since Voyager 1 and Io were both near Jovian midnight. In Figure 3 the magnetic equator is shown horizontal, marked with the distance in Jovian radii, and the dipole offset was ignored. The approximate position of the Io plasma torus is shown by a dashed circle, one third of the way between the magnetic and rotational equators. The dipole magnetic field line in Figure 3, at $L = 6$, could be either that of the torus or the flux tube through Io itself, and its possible distortion near the planet was also ignored. Although it might be inadequate at the lower frequencies [see *Lecacheux*, 1981, Figures 5*b* and 5c], wave refraction by the torus was neglected and the ray paths were assumed to be straight.

Source locations. The projections clearly indicate that the emissions originated in the northern hemisphere. Furthermore, the altitude progression with decreasing frequency suggests a cyclotron source along a given field line, probably that near $L = 6$ associated either with the torus or with the moon Io, itself. In support of this concept, the cyclotron frequency deduced for a radial distance of 2 R_J from the magnetic model of *Acuña and Ness* [1976, Figure 3] was included in Figure 3, along with its extrapolation upward, inversely with the cube of the distance. The projections at 0.75 and 1 MHz would certainly be consistent with a source at the cyclotron fundamental.

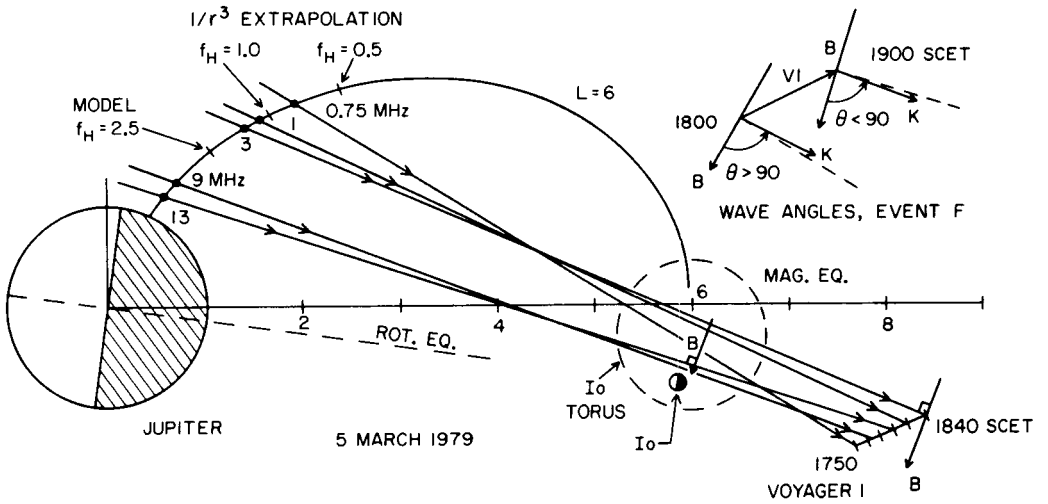

Fig. 3. The Jovian decametric wave paths deduced from the Faraday cusps and polarization reversals in Figures 1 and 2, with respect to Jupiter, its moon Io, the $L = 6$ dipole field line through Io, and the position of Voyager 1 during the observation. The Io plasma torus is shown schematically as a dashed circle situated between the magnetic and rotational equators, and the source cyclotron frequency [after *Acuña and Ness*, 1976] is shown by tick marks on the field line. The inset shows how the wave angle at Voyager 1 (for a frequency of 1 MHz) changed from obtuse to acute during the observing period. The pertinent waves seem to have originated as extraordinary cyclotron emissions from the northern hemisphere, possibly near the Io flux tube.

However, considering the projection accuracy and the possible torus refraction at these lower frequencies, this result cannot be considered conclusive, especially since the 3-MHz projection, for the reversal event E in Figure 1, might equally well have been associated with a second-harmonic emission.

If the source does occur along an $L = 6$ field line, it must have been somewhere in the midnight quadrant facing Voyager 1, since the projections at the lower frequencies would otherwise have missed that field line entirely. For instance, if the active field line were near dusk or dawn, then the 0.75-MHz source would have appeared to lie almost 1 R_J above the maximum distance of that field line from the magnetic equator. By a similar argument, it is unlikely that the emissions could have originated in the sunlit hemisphere. Again, this result is not considered conclusive, since there is no guarantee that the $L = 6$ field line was responsible for the emissions, and the projections would also be consistent with cyclotron emissions from higher latitudes or even from directly over the pole. However, it would clearly be consistent with a source near the Io flux tube, as some of the emission theories would require, since Io was then also in the midnight quadrant (having just before been visited by Voyager 1).

Wave mode. At the lower frequencies, where the polarization sensing capabilities of the PRA antenna system are most reliable, the observed rotation sense of the wave electric vector was left handed before the reversal (astronomical convention) and right handed afterward. Since the wave angle at the spacecraft was obtuse before the change, and acute afterward, as is shown by the inset in Figure 3, the polarization sense must have been right handed with respect to the magnetic field component in both instances (plasma convention). This implies that the observed wave mode was extraordinary. Since the wave angles to the magnetic field, both at the source and at the torus entry point (see Figure 3), were similarly acute, this implies that the emitted wave mode was also extraordinary.

DISCUSSION

Two seemingly insignificant features of the wave observations, the fringe cusps and the polarization reversals, have thus produced a rather complete picture of where those particular waves originated. As shown in Figure 3, they apparently came from the northern hemisphere, at progressively lower altitudes with increasing frequency and at roughly those altitudes which would be expected for a source at the cyclotron frequency. Furthermore, the nature of the polarization sense reversals suggests that the emitted wave was extraordinary.

Source density. Moreover, the occurrence of a noncircular limit polarization at 10 MHz would suggest a low source plasma density, quite analogous to that in the auroral plasma cavity found to occur with auroral kilometric radiation (AKR) at the earth [*Calvert*, 1981*b*]. Although a precise determination would be difficult, a rough estimate for the source density can be deduced as follows: For $f \gg f_H$ and $\beta \ll 2$ the element of differential phase shift from (3) and (5) becomes

$$d\phi = 2\pi f_N^2 f_H \, dh/f^2 c \tag{8}$$

where $dh = \Delta z \cos\theta$ is the more or less vertical height element, which would equal $-r\, df_H/3f_H$ for a dipole magnetic field. The integral of $d\phi$ outward from an arbitrary altitude where the cyclotron frequency is f_H yields

$$\phi = 2\pi f_N^2 f_H r/3f^2 c \tag{9}$$

for the total phase shift above that altitude. Now, on the assumption that a total terminal phase shift of less than π would produce a limit polarization characteristic of that altitude, an upper limit for the plasma frequency f_N is given by

$$f_N^2(\text{kHz}) < 6.3f(\text{MHz})(f/f_H)/r(R_J) \tag{10}$$

in which the units are indicated for Jupiter and f/f_H is a dimensionless quantity dependent upon the observed polarization and wave direction according to (1) and (2). In order to account for the fringes above 10 MHz at A in Figure 1, it is estimated that a polarization of at least $2j$ would be required, and that would indicate that β was at least 1.5 and thus that f/f_H was less than 1.5 for the 68° wave angle found in Figure 3. Accordingly, the plasma frequency near the source must have been less than 8 kHz, and hence the plasma density must have been less than 0.8 cm^{-3}. This is in surprisingly good agreement

with the lower limit to the plasma density on similar field lines of 0.5 cm^{-3} found by *Gurnett et al.* [1981] from the upper whistler cutoff frequencies also observed with Voyager 1.

Of course, it remains unknown whether these low source plasma densities are local or transient, as they are at the earth. The plasma-cyclotron frequency ratio, f_N/f_H (which must be low to produce cyclotron resonant emission), was apparently less than 10^{-3}, in contrast with 0.02 in the heart of the AKR source region [*Calvert*, 1981*b*]. This ratio, however, probably pertains to a region well above and outside the source, since $f/f_H = 1.3$ occurs at roughly 0.2 R_J above the cyclotron level. The actual source plasma-cyclotron ratio could be somewhat larger, especially if the emission originates like AKR, from local, field-aligned density enhancements [*Calvert*, 1982*a*].

AKR analogy. Although it is hardly a surprise, the Jovian source pictured in Figure 3 is quite analogous to that of AKR, since it exhibits all of the principal AKR properties deduced from the crucial ISIS 1 satellite observations [*Benson and Calvert*, 1979; *Calvert*, 1981*a*]. The emission appears to occur at the cyclotron frequency, in the extraordinary wave mode, at large angles with respect to the magnetic field (here 52° and 68° at 1 and 10 MHz), and from a region of quite low plasma density. The current observations are thus evidence that the pertinent Jovian emissions probably arise from the same basic process, which is now believed to be the Doppler-shifted cyclotron instability of *Melrose* [1976] and *Wu and Lee* [1979]. The principal differences seem to be the apparently lower plasma-cyclotron frequency ratio at Jupiter and the possible association with the Io flux tube.

Source classification. It is hard to determine which of the previously known Jovian radio sources might have produced the emissions analyzed here. Based initially on earthbound observations, the classification scheme for such sources depends upon the statistical occurrence of radio signals as a function of the Io phase (γ_{Io}) and the system III longitude (λ_{III}) with respect to the observer [see *Carr and Desch*, 1976, Figure 2]. This classification, however, becomes dubious at the lower frequencies, and there is no guarantee that it should persist when the observer is very close to the planet, since the proximity should affect the observing directions. Besides, individual events like this one (for which $\gamma_{Io} = 180° \pm 1.3°$, $\lambda_{III} = 60° \pm 15°$, and no classical source exists) always seem to enjoy thwarting statistical classification schemes.

CONCLUSIONS

The Faraday fringe cusps and polarization sense reversals found in the Voyager 1 PRA observations shortly after the Jovian encounter indicate a decametric radio source in the northern hemisphere which is quite analogous to that of AKR at the earth. Between 1 and 10 MHz the source distance from the planetary center decreased from 2.5 to 1.4 R_J, approximately following the ambient cyclotron frequency. The emissions appeared to originate, possibly near the $L = 6$ Io flux tube, in the extraordinary wave mode and at moderately large angles to the magnetic field direction (as depicted in Figure 3). Moreover, the plasma density near the 10-MHz source was apparently less than 0.8 cm^{-3}.

Acknowledgments. This work was part of the Jupiter Data Analysis Program and was funded partly by NASA grant NAGW-256, partly by The University of Iowa, and partly by NASA grant NGL-16-001-043. The Voyager data were obtained from the National Space Science Data Center, Greenbelt, Maryland, and the ephemeris for Voyager 1 was provided by R. R. Anderson and W. S. Kurth. Thanks are due C. K. Goertz, W. S. Kurth, B. A. Randall, and R. R. Anderson for numerous useful discussions, and especially R. R. Anderson, who helped me through a particularly rocky review.

The Editor thanks T. D. Carr and two other referees for their assistance in evaluating this paper.

REFERENCES

Acuña, M. H., and N. F. Ness, The main magnetic field of Jupiter, *J. Geophys. Res.*, *81*, 2917–2922, 1976.

Allis, W. P., S. J. Buchsbaum, and A. Bers, *Waves in Anisotropic Plasmas*, MIT Press, Cambridge, Mass., 1963.

Bagenal, F., and J. D. Sullivan, Direct plasma measurements in the Io torus and inner magnetosphere of Jupiter, *J. Geophys. Res.*, *86*, *8447–8466*, 1981.

Bagenal, F., J. D. Sullivan, and G. L. Siscoe, Spatial distribution of plasma in the Io torus, *Geophys. Res. Lett.*, *7*, 41–44, 1980.

Benson, R. F., and W. Calvert, ISIS-1 observations at the source of auroral kilometric radiation, *Geophys. Res. Lett.*, *6*, 479–482, 1979.

Birmingham, T. J., J. K. Alexander, M. D. Desch, R. F. Hubbard, and B. M. Pedersen, Observations of electron gyroharmonic waves and the structure of the Io torus, *J. Geophys. Res.*, *86*, 8497–8507, 1981.

Broadfoot, A. L., M. J. S. Belton, P. Z. Takacs, B. R. Sandel, D. E. Shemansky, J. B. Holberg, J. M. Ajello, S. K. Atreya, T. M. Donahue, J. L. Bertaux, J. E. Blamont, D. F. Strobel, J. C. McConnell, A. Dalgarno, R. Goody, and M. B. McElroy, Extreme ultraviolet observations from Voyager 1 encounter with Jupiter, *Science*, *204*, 979–982, 1979.

Brown, R. A., A model of Jupiter's sulphur nebula, *Astrophys. J.*, *206*, L179–L183, 1976.

Budden, K. G., *Radio Waves in the Ionosphere*, Cambridge University Press, New York, 1961.

Calvert, W., The signature of auroral kilometric radiation on ISIS 1 ionograms, *J. Geophys. Res.*, *86*, 76–82, 1981*a*.

Calvert, W., The auroral plasma cavity, *Geophys. Res. Lett.*, *8*, 919–921, 1981*b*.

Calvert, W., A feedback model for the source of auroral kilometric radiation, *J. Geophys. Res.*, *87*, 8199–8214, 1982*a*.

Calvert, W., The source location and polarization of Jovian Io B radio emissions (abstract), *Eos Trans AGU*, *63*, 1062, 1982*b*.

Carr, T. D., and M. D. Desch, Recent decametric and hectrometric observations of Jupiter, in *Jupiter*, edited by T. Gehrels, pp. 693–737, University of Arizona Press, Tucson, 1976.

Goertz, C. K., Polarization of Jovian decametric radiation, *Planet. Space Sci.*, *22*, 1491–1500, 1974.

Gurnett, D. A., F. L. Scarf, W. S. Kurth, R. R. Shaw, and R. L. Poynter, Determination of Jupiter's electron density profile from plasma wave observations, *J. Geophys. Res.*, *86*, 8199–8212, 1981.

Lecacheux, A., Ray tracing in the Io plasma torus: Application to the PRA observations during Voyager 1's closest approach, *J. Geophys. Res.*, *86*, 8523–8528, 1981.

Levy, G. S., D. W. Green, H. N. Royden, and G. E. Wood, Dispersive Doppler measurements of the electron content of the torus of Io, *J. Geophys. Res.*, *86*, 8467–8470, 1981.

Melrose, D. B., An interpretation of Jupiter's decametric radiation and the terrestrial kilometric radiation as direct amplified gyroemission, *Astrophys. J.*, *207*, 651–662, 1976.

Tokar, R. L., D. A. Gurnett, F. Bagenal, and R. R. Shaw, Light ion concentration in Jupiter's inner magnetosphere, *J. Geophys. Res.*, *87*, 2241–2245, 1982.

Warwick, J. W., J. B. Pearce, R. G. Peltzer, and A. C. Riddle, Planetary radio astronomy experiment for Voyager missions, *Space Sci. Rev.*, *21*, 309–327, 1977.

Warwick, J. W., J. B. Pearce, A. C. Riddle, J. K. Alexander, M. D. Desch, M. L. Kaiser, J. R. Thieman, T. D. Carr, S. Gulkis, A. Boischot, C. C. Harvey, and B. M. Pedersen, Voyager 1 planetary radio astronomy observations near Jupiter, *Science*, *204*, 995–998, 1979*a*.

Warwick, J. W., J. B. Pearce, A. C. Riddle, J. K. Alexander, M. D. Desch, M. L. Kaiser, J. R. Thieman, T. D. Carr, S. Gulkis, A. Boischot, Y. Leblanc, B. M. Pedersen, and D. H. Staelin, Planetary radio astronomy observations from Voyager 2 near Jupiter, *Science*, *206*, 991–995, 1979*b*.

Wu, C. S., and L. C. Lee, A theory of the terrestrial kilometric radiation, *Astrophys. J.*, *230*, 621–626, 1979.

(Received December 21, 1982;
revised April 21, 1983;
accepted April 25, 1983.)

GEOPHYSICAL RESEARCH LETTERS, VOL. 12, NO. 4, PAGES 179-182, APRIL 1985

TRIGGERED JOVIAN RADIO EMISSIONS

W. Calvert

Department of Physics and Astronomy, The University of Iowa, Iowa City, Iowa 52242

Abstract. Certain jovian radio emissions seem to be triggered from outside, by much weaker radio waves from the sun. Recently found in the Voyager observations near Jupiter, such triggering occurs at hectometric wavelengths during the arrival of solar radio bursts, with the triggered emissions lasting sometimes more than an hour as they slowly drifted toward higher frequencies. Like the previous discovery of similar triggered emissions at the earth, this suggests that Jupiter's emissions might also originate from natural radio lasers.

Introduction

Presumably the terrestrial counterpart of Jupiter's famous decametric radio emissions, the auroral kilometric radiation (AKR) consists of intense radio emissions from the earth's auroral zone at frequencies between about 50 and 600 kHz [Gurnett, 1974]. Since the AKR had previously always been considered a spontaneous result of certain wave instabilities [Melrose, 1976; Wu and Lee, 1979; among others], it was quite surprising to find that the AKR sometimes seemed to be triggered by incoming type III solar radio bursts [Calvert, 1981]. Perhaps equally surprising, it has now been found that certain jovian radio emissions also exhibit such triggering.

The pertinent emissions occurred at hectometric wavelengths, often extending up to an observational frequency limit of 1.3 MHz imposed by the low-band Voyager radio spectrograms on which they appear. Unobservable through the earth's ionosphere, such hectometric jovian emissions (designated 'HOM' by the Voyager wave team) were first detected with Voyager a few months before each of the jovian encounters, extending down to about 0.5 MHz and quite distinct from the kilometric emissions (KOM) at lower frequencies [Boischot et al., 1981]. Like the decametric component, they exhibit strong dependence on Jupiter's rotational phase, plus some Io control down to at least 1.8 MHz. They also vary with the observing latitude and local time, and show a propensity for systematic frequency drifts [Alexander et al., 1981].

Being pertinent background, the AKR triggering will be reviewed first, followed by examples of jovian triggering observed with Voyager. The observed occurrence of triggering will then be discussed, primarily to verify the statistical significance of the effect.

AKR Triggering

Triggered AKR was discovered using ISEE-1 radio spectrograms on which the AKR was found to begin preferentially during type III bursts, usually starting at a single frequency near the burst's leading edge and subsequently expanding to fill a broader spectrum lasting long after the burst itself had completely disappeared [Calvert, 1981]. For the available 1979 ISEE-1 observations, it was verified that the AKR onsets during type III bursts couldn't have been accidental, to a statistical confidence level (unity minus the probability of accidental alignment) of 99.7%. About one third of the strongest type III bursts seemed to be capable of triggering AKR, with triggered AKR comprising about one tenth of that observed.

It was clear from the observed onset timing that the incoming type III radio waves must have caused the observed triggering, rather than some other agent of the type III burst's causative solar flare [see Smith and Smith, 1963]. In most cases, the triggering seemed to occur just when the burst, in executing its characteristic downward frequency sweep, first reached the pertinent frequency. This being delayed ten or more minutes after the optical flare, the onsets presumably weren't a prompt flare effect, attributable to solar photons. The observed onsets, moreover, generally occurred either well before or in the absence of energetic flare electrons reaching the earth. Other flare effects occurring much later, the incoming waves must have been responsible.

The AKR being quite variable, observations of triggering are subject to the obvious uncertainty of identifying onsets. Farrell [1984] recently sought to remove this difficulty by relying instead upon the average AKR signal strength, measured during one-hour intervals before and after an independently selected set of type III bursts. For 200 such events, using IMP-8 in the evening sector to detect the AKR and ISEE-3 sunward of the earth both to detect the type III bursts and to measure the burst signal which had to be deducted, he found statistically significant increases of the AKR signals following bursts at both 178 and 500 kHz. This independent test clearly confirmed the AKR triggering.

Despite certain private skepticism, the evidence for triggered AKR still seems quite conclusive. Finding the same effect at Jupiter clearly lends support by analogy and suggests that a susceptibility to triggering must be a universal property of such emissions.

Jovian Triggering

The evidence for triggered jovian emissions was found using special high-resolution low-band spectrograms (kindly provided by M. L. Kaiser and J. K. Alexander) of the Voyager planetary radio astronomy (PRA) instruments [Warwick et al., 1977]. These spectrograms, of which figures 1, 2, and 3 are examples, show the sequential six-second PRA measurements without averaging, each having a one kilohertz bandwidth in 70 channels

Paper number 5L6461.
0094-8276/85/005L-6461$03.00

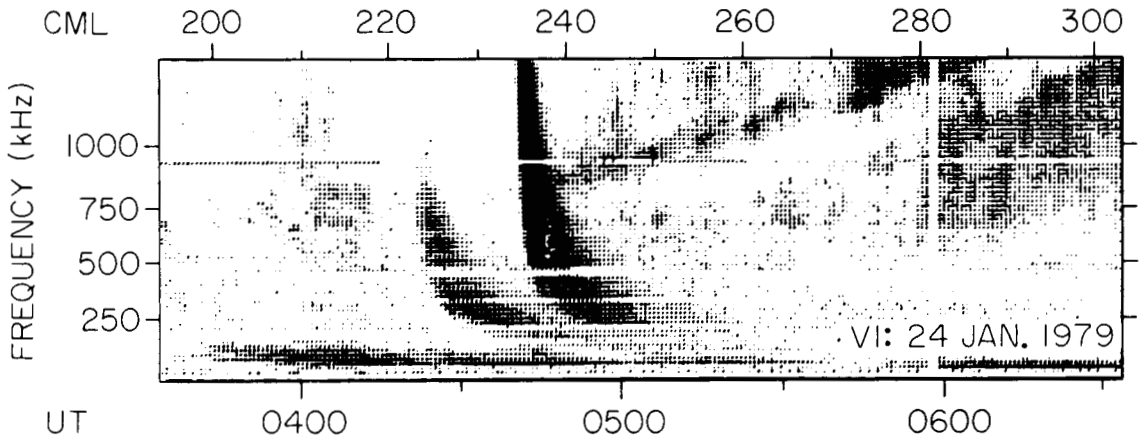

Fig. 1. The apparent triggering of narrowband jovian hectometric radio emissions by the stronger of two type III solar radio bursts, observed with Voyager 1 well before encounter. For this and subsequent PRA spectrograms, the system III (1965) central meridian longitude (CML) is that of Voyager and the observing time was adjusted to equal the universal time (UT) at the earth.

extending up to 1.3 MHz. With stronger signals shown as darker shadings, such spectrograms often revealed features which were hard to recognize either in the noisier high-band spectrograms above 1.3 MHz or in the more generally-available compressed low-band spectrograms. The data set, for both spacecraft, extended from about two months before each of the Jovian encounters to shortly thereafter. The pertinent periods, however, were those more than about a month before encounter, while the receiver gains were still at maximum and the hectometric signals from Jupiter were still less than overwhelming, since that facilitated detecting the type III bursts.

Figure 1 shows a Voyager 1 spectrogram recorded about forty days before encounter, at a distance of 573 R_J (4.1×10^7 km). In this and the other cases to be presented, Voyager 1 was at approximately 3° north joviographic latitude and 10.4 to 10.5 hr jovian local time (about 23° west of the sun, as viewed from Jupiter). Two type III bursts, characterized by their rapid downward frequncy drifts and increasing durations, appear in this spectrogram at 0425 and 0440 UT. The second obviously seems to have triggered a rising band of jovian hectometric emissions beginning at 850 kHz. This emission, having a bandwidth of about 100 kHz, rose at a rate of 6 kHz per minute and disappeared at the low-band's 1.3 MHz upper frequency limit about one hour later. The lack of hectometric signals beforehand presumably wasn't instrumental, the PRA having no automatic gain control and the unrelated kilometric signals below 200 kHz being continuous. Although they showed similar drifts, it isn't clear whether the subsequent broadband hectometric signals were also triggered.

Figure 2 shows a second example, recorded somewhat earlier while Voyager 1 was at 856 R_J (6.1×10^7 km). Here the triggering seems to have occurred at about 650 kHz, during the type III burst at 2320 UT, and the resulting hectometric signals drifted upward at the slower rate of 4 kHz/min. After about one-half hour, these signals merged with others which may or may not have been related to the triggering.

A third example is shown in figure 3, recorded with Voyager 1 at 306 R_J (2.2×10^7 km). In this case, the hectometric signal originated at 750 kHz, drifted upward at 7 kHz/min, and it seems to have been accompanied by broadband triggering at higher frequencies.

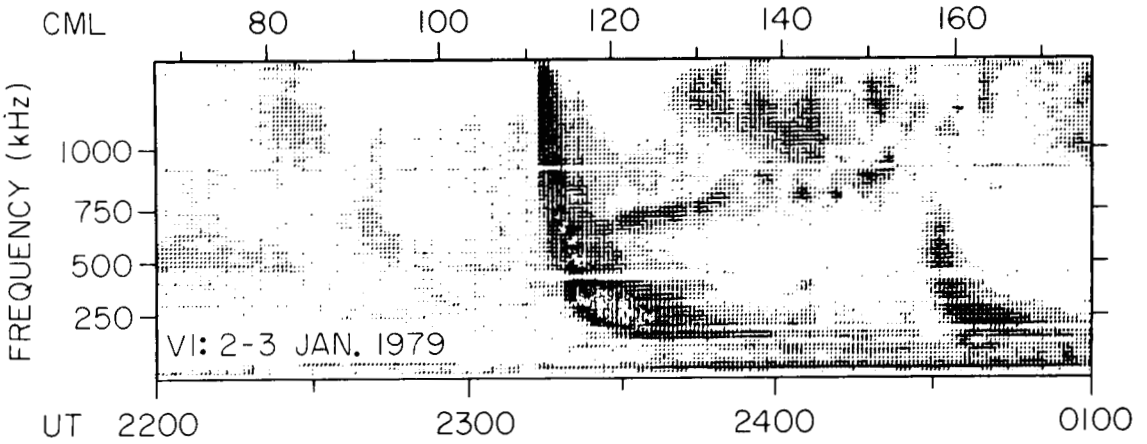

Fig. 2. Narrowband triggering of somewhat shorter duration and slower drift, plus other signals at higher frequencies which may or may not be related. The white regions in the midst of the type III burst are artifacts of photographic reproduction.

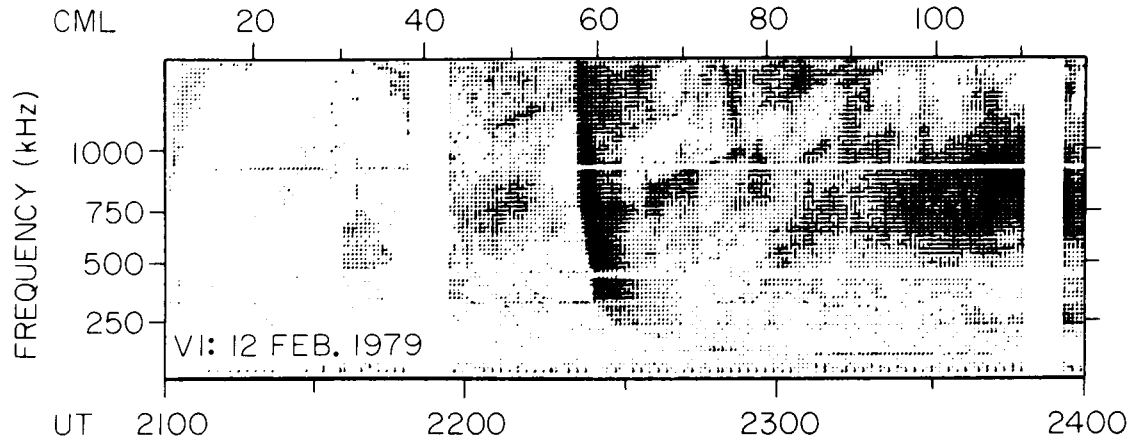

Fig. 3. Narrowband triggering seemingly accompanied by broadband triggering at higher frequencies. The brief signal absences just before 2200 and 2400 represent data gaps.

More than a dozen other cases like figures 1, 2, and 3 have been found, using both spacecraft. Most exhibited rising bands like those shown, having bandwidths less than 200 kHz, lasting twenty minutes or more, and rising at a few kilohertz per minute. Although this seems to be the outstanding signature of triggered jovian hectometric emissions, in a few cases broadband triggering appeared to fill most of the spectrum above 500 kHz, and in one case the triggered signals extended well into the PRA high band, up to roughly 10 MHz.

Occurrence

In order to test whether the observed coincidences of hectometric onsets with type III bursts might have been accidental, all of the available January 1979 Voyager 1 spectrograms were examined for both type III bursts and narrowband hectometric onsets, using the criteria just described. In 254 hours of observation (representing 34% coverage for the month), 28 type III bursts and 27 hectometric onsets were found, including five cases which were coincident within the type III burst's duration at the pertinent frequencies, of twenty minutes or less. The bursts and narrowband onsets thus occurred at approximately the same rate, of 0.1 per hour. Had the two been statistically independent, there should have been scarcely one accidental twenty-minute coincidence, that being $(0.1/3)^2$ for 762 such intervals. The odds of finding at least five, according to Poisson statistics [see Feller, 1950] should have been only 0.003 or just one chance in three hundred. As with the AKR triggering, this implies a confidence level of 99.7%

This exercise was repeated using the one month of Voyager 2 radio spectrograms between April 20 and May 19, 1979. In 594 hours of observation (83% coverage), 41 bursts and 40 narrowband onsets were found, including six coincidences. Again only one accidental coincidence would have been expected, and the probability of there being six, thanks to the larger sample size, is 0.0003, or one chance in three thousand, for a confidence level of 99.97%. Taken collectively with the Voyager 1 results, they imply a probability of one in a million and a confidence level of 99.9999%. This constitutes overwhelming confirmation that the coincident hectometric onsets couldn't have been accidental.

The observed type III bursts and hectometric onsets for both months are shown in figure 4, versus the central meridian longitude (CML) of Voyager. Except for a presumably accidental peak attributed to burst groups, the type III bursts were reasonably independent of CML, implying as expected, no jovian control of the sun. The narrowband hectometric onsets, on the other hand, showed a marked preference for 70° and 280°, reflecting the trend previously reported for all hectometric emissions by Alexander et al. [1981]. The coincident onsets, shaded black in the figure, showed no obvious preference for the same

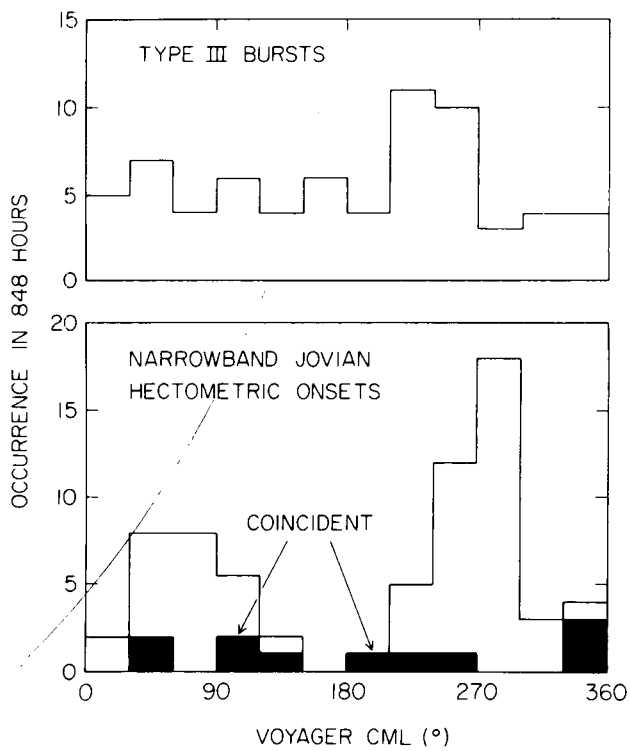

Fig. 4. The occurrence of type III solar bursts and narrowband hectometric onsets versus Voyager's CML during one month each for Voyagers 1 and 2. Coincident onsets are shown solid.

CML values. This further implies that the coincidences weren't accidental and suggests that the susceptibility to triggering is probably independent of Jupiter's phase.

Discussion

Because of the great solar distance of Jupiter and the lack of perceptible triggering delays, it is quite certain the solar electrons accompanying type III bursts could not have been responsible for the observed jovian triggering. Even at half the speed of light, such electrons (having an atypically high energy of 64 keV) should have been delayed at least forty minutes, not allowing for their presumably longer spiral trajectories. As with the AKR, the triggering seems to have been caused by the incoming type III radio waves.

The additional light delay to Voyager via Jupiter should have been up to about four minutes. In all cases studied, this expected delay between the causitive solar burst and the triggered jovian emission was masked by the longer burst durations.

Except for the feedback theory originally inspired by the discovery of triggered AKR [Calvert, 1981; 1982], a susceptibility to triggering is at variance with all other existing production theories. Feedback oscillators, on the other hand, would readily be triggerable if their feedback and gain were just barely insufficient for oscillation and an incoming wave were enough to make up the loop gain shortfall. Acting somewhat like old-time regenerative shortwave radio receivers, such marginally stable radio lasers could be forced into oscillation by a relatively weak wave. Then, provided some side-effect of the resulting forced oscillation increased the loop gain, such oscillators might remain oscillating after the triggering wave disappears.

Conclusions

It has been found that jovian hectometric radio emissions are occasionally triggered by incoming type III solar radio bursts. This triggering seems to occur between about 500 and 900 kHz, producing rising bands of emission having bandwidths of typically 100 to 200 kHz, durations of twenty minutes or more, and upward drift rates of a few kilohertz per minute. Eleven such cases have been identified in the Voyager PRA observations between one and two months before encounter. From the observed occurrence rates of the type III bursts and the hectometric onsets, it was verified that these apparent triggerings couldn't have been accidental alignments.

The jovian triggerings are believed comparable to the similar triggerings of AKR at the earth. This implies a new similarity between the jovian and terrestrial emissions and suggests that both originate from radio laser oscillators, since only such sources should be readily triggerable.

Acknowledgements. This work was supported by NASA grants NAG5-225, NAGW-256, and NGL 16-001-043. W. S. Kurth provided the pertinent Voyager ephemeris. I apologize to M. L. Kaiser for implying his support of the previous AKR work.

References

Alexander, J. K., T. D. Carr, J. R. Thieman, J. J. Schauble, and A. C. Riddle, Synoptic observations of Jupiter's radio emissions: Average statistical properties observed by Voyager, J. Geophys. Res., 86, 8529-8545, 1981.

Boischot, A., A. Lecacheux, M. L. Kaiser, M. D. Desch, J. K. Alexander, and J. W. Warwick, Radio Jupiter after Voyager: An overview of the planetary radio astronomy observations, J. Geophys. Res., 86, 8213-8227, 1981.

Calvert, W., The stimulation of auroral kilometric radiation by type III solar radio bursts, Geophys. Res. Lett., 8, 1091-1094, 1981.

Calvert, W., A feedback model for the source of auroral kilometric radiation, J. Geophys. Res., 87, 8199-8214, 1982.

Farrell, W. M., A statistical study of solar type-III bursts and auroral kilometric radiation onsets, thesis, University of Iowa, 1984.

Feller, W., An Introduction to Probability Theory and Its Applications, Wiley (New York), 1950.

Gurnett, D. A., The Earth as a radio source: Terrestrial kilometric radiation, J. Geophys. Res., 79, 4227-4238, 1974.

Melrose, D. B., An interpretation of Jupiter's decametric radiation and the terrestrial kilometric radiation as direct amplified gyroemission, Astrophys. J., 207, 651-662, 1976.

Smith, H. J. and E. V. P. Smith, Solar Flares, Macmillan (New York), 1963.

Warwick, J. W., J. B. Pearce, R. G. Peltzer, and A. C. Riddle, Planetary radio astronomy experiment for voyager missions, Space Sci. Rev., 21, 309-327, 1977.

Wu, C. S., and L. C. Lee, A theory of the terrestrial kilometric radiation, Astrophys. J., 230, 621-626, 1979.

(Received February 5, 1985;
accepted February 18, 1985.)

GEOPHYSICAL RESEARCH LETTERS, VOL. 12, NO. 9, PAGES 625-626, SEPTEMBER 1985

AFFIRMATION OF TRIGGERED JOVIAN RADIO EMISSIONS AND THEIR ATTRIBUTION TO COROTATING RADIO LASERS

W. Calvert

Department of Physics and Astronomy, The University of Iowa, Iowa City, Iowa 52242

Abstract. The diverse criticisms of jovian radio triggering, by Desch and Kaiser, are considered invalid primarily because they stemmed from ignoring the original event criteria. Moreover, attributing the observed triggerings to accidental encounters with a constant rotating beam is unjustified, as should have been obvious from the original analysis, since they occurred at the wrong jovian phases. On the other hand, there is nothing wrong with a rotating source also being triggerable, and it is proposed that the triggered emissions originate from just such sources.

Implying generation by natural radio lasers, the discovery of externally-triggered jovian radio emissions [Calvert, 1985a] was considered a breakthrough for understanding such planetary radiations. The observations of triggering, however, have been questioned by Desch and Kaiser [1985], who found less statistical evidence for such events in the same Voyager radio observations, and this paper will answer their objections.

Although I respect Desch and Kaiser, in this instance I find them less than objective. They began with firmly-held doubts about triggering [Kaiser, private communication, 1981 to present], and ever since have been casting about for some reason to reject the concept.

Their doubts seem rooted in a mistaken belief that triggering is bizarre and uncommon. The effect, however, is readily demonstratable with suitably-modified audio amplifiers, as was done before an audience at the past spring meeting of the American Geophysical Union [Calvert, 1985c].

The radio triggering at Jupiter was considered a second instance of the same phenomenon previously found at the earth [Calvert, 1981, 1985b] and independently confirmed by Farrell [1985]. By attacking only the statistical significance of the triggering at only one planet, Desch and Kaiser have dealt with only part of the issue.

The principal evidence for triggering in the Voyager radio spectrograms was the sudden onset of certain specific features during incoming type III solar radio bursts, often simultaneously over a range of frequencies. An 'onset' in the original study pertained only to these specific spectral features, and although not explicitly stated, a prior absence of jovian activity was not considered essential (as in my Figure 3), since that would have favored occasions without suitable radio lasers [Calvert, 1982] pointing toward Voyager and waiting to be triggered.

The statistical significance of triggering was asserted only for the narrowband rising features "having bandwidths less than 200 kHz, lasting twenty minutes or more, and rising at a few kilohertz per minute." Although broadband triggering was also pointed out, such events were completely excluded from my statistical analysis.

Desch and Kaiser, however, have ignored my event criteria and adopted new criteria of their own, requiring the much less specific "no jovian activity followed by sharply defined emission." They then "construed" triggering rather than simply trying to observe it. When this difference of criteria was pointed out to them, they subsequently "tightened" their criteria to include events "like" their Figure 1a (or my Figure 2). When asked specifically whether they had applied my criteria, their answer was "no". Their different results are attributed to this intentional choice of different event criteria.

In other words, although they purport to have examined my narrowband and broadband triggered events, they really have examined neither. Instead, they have simply examined something else and asserted that that was not statistically significant. Clearly, they have not tested the hypothesis they were seeking to disprove.

The difference of criteria can be illustrated with their own Figure 2, which shows brief triggering by a type III burst in the lower panel near 21 hr (although much compressed compared to the previous figures). Although hardly obvious at first glance, and difficult to verify without high-resolution spectrograms, that event came close to satisfying my criteria for narrowband onsets, since it occupied about 200 kHz, lasted roughly 15 minutes (four dots width), and seemed to drift upward at about 4 kHz/min. For Desch and Kaiser to have included such a case inadvertently clearly signifies that they have not honed their skills for finding such events. (This case also emphasizes the need to ignore prior activity, since the triggered feature was part of ongoing emissions detected in the other Voyager receiver channel.)

Their demonstration with artificial type III bursts signifies nothing extra, since it equally depended upon their original non-specific event criteria and yielded a spread which was consistent with Poisson statistics, given their stated mean. In the original analysis of the same data, the expected mean for accidental narrowband alignments was one event, as was the standard deviation (since the standard deviation of a Poisson distribution is simply the square root of the mean). This implies that the observed five coincident onsets were four standard deviations greater than the mean and hence quite significant. With their stated means of 3.6 to 4.6, it would have required at least eleven events to have had comparable significance. It was wrong of them to imply that a few cases never matter when the standard deviations were different.

Paper number 5L6640.
0094-8276/85/005L-6640$03.00

Their comparison with the work of Farrell [1985] is decidedly inappropriate. Farrell carefully measured the average signal increase attributable to triggering and established its significance, whereas Desch and Kaiser have simply counted the occurrence of increases. These two are not the same, and what they have really done is to count onsets again.

Desch and Kaiser found eleven increases during type III bursts, and yet they reported only five potential triggerings. According to the above analysis, eleven should have been quite significant. What was wrong with the other six (presumably their criteria again), and why were the eleven not considered significant?

If the results of Farrell are any indication, one should expect infrequent large increases to typify triggering, rather than an abundance of increases. This also seems borne out by my study, where only eleven triggerings (different from their eleven) were found to accompany 69 type III bursts. By expecting otherwise, Desch and Kaiser are demanding more of the phenomenon than they should and simply slaying a paper tiger of their own manufacture.

In their Figure 2, Desch and Kaiser pointed out their "240° CML event," which was supposed to occur when a jovian central meridian longitude of 240° was facing Voyager. However, those in the figure actually started at 275°±4°. They further asserted that this event persists for repeated rotations, even though it was absent from the Voyager 2 observations on the very next one. Although it is hard to be certain with the complex Voyager radio data, this possibly persistent narrowband feature presumably accounts for the peak in my Figure 4 centered on about 280°, although that would imply that their "240°" event does not seem to occur at 240°.

Desch and Kaiser have implied (and erroneously attributed to me) that most of the observed alignments were with their 240° event. My Figure 4 clearly showed that this was untrue, nor was it true for the Voyager 1 events alone (that being a deduction on their part from examining triggered events which they had claimed earlier did not exist). The whole purpose of my Figure 4 was to eliminate accidental alignments with systematic features like their 240° event, regardless of how they originated.

Desch and Kaiser might have meant that their so-called 240° event sometimes extends forward to as far as 240°, and that my Figure 1 might be attributed to just such a case. Although that interpretation might have some merit, such advanced onsets would also imply triggering and give rise to the concept that the triggered features resulted from triggerable beams that rotate with the planet (in this case occupying about 6° of jovian longitude, according to the signal durations in my Figure 1.)

Desch and Kaiser attribute all of the observed onsets to rotation, insisting that the source was "almost always" emitting. They offered no valid proof for this repeated assertion (their Figure 3 notwithstanding), nor did they quantify what was meant by "almost" and "near[ly]." As long as they must retain such qualifiers, it makes little logical sense to infer that all the onsets must have been rotational, nor that none could have had any other physical significance. They have, in effect, assumed that beams which rotate with the planet are not triggerable, and to offer that as proof against triggering constitutes circular reasoning.

With their Figure 3, Desch and Kaiser sought to demonstrate that onsets like mine were purely rotational. However (again bearing in mind the compressed time scale), any narrowband triggerings in the upper panel would have been completely obscured in the lower, and the prompt broadband triggered features like those in my Figure 3 were completely absent (their concept of "almost identical" presumably allowing for this). The most that their Figure 3 actually shows is that onsets according to their own criteria might have been rotational.

I have examined all of the Voyager compressed spectrograms for the entire year of 1979 and found no obvious inconsistencies with triggering. I found some cases in which the triggering appeared simultaneous in different directions, and others which were consistent with triggerable rotating beams.

It should be noted that triggering implies lasing, and hence also a ready explanation for the rotating beams which they have found, since all laser emissions are inherently beamed (by virtue of their coherence). Moreover, the beam directions should presumably be fixed by density structures at the source, and hence they should rotate with the planet. This, in fact, is the best reason yet for why the jovian emissions ought to be beamed and rotate with the planet.

I am forced to admit that Kaiser [private communication, 1985] has actually caught me in a error, since I previously mistook the 48-second high-resolution spectrograms for six-second measurements. Apart from that, I would change nothing of my paper as a result of his and Desch's efforts, nor do I feel that the discovery of triggering should be put to rest without a truly realistic and detailed examination.

Acknowledgements. This work was supported by NASA grants NAGW-256 and NGL-16-001-043. The compressed Voyager radio spectrograms were provided by the National Space Science Data Center, Greenbelt, Maryland.

References

Calvert, W., The stimulation of auroral kilometric radiation by type III solar radio bursts, Geophys. Res. Lett., 8, 1091-1094, 1981.

Calvert, W., A feedback model for the source of auroral kilometric radiation, J. Geophys. Res., 87, 8199-8214, 1982.

Calvert, W., Triggered jovian radio emissions, Geophys. Res. Lett., 12, 179-182, 1985a.

Calvert, W., Auroral kilometric radiation triggered by type II solar radio bursts, Geophys. Res. Lett., 12, 377-380, 1985b.

Calvert, W., Triggered jovian radio emissions (abstract), EOS Trans. AGU, 66, 343, 1985c.

Desch, M. D., and M. L. Kaiser, On the proposed triggering of jovian radio emissions, Geophys. Res. Lett., this issue, 1985.

(Received July 12, 1985;
accepted, July 16, 1985)

GEOPHYSICAL RESEARCH LETTERS, VOL. 13, NO. 4, PAGES 370-372, APRIL 1986

AKR SIGNAL INCREASES CAUSED BY TRIGGERING

W. M. Farrell, W. Calvert, and D. A. Gurnett

Department of Physics and Astronomy, The University of Iowa, Iowa City, Iowa 52242

Abstract. This paper presents a study of the amplitude increases which accompany the triggering of auroral kilometric radiation (AKR) by Type-III solar radio bursts. IMP-8 data were used to determine the signal increases observed during one-hour periods before and after Type-III bursts at 100 kHz, 178 kHz and 500 kHz and these were compared with similar observations when the Type-III bursts were absent. The results indicate that between 8 to 16% of the Type-III bursts caused statistically significant intensity increases and that infrequent large signal increases of sometimes 20 dB or more tended to characterize the triggered AKR, rather than a large proportion of small increases.

Introduction

Previous studies have indicated that Type-III bursts are capable of triggering AKR onsets [Calvert, 1981; Farrell and Gurnett, 1985], and this observation has become an important factor in determining the exact mechanism of AKR generation. This paper presents a study in which the AKR wave amplitudes before and after Type-III bursts were examined to further characterize the triggered AKR events.

During recent years, the processes which generate Earth's intense auroral kilometric radiation have been the subject of considerable investigation. Although many such processes have been proposed, only the amplification by cyclotron resonance [Ellis, 1965; Melrose, 1976; Wu and Lee, 1979] has achieved much general acceptance. Although cyclotron resonance plays an important role in AKR generation, it is not clear whether amplification alone explains all of the AKR's features. A more comprehensive model has been introduced where a radio wave laser [Calvert, 1982] generates the intense AKR signals. This laser model explains AKR's observed signal intensities, its source location and its spectral fine structure.

The laser model of the AKR generation was spawned by the observation of triggered AKR. Initially, solar Type-III bursts and AKR were perceived to be unrelated phenomena. However, cases were found in which Type-III bursts and AKR were temporally aligned, indicating that stimulation was involved [Calvert, 1981]. The phenomena became known as triggered AKR when it was clear that incoming Type-III bursts were responsible [ibid; Calvert, 1985a, 1985b, 1985c]. Figure 1 shows an ISEE-1 spectrogram with a Type-III bursts and triggered AKR.

Critics of the triggering concept have suggested that the emissions' temporal alignments were accidental [Desch and Kaiser, 1985]. If indeed Type-III bursts are unrelated to AKR, then the probability of detecting AKR before and after Type-III bursts should be equal. In a previous study [Farrell and Gurnett, 1985], a superposed epoch analysis was performed on over 140 Type-III bursts to determine if AKR was triggered by the bursts. In that study, ISEE-3 (at the L-1 Legrange point approximately 200 R_E on the sunward side of the earth) was used to detect isolated Type-III bursts, and IMP-8 (in a relatively close earth orbit) was used to detect the AKR. For each of the Type-III bursts examined in that study, intensities were measured with both satellites in two-hour periods extending from one hour before to one hour after the initial appearance of the Type-III burst. Each of the two-hour event intervals were then analyzed by a two-step process: First, the ISEE-3 measurements for each event were subtracted from the corresponding IMP-8 measurements, effectively subtracting the Type-III burst intensities out of the IMP-8 measurements. Next, the intensities for all the event intervals were averaged as a function of the time with respect to the burst. This analysis was done at three frequencies: 100 kHz, 178 kHz and 500 kHz. The results of this superposed epoch analysis showed statistically significant average intensity increases after Type-III bursts at both 178 kHz and 500 kHz, and thus that the emissions' temporal alignment was not accidental, but a direct result of the Type-III bursts triggering the AKR.

Analysis Procedure

Although the superposed epoch analysis clearly confirmed the AKR triggering, it did not indicate directly the probability of finding triggered AKR events, and a new study was performed to find that probability. This study follows the same basic procedure as the superposed epoch analysis,

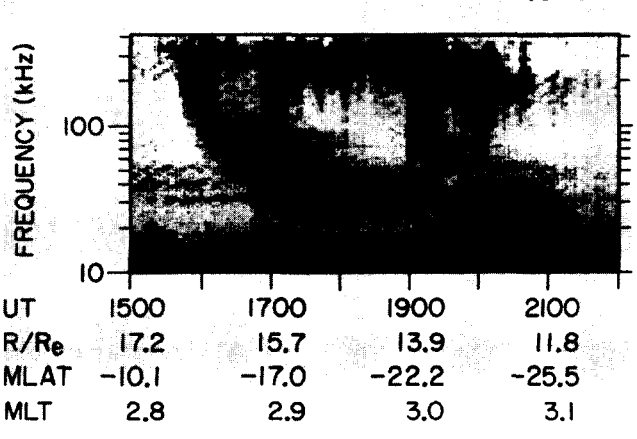

Fig. 1. An ISEE-1 spectrogram showing a Type-III burst which apparently triggered the subsequent AKR.

Paper number 6L6016.
0094-8276/86/006L-6016$03.00

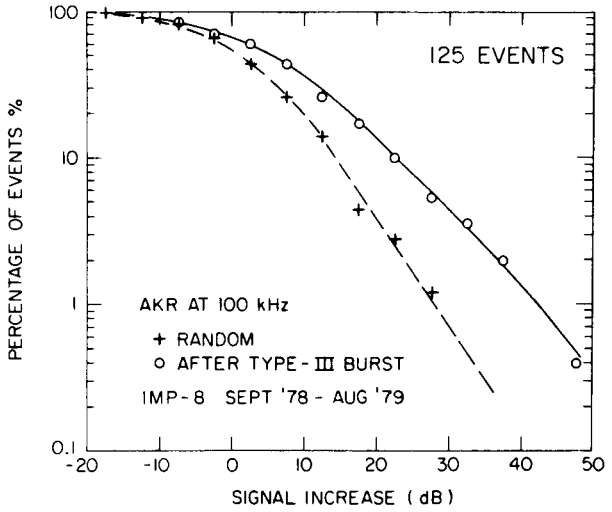

Fig. 2. The cumulative distribution of AKR intensity increases associated with Type-III bursts (circles) compared with comparable randomly-selected intervals (crosses), for consecutive one-hour periods at 100 kHz. Note that consistently more large signal increases (> 20 dB) accompanied the Type-III events, clearly signifying the triggering of the AKR.

where the ISEE-3 and IMP-8 measurements were used to detect Type-III bursts and AKR, respectively. Again, for each event, the ISEE-3 measurements were subtracted from the corresponding IMP-8 measurements. However, rather than averaging the events, as was done in the superposed epoch analysis, a preceeding-hour average and a following-hour average were calculated for each event. The triggering of AKR should then be indicated by changes between these two averages.

In order to determine if triggering had occurred, a control group consisting of randomly selected two-hour intervals was also used. These intervals were analyzed following the same procedure. The intensity changes measured from these intervals were taken to indicate the intensity changes which should have been expected if only randomly occurring AKR were being detected. Consequently, comparing the distribution of these intensity changes to the distribution of intensity changes from the Type-III bursts' data set, the number of triggered AKR events can be estimated.

Results

A comparison of the Type-III and control group intensity change distributions clearly indicates that triggered AKR was being detected. Figures 2, 3 and 4 show the cumulative distributions for both the control group and that with Type-III bursts at 100 kHz, 178 kHz and 500 kHz, respectively. Note that at all three frequencies, the distributions with Type-III bursts had a greater number of events with large signal increases. This result is expected only if the Type-III bursts were consistently triggering the AKR.

At 100 kHz, 13.5% of the events with Type-III bursts had more than a 20 dB signal increase, while only 3.5% of the control group's events were above this same level--almost a factor of four difference. At 178 kHz, 5.4% of the events with Type-III bursts were above a 20 dB signal increase whereas only .45% of the control group's events were above that same level--over a factor of ten difference. At 500 kHz, 6% of the events in the Type-III bursts set were above a 20 dB signal increase, whereas only 1.0% of the control group's events were above that level--a factor of six difference. In all three cases, the number of Type-III events with signal increases larger than about 20 dB was much greater than those of the control group; a result expected of triggered AKR.

Statistical Significance

The results thus show an excess of large signal increases following Type-III bursts, and in order to determine the statistical significance of this result, a count was made of the number of Type-III events exceeding two standard deviations of the control group. This number was then compared to the number of control group events above the same level. A probability for accidentally finding the observed number of Type-III events above two standard deviations was then calculated with Poisson's statistics using the number of control group events above two standard deviations as the expected number of accidental events.

At 100 kHz, 12 events from the Type-III burst set were above two standard deviations (21 dB), while only 4 events from the control group were above that level. The probability of finding this many Type-III events beyond two standard deviations is less than .1%, implying that the 12 events were quite statistically significant. At 178 kHz, 13 events from the Type-III burst set were above two standard deviations (10 db), whereas only 4 events from the control group were above that level. Again, the probability of finding this many Type-III events beyond two standard deviations is quite small (less than .05%) and that indicates that the 13 events were also quite statistically significant. At 500 kHz, 7 events from the Type-III burst set were above two standard deviations (14.6 db) while only 2 events from the control group were above that level. The probability of finding that many Type-III events above two standard deviations is less than .5%. This indicates again that the 7

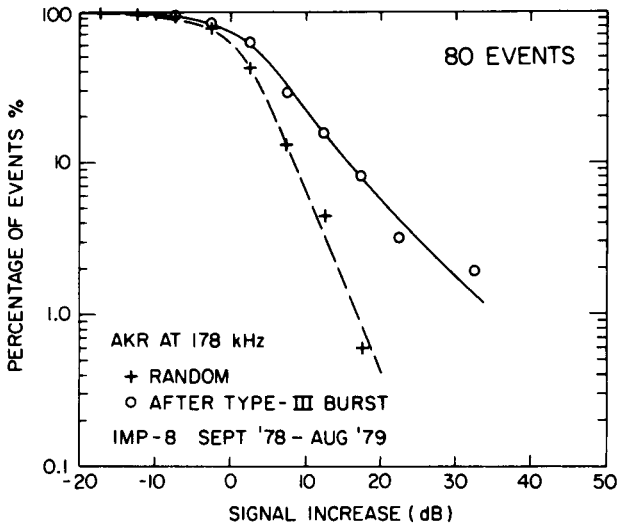

Fig. 3. The same as Figure 2, for 178 kHz.

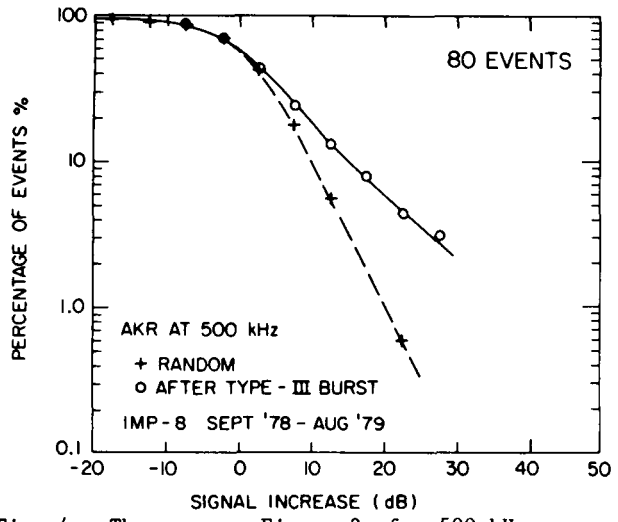

Fig. 4. The same as Figure 2, for 500 kHz.

events also were statistically quite significant. Note that at all three frequencies the number of Type-III events above two standard deviations is statistically significant to a confidence level of at least 99.5%.

Discussion

The superposed epoch analysis previously showed statistically significant intensity increases following Type-III bursts only at 178 kHz and 500 kHz. However, it was not clear from that analysis whether the increases were due to small intensity increases following many Type-III events or large intensity increases following only a few Type-III events. The results of this study show that 9.6%, 16.3% and 8.8% of the Type-III events had intensity increases greater than two standard deviations at 100 kHz, 178 kHz and 500 kHz, respectively, indicating that only a few of Type-III events with large signal increases accounted for the statistically significant intensity increases that were measured in the superposed epoch analysis.

In the superposed epoch analysis, the intensities at particular times from each event were added together, so events with the strongest signals contributed the most to the overall total intensities. In effect, each event in the superposed epoch analysis was weighted by its intensity. The superposed epoch analysis did not show statistically significant intensity increases at 100 kHz presumably because they were drowned out by the more intense random AKR. In the current analysis, however, all events had equal weight, and triggered AKR was relatively easy to detect at all three frequencies.

As previously pointed out [Calvert, 1981; 1982], these observations imply that the generation of AKR involves true lasing rather than open-loop "maser" amplification acting alone. Simply because the triggered AKR continues to persist long after the triggering solar signals have disappeared, they imply states of oscillation within the source which are capable of continuing independently once they have gotten started. Although the exact triggering mechanism remains to be clarified, by analogy with triggerable electronic oscillator circuits like regenerative shortwave radio receivers, this in turn would imply the sort of closed-loop wave feedback oscillations which are the essence of lasing [e.g., see Verdeyen, 1981]. The significance of these measurements, therefore, beyond confirming the remarkable external triggering of planetary radio emissions, is that they also imply radio lasing at the source.

Conclusions

The analysis presented here conclusively confirms the original conclusion that Type-III bursts sometimes trigger onsets of AKR [Calvert, 1981]. It was shown that the AKR intensity changes during Type-III bursts involved a statistically-significant number of events with large signal increases, above about 15 to 20 db. It was concluded that between 8-16% of incoming Type-III bursts trigger AKR onsets.

Acknowledgements. We are grateful to Bob Stone and Bob MacDowall for their ISEE-3 3-D radio mapping experiment data and to Fred Scarf for his ISEE-3 plasma wave investigation data. Terry Averkamp and Larry Granroth deserve thanks for valuable input on data reduction and analysis. John Birkbeck also deserves our thanks for a fine drafting job.

The research was supported by NASA through contract NAS5-28701 with Goddard Space Flight Center and grant NGL-16-001-043 with NASA Headquarters, plus also for W. Calvert, NASA grant NAGW-256.

References

Calvert, W., The stimulation of auroral kilometric radiation by Type-III solar radio bursts, Geophys. Res. Lett., 8, 1091, 1981.

Calvert, W., A feedback model for the source of auroral kilometric radiation, J. Geophys. Res., 87, 8199-8214, 1982.

Calvert, W., Triggered jovian radio emissions, Geophys. Res. Lett., 12, 179-182, 1985a.

Calvert, W., Affirmation of triggered Jovian radio emissions and their attribution to corotating radio lasers, Geophys. Res. Lett., 12, 625-626, 1985b.

Calvert, W., Auroral kilometric radiation triggered by Type-II solar radio bursts, Geophys. Res. Lett., 12, 377-380, 1985c.

Desch, M. D., and M. L. Kaiser, On the proposed triggering of Jovian radio emissions, Geophys. Res. Lett., 12, 621-624, 1985.

Ellis, G. R. A., The decametric radio emissions of Jupiter, Radio Science, 69D, 1513-1530, 1965.

Farrell, W. M., and D. A. Gurnett, The statistical study of solar Type-III bursts and auroral kilometric radiation onsets, J. Geophys. Res., 90, 9634-9640, 1985.

Melrose, D. B., An interpretation of Jupiter's decametric radiation and the terrestrial kilometric radiation as direct amplified gyroemission, Astrophys. J., 207, 651, 1976.

Verdeyen, J. T., Laser Electronics, (Prentice-Hall, Englewood Cliffs, New Jersey), 1981.

Wu, C. S., and L. C. Lee, A theory of the terrestrial kilometric radiation, Astrophys. J., 230, 621-626, 1979.

(Received January 17, 1986
accepted February 12, 1986)

GEOPHYSICAL RESEARCH LETTERS, VOL. 13, NO. 11, PAGES 1105-1108, NOVEMBER 1986

SATELLITE INTERFEROMETRIC MEASUREMENTS OF AURORAL KILOMETRIC RADIATION

M. M. Baumback[1], D. A. Gurnett[1], W. Calvert[1] and S. D. Shawhan[2]

[1]Dept. of Physics and Astronomy, University of Iowa, Iowa City, IA 52242
[2]NASA Headquarters, 400 Maryland Ave., Washington, DC 20546

Abstract. The first satellite interferometric measurements of auroral kilometric radiation (AKR) were performed by cross-correlating the waveforms detected by the ISEE 1 and ISEE 2 spacecraft. Such correlations were measured at 125 and 250 kHz for projected baselines perpendicular to the source direction ranging from 20 to 3868 km. High correlations were found for all projected baselines, with little or no tendency to decrease even for the longest baselines. These results must be interpreted differently for incoherent and coherent radiation. For incoherent radiation, the correlation as a function of the baseline is the Fourier transform of the source brightness distribution, and this implies an average source region diameter for all of the bursts analyzed of less than about 10 km. For such small source diameters, the required growth rates are too large to be explained by existing incoherent theories, strongly indicating that the radiation must be coherent. For coherent radiation, an upper limit to the source region diameter can be inferred instead from the angular width of the radiation pattern. The close similarity of the spectra at the longest baselines indicates that the angular width of the radiation pattern must be at least 2.5°, implying that the diameter of the source must be less than about 20 km. At present, the proposed closed-loop radio lasing model is the only known mechanism for providing sources this small.

Introduction

The purpose of this paper is to present the first satellite interferometric measurements of auroral kilometric radiation (AKR). AKR is the most intense electromagnetic radiation generated in the earth's magnetosphere, occurring in the frequency range from 50 to 700 kHz with an average radiated power of approximately 10^7 watts [Gallagher and Gurnett, 1979]. Gurnett [1974] showed that AKR is associated with discrete auroral arcs. Polarization and direction-finding measurements [Kaiser et al., 1978; Shawhan and Gurnett, 1982; Mellott et al., 1984; Kurth et al., 1975; Calvert, 1985] have shown that the radiation is generated along auroral field lines at frequencies near the local electron cyclotron frequency mainly in the right-hand polarized extraordinary mode. The spectrum has clearly defined upper and lower cutoff frequencies which fluctuate over a wide range on a time scale of tens of minutes. High resolution measurements [Gurnett et al., 1979] show that the spectrum consists of numerous narrowband bursts with bandwidths sometimes less than 100 Hz.

Paper number 6L6379
0094-8276/86/006L-6379/$03.00

Although a variety of mechanisms have been proposed for the generation of AKR, only the Doppler-shifted cyclotron resonance instability [Melrose, 1976; Wu and Lee, 1979] has gained general acceptance. Omidi and Gurnett [1984] computed the path integrated growth rates for this mechanism and concluded that even with electron velocity distributions much steeper than those which are observed, a 70 km amplification length is required to explain the observed AKR intensity. Recently, Calvert [1982] has proposed an AKR generation model involving wave feedback very similar to an optical laser, with local density irregularities serving as mirrors. The laser model predicts discrete bursts of nearly monochromatic radiation, very similar to those which are observed. The laser model also requires less wave growth than amplification alone, since the only requirement is that the net gain around the feedback path be greater than one.

The interferometric measurements presented in this study are from the ISEE 1 and 2 spacecraft which are in nearly identical eccentric earth orbits with apogees at geocentric radial distances of about 23.7 R_E. With these orbits the spacecraft can detect AKR emissions from the auroral region as illustrated in Figure 1. ISEE 1 and 2 have identical wideband receivers that can be tuned to a variety of frequencies from 31 kHz to 2 MHz. The bandwidth of the receivers is 10 kHz. The electric field waveforms detected by the two spacecraft are converted to a frequency range of 0.65 to 10.0 kHz for transmission to the ground where they are recorded on analog tapes at the NASA telemetry stations. The waveforms can then be cross-correlated to perform interferometric measurements. See Shawhan [1979] for a description of the wideband receivers and interferometry system.

Long Baseline Interferometry

For simplicity and ease of data processing, the cross-correlations were performed with a one-bit correlator. For such a correlator, the actual correlation must be computed using the equation [Weinreb, 1963],

$$\rho_m = \sin(\tfrac{\pi}{2} C_o) \tag{1}$$

where C_o is the correlator output. In the presence of receiver and telemetry noise, the correlation must also be corrected for the signal-to-noise ratio according to the relation

$$\rho = [\langle S_1^2/V_1^2\rangle\langle S_2^2/V_2^2\rangle]^{-1/2}\rho_m \tag{2}$$

where S_1 and S_2 are the signal voltages, V_1 and V_2 are the signal-plus-noise voltages, ρ_m is the correlation computed from Equation 1, and the

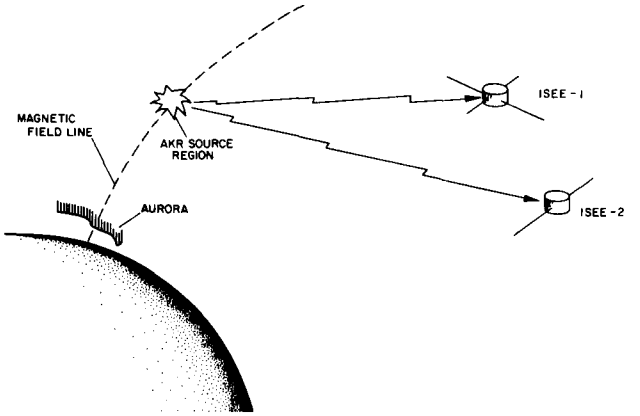

Fig. 1. From nearly identical orbits, both ISEE 1 and ISEE 2 can detect AKR emissions from the auroral region. From the cross-correlation of the detected signals and the observed radiation pattern, an upper limit to the apparent source region diameter can be determined.

angle brackets represent time averages over the periods of measurement.

Correlation measurements must be interpreted differently for incoherent and coherent sources. For an incoherent source, the radiation emitted from different elements in the source region is uncorrelated, whereas for a coherent source the radiation emitted from different elements in the source region is correlated. For an incoherent source, it is customary to interpret the interferometer output as the Fourier component of the two-dimensional source region brightness. The correlation for a source region with brightness distribution S(x,y) is

$$\rho(u,v) = \int\int S(x,y)e^{-i(2\pi/\lambda)(ux+vy)}dxdy \qquad (3)$$

where u and v are the x and y projections of the baseline between the two spacecraft, and x and y are the angular source-region coordinates. Since ISEE 1 and 2 can only measure the correlation at one baseline for each individual event, the source region brightness distribution must be modeled, and for this we have used a Gaussian brightness model. For a circular two-dimensional Gaussian brightness distribution the correlation can be shown to be

$$\rho = e^{-(\pi b\alpha/2\lambda)^2} \qquad (4)$$

where α is the angular width of the source region, b is the projected baseline of the interferometer, and λ is the wavelength. Equation 4 shows that for an incoherent source the correlation rapidly drops to zero if the angular width of the source exceeds λ/b.

For coherent radiation, the radiation emitted from different elements in the source region is correlated, and the traditional method of interferometry analysis (Equation 4) cannot be used. However, the apparent width of the radiation pattern may be used to estimate an upper limit to the source diameter. The angular width of the radiation pattern is limited by diffraction and is approximately λ/d, where d is the diameter of the source. For the specific case of a Gaussian brightness distribution, the source diameter is given by

$$d = \frac{\lambda}{\pi \sin(\theta/2)} \qquad (5)$$

where θ is the angular width between the 1/e power points of the radiation pattern.

Results

Correlations have been measured at projected baselines ranging from 20 to 3868 km at frequencies of 125 and 250 kHz. Most of the measurements were made on the nightside of the earth at radial distances greater than 10 R_E. A typical example of the correlations observed is shown in Figure 2. The top two panels show the spectra of a series of AKR bursts received by ISEE 1 and 2 and the bottom panel shows the measured cross-correlation. The sinusoidal modulation of the correlation is caused by the difference in frequency of the local oscillators in the two receivers as well as other slow variations in the spacecraft-source geometry. The amplitude of the sine wave gives the measured correlation ρ_m. The correlation for this event, after correcting for the signal-to-noise ratio is $\rho = 0.81$. If the source is assumed to be incoherent with a Gaussian brightness distribution, the source size can be computed from Equation 4. With a baseline length of b = 3260 km, the angular size of the source turns out to be $\alpha = 1.08 \times 10^{-4}$ rad. Using the source-to-spacecraft distance for this event, which was about 13.4 R_E, the source diameter is estimated to be about 9 km.

Correlation measurements similar to that shown in Figure 2 have been performed for 52 events extending over a large range of baselines. Figure 3 shows a plot of the correlation as a function of the projected baseline for all of the bursts analyzed. Each point in Figure 3 represents the average correlation measured for about

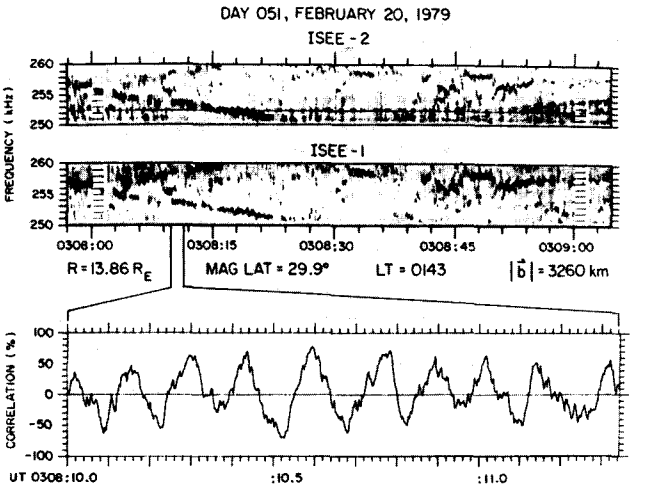

Fig. 2. The top two panels show the spectra of a series of AKR bursts observed by ISEE 1 and ISEE 2. The bottom panel shows the correlation for one of these bursts. The sinusoidal modulation is caused primarily by the difference in the two local oscillator frequencies.

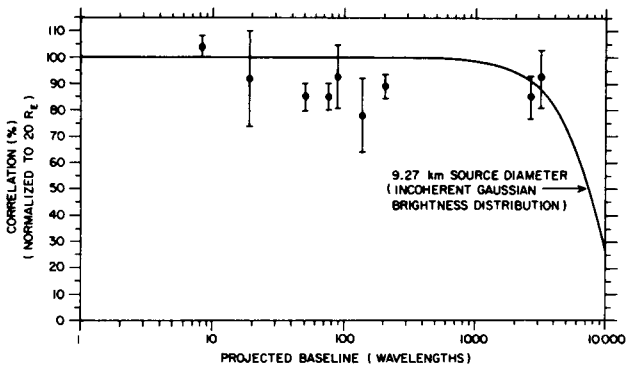

Fig. 3. The best fit of the correlation amplitude as a function of baseline to a Gaussian brightness distribution implies a source diameter of less than 9.27 km for incoherent sources. The source region diameter is determined primarily by the correlation at the longest baseline.

five separate events at each baseline. Since the angular size of the source depends upon the source-spacecraft distance, these correlations have been normalized to a fixed source distance of 20 R_E. This plot shows that the correlation is essentially constant and slightly less than 100% out to the longest baselines which were available. The best fit of Equation 4 through the available points gives a source diameter of 9.27 km. However, since the observed correlations remained high even for the longest baselines, this constitutes only an upper limit for the apparent source size, and it could actually be much smaller. These measurements show that if the source is incoherent then the source region must be very small, less than about 10 km.

If the source is assumed to have a coherent Gaussian-shaped radiation pattern, the source diameter can be computed from Equation (5). Because nearly identical spectra are observed by both spacecraft at the largest available baseline separations, again only an upper limit to the source diameter can be determined. For the longest baseline (~ 3868 km) the angular width of the radiation pattern at apogee must have been at least 2.5°. The corresponding source diameter then must therefore be no larger than about 20 km at 250 kHz.

Discussion

A successful theory for the generation of AKR must account for the high correlations obtained from these interferometric measurements. Two models for the generation of AKR will be examined to determine if high correlations can be explained. The first model assumes that AKR is simply amplified galactic background radiation, as assumed by Omidi and Gurnett [1982] and tacitly assumed by most others [Melrose, 1976; Wu and Lee, 1979; etc.]. For large source diameters, the solid angle of the amplified galactic radiation received by each spacecraft is the same as the angular size of the source region as viewed from the spacecraft. For small source diameters, comparable to the wavelength of the radiation, diffraction effects spread the waves over a wider angle and permit a larger solid angle of the amplified galactic background noise to be received by the two spacecraft. The cross-correlation between the signals detected by the spacecraft is given by the ratio $\Delta\Omega/\Omega$, where $\Delta\Omega$ is the overlap in the solid angle of the amplified galactic background noise viewed by the two spacecraft and Ω is the total solid angle. For angular spacecraft separations greater than the angular size of the source, as was usually the case for ISEE 1 and 2, the geometric solid angles never overlap, as illustrated in the top panel of Figure 4, and the correlation should always have been zero. However, to account for the high observed correlations, the actual solid angles of the amplified galactic background radiation must overlap almost completely. This requires that the source region diameters must be only a few kilometers so that diffraction effects can produce the required overlap, as illustrated in the bottom panel of Figure 4. For such small source diameters very high growth rates (perhaps exceeding 10 dB per kilometer) are required to produce the observed intensities. Such high growth rates are much greater than those estimated for the cyclotron instability [Wu and Lee, 1979; Melrose, 1976; Omidi and Gurnett, 1982]. This result strongly implies that the radiation must be coherent.

Calvert [1982] has proposed wave amplification

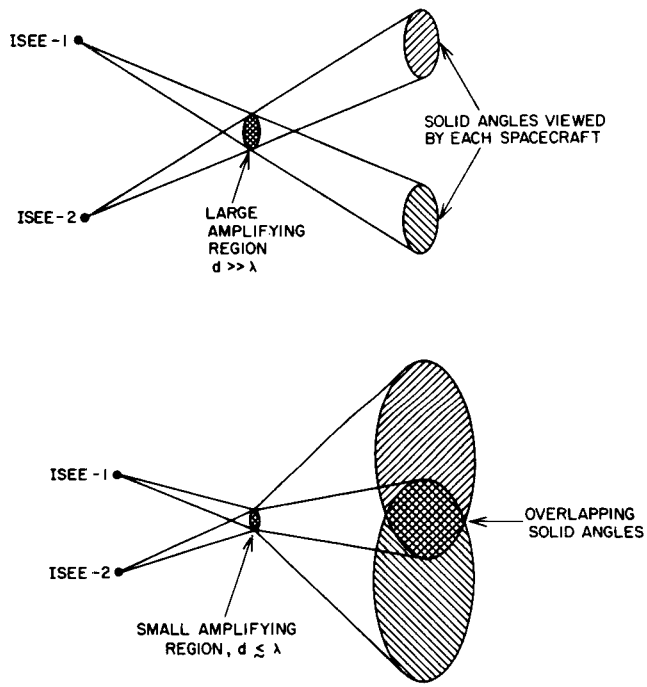

Fig. 4. The top panel illustrates that for angular spacecraft separations greater than the angular source size, the solid angles of amplified galactic background radiation illuminating each spacecraft would not overlap and the detected signals should be uncorrelated. The bottom panel illustrates that for source region diameters comparable to the wavelength of the radiation, diffraction effects could produce solid angles which overlap and produce a correlation (although such small sources would seem to require unrealistically high growth rates).

with feedback to explain the observed intensity and discrete structure of the AKR. This mechanism also has the merit of producing a coherent source with an angular size in agreement with these observations. According to this theory, the apparent laser length can be determined from the observed spacings of the discrete AKR components and was found to be about 25 km. By straightforward laser theory [see Verdeyen, 1981], this implies an exit spot width of about 5 km and a beamwidth of about 10°, entirely consistent with the new interferometric observations.

Conclusions

For a source emitting incoherent radiation, the correlation measurements imply a source region diameter of less than about 10 km. For coherent radiation, the radiation pattern must have an angular width of at least 2.5°, and hence a source region diameter of less than about 20 km. The high correlations observed are totally inconsistent with simple amplification of galactic background radiation (unless the amplifying regions are smaller than expected and the growth rates are substantially larger than predicted), but they are consistent with the proposed coherent laser mechanism of Calvert [1982].

Acknowledgments. This research was supported in part by the National Aeronautics and Space Administration under Contracts NAS5-26819 and NAS5-28701, Grants NAG5-118 NASA/HQ, NGL-16-001-002, and NGL-16-001-043 and by the Office of Naval Research under Grant N00014-85-K-0404. The work of W. Calvert was also supported by NASA Grant NAGW-256.

References

Calvert, W., A feedback model for the source of auroral kilometric radiation, J. Geophys. Res., 87, 8199-8214, 1982.

Calvert, W., DE-1 Measurements of AKR wave directions, Geophys. Res. Lett., 12, 381-384, 1985.

Gallagher, D. L., and D. A. Gurnett, Auroral kilometric radiation: Time-averaged source location, J. Geophys. Res., 84, 6501-6509, 1979.

Gurnett, D. A., The earth as a radio source: Terrestrial kilometric radiation, J. Geophys. Res., 79, 4227-4238, 1974.

Gurnett, D. A., R. R. Anderson, F. L. Scarf, R. W. Fredricks, and E. J. Smith, Initial results from the ISEE-1 and -2 plasma wave investigation, Space Sci. Rev., 23, 103-122, 1979.

Kaiser, M. L., J. K. Alexander, A. C. Riddle, J. B. Pearce, and J. W. Warwick, Direct measurements by Voyagers 1 and 2 of the polarization of terrestrial kilometric radiation, Geophys. Res. Lett., 5, 857-860, 1978.

Kurth, W. S., M. M. Baumback, and D. A. Gurnett, Direction-finding measurements of auroral kilometric radiation, J. Geophys. Res., 80, 2764-2770, 1975.

Mellott, M. M., W. Calvert, R. L. Huff, D. A. Gurnett, and S. D. Shawhan, DE-1 Observations of ordinary mode and extraordinary mode auroral kilometric radiation, Geophys. Res. Lett., 11, 1188-1191, 1984.

Melrose, D. B., An interpretation of Jupiter's decametric radiation and the terrestrial kilometric radiation as a direct amplified gyroemission, Astrophys. J., 207, 651-662, 1976.

Omidi, N., and D. A. Gurnett, Growth rate calculations of auroral kilometric radiation using the relativistic resonance condition, J. Geophys. Res., 87, 2377-2383, 1982.

Omidi, N., and D. A. Gurnett, Path integrated growth of auroral kilometric radiation, J. Geophys. Res., 89, 10,801-10,812, 1984.

Shawhan, S. D., Description of the ISEE satellite-to-satellite kilometric wavelength interferometer system, Ann. des Telecommunications, 35, 266-272, 1979.

Shawhan, S. D., and D. A. Gurnett, Polarization measurements of auroral kilometric radiation by Dynamics Explorer-1, Geophys. Res. Lett., 9, 913-916, 1982.

Verdeyen, J. T., Laser Electronics, Prentice-Hall, Englewood Cliffs, New Jersey, 1981.

Weinreb, S., A digital spectral analysis technique and its application to radio astronomy, Tech. Rep. 412, Research Laboratory of Electronics, M.I.T., Cambridge, 1963.

Wu, C. S. and L. C. Lee, A theory of the terrestrial kilometric radiation, Astrophys. J., 230, 621-626, 1979.

(Received September 19, 1986;
accepted October 7, 1986)

GEOPHYSICAL RESEARCH LETTERS, VOL. 14, NO. 2, PAGES 119-122, FEBRUARY 1987

THE MINIMUM BANDWIDTHS OF AURORAL KILOMETRIC RADIATION

M. M. Baumback[1] and W. Calvert

Physics and Astronomy, The University of Iowa, Iowa City, Iowa 52242

Abstract. The bandwidths of the discrete spectral components of the auroral kilometric radiation can sometimes be as narrow as 5 Hz. Since this would imply an apparent source thickness of substantially less than the wavelength, it is inconsistent with the previous explanation for such discrete components based simply upon vertical localization of a cyclotron source. Instead, such narrow bandwidths can only be explained by radio lasing.

Introduction

The earth's intense auroral kilometric radiation (AKR), which is generated above the auroral zone at frequencies of 50 to 700 kHz in conjunction with discrete auroral arcs, is now generally attributed to the Doppler-shifted electron-cyclotron instability of Ellis [1965], Melrose [1976], and Wu and Lee [1979], among others. The principal current question is whether this instability operates alone, simply amplifying the background cosmic radio noise, or whether it operates in conjunction with local density irregularities which serve as mirrors and provide the closed-loop wave feedback which is required for natural radio lasing [Calvert, 1982]. Previously we have examined the spatial coherence of the AKR, with the conclusion (barring sources of unreasonably small size) that only lasing can account for the high levels of coherence which were observed [Baumback et al., 1986]. Here we shall examine a related but equally-significant property which signifies lasing, that of the AKR's spectral monochromaticity, again with the conclusion that only lasing can account for the extremely narrow bandwidths which are sometimes observed.

A laser produces monochromaticity in exactly the same way as any other closed-loop feedback oscillator, by the signal amplitude increasing to saturation and the consequent spectral quenching of adjacent frequencies [see Calvert, 1982, 1986]. A stable, ideal laser, in fact, should produce a truly monochromatic output, regardless of its size or internal structure, with no spectral bandwidth whatsoever. In actuality, of course, there are always secondary effects, like motion of the mirrors, temporal variations of the peak loop gain, or background noise, which can broaden the actual bandwidth, but to first order the spectral bandwidth of a laser should be zero.

Although first discovered when the AKR was found to be externally triggerable [Calvert, 1981, 1985], the principal evidence that the AKR originates from natural radio lasing has always been its discrete emission spectrum [Calvert, 1982]. Examined with sufficiently-fine spectral resolution, in fact, the AKR is virtually always found to consist of multiple discrete spectral components [Gurnett et al., 1979; Gurnett and Anderson, 1981]. Previously typifying it as having bandwidths of about 1 kHz, Gurnett and Anderson [1981] attributed such spectral discreteness to localized sources emitting at the electron cyclotron frequency; a 1 kHz bandwidth corresponding to a vertical thickness of about 15 kilometers.

In this paper we shall examine the minimum spectral bandwidths which are observed in the AKR emission spectrum with ISEE-1, with the conclusion that those bandwidths can sometimes be as narrow as only about 5 Hz. Since this would correspond to a vertical source thickness of only about 80 meters, which is substantially less than both the emitted wavelength or the size of any known vertical structure of the aurora, it is further concluded that the source-localization hypothesis must be discarded in favor of radio lasing.

Observations

Figure 1 is a radio spectrogram from the ISEE-1 swept frequency receiver showing AKR between its lower frequency cutoff at about 100 kHz and the 400 kHz upper frequency limit of the receiver, with the portion that has been chosen for further analysis indicated by an arrow. The ISEE-1 and ISEE-2 spacecraft also include identical "wideband" receivers with 10 kHz bandwidths which can be tuned to a variety of frequencies between 31 kHz and 2 MHz. For the measurements presented below, the ISEE wideband receivers con-

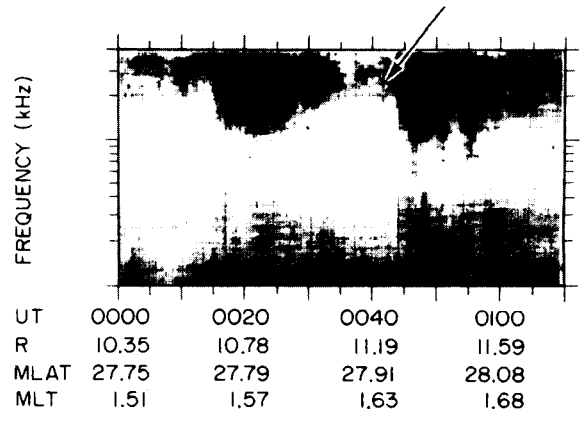

Fig. 1. An ISEE 1 radio spectrogram showing AKR between about 100 kHz and the upper frequency limit of 400 kHz, with the portion chosen for further analysis (during a relatively quiet period between stronger bursts) indicated by an arrow.

[1]M. M. Baumback now at Sachs/Freeman Assoc., 1401 McCormick Dr., Landover, MD 20785.

Paper number 6L6416.
0094-8276/87/006L-6416$03.00

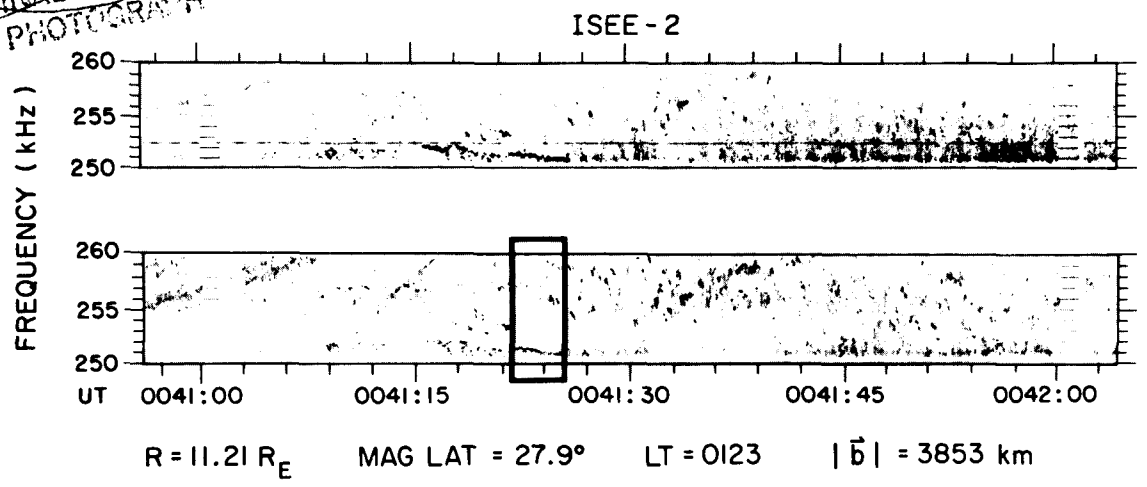

Fig. 2. A conventional spectral analysis of the analog AKR signals received by both ISEE-1 and ISEE-2, showing boxed the portion subsequently analyzed by digital techniques. These records illustrate the similarity of the AKR spectral fine structure observed by both spacecraft even at their largest projected separations (here 3853 km), with the apparent amplitude differences being attributed to the somewhat different beaming of different components.

verted the waveforms received in the 250 to 260 kHz frequency range directly to the 0.65 to 10.0 kHz range for transmission to the ground, where they were recorded on analog tapes for later analysis.

In Figure 2 are the ISEE-1 and ISEE-2 high resolution spectrograms for a one-minute interval of this data showing various discrete AKR emissions. Although the apparent bandwidth of most of these discrete emissions is typically about 1 kHz, sometimes the bandwidth can be considerably more narrow. For instance, although at 0041:00 UT there are several emissions with bandwidths of about 1 kHz drifting from 255 to 260 kHz, between 0041:15 and 0041:27 UT there are much more narrow AKR emissions at a frequency of about 251 kHz. A four-second interval of these narrowband emission was chosen for further analysis, as shown boxed.

Figure 3 shows a single spectrum from this event containing a very narrow spectral peak at 251.4 kHz. The width of this spectral peak is virtually indistinguishable from the width obtained with monochromatic test signals, implying that the bandwidth of this emission was less than the 20 Hz resolution of the spectrum analyzer. The inset in Figure 3 is a series of spectra covering this four-second interval and showing many other discrete spectral peaks of comparable width.

Figure 4 is a spectrogram produced from the same spectrum analyzer data as that in Figure 3, but covering only the 250.0 to 252.5 kHz frequency range and a one-second time interval.

Autocorrelation Analysis

By autocorrelation techniques, signal bandwidths can be calculated to somewhat better precision than is possible with a spectrum analyzer. Since the autocorrelation $\rho(\tau)$ of a signal $f(t)$ is the Fourier transform of its power spectrum, the spectrum can be reconstructed from the autocorrelation by the inverse Fourier transform. For signals which are not time stationary, an approximation to the autocorrelation for short time intervals $\rho_c(t,\tau)$ can be computed from the equation

$$\rho_c(t,\tau) = \frac{\sum_{k=0}^{n} W(k\Delta t)\, f(t-k\Delta t+\frac{\tau}{2})\, f(t-k\Delta t-\frac{\tau}{2})}{\sum_{k=0}^{n} W(k\Delta t)} \qquad (1)$$

where t is the time, τ is the time lag, Δt is the time interval between samples (7 μsec), W is an exponential weighting function (in this case giving the equivalent of a 14 millisecond integration time constant) and n is an integer large enough so that $n\Delta t$ is always much greater than the time constant. In this analysis, the one-bit method for computing autocorrelations was used [Weinreb, 1963]. With such methods, the computed

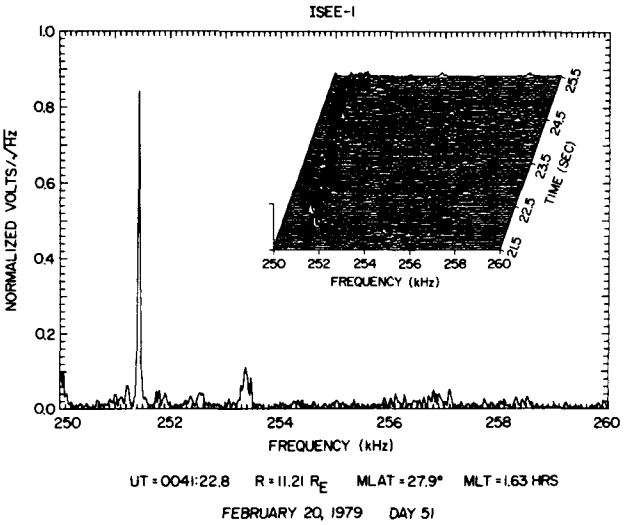

Fig. 3. A single spectrum from the segment boxed in Figure 2, showing an apparent bandwidth which is virtually indistinguishable from the optimum resolution of the technique (20 Hz), plus an inset showing the sequence of spectra for that segment.

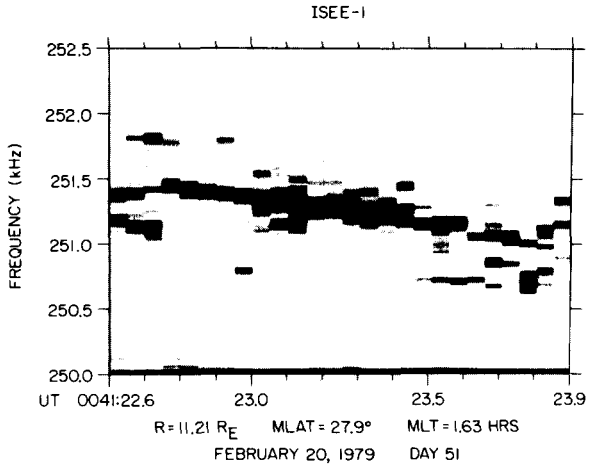

Fig. 4. A somewhat smaller portion of Figure 3 displayed as a spectrogram, with the smallest rectangular pixels indicating the combined spectral/temporal resolution of the technique.

autocorrelation $\rho_c(t,\tau)$ must be corrected by

$$\rho(t,\tau) = \sin\left(\pi\rho_c(t,\tau)/2\right) \qquad (2)$$

to obtain the actual autocorrelation $\rho(t,\tau)$.

The correlations, computed for a number of different times, were Fast Four Transformed (FFT) from the lag domain to the frequency domain in order to produce the spectrogram shown in the top panel of Figure 5. For this spectrogam the autocorrelation was calculated for time lags of up to 85.5 milliseconds, giving an effective frequency resolution of about 6 Hz. Since the bandwidths of these discrete emissions are comparable to the frequency resolution, a uniform FFT weighting function was chosen, giving a somewhat sharper frequency resolution despite its having somewhat larger spurious side lobes. A comparison of Figure 4 (produced by the conventional spectrum analyzer) with Figure 5 (produced by transforming the autocorrelation) clearly shows that the transformed autocorrelation replicates the same spectral features with better resolution.

An estimate for the bandwidth can be calculated directly from the autocorrelation by assuming a spectral shape for the emission. Since the actual spectral shape of the emissions is unknown, we have modeled the spectral shape as a Gaussian, assuming that there was only one spectral peak. For a Gaussian shape, the autocorrelation is

$$\rho(\tau) = e^{-(\Delta\omega\tau/4)^2}\cos(\omega\tau) \qquad (3)$$

where ω is the center frequency of the emission and $\Delta\omega$ is the bandwidth between the 1/e power points of the signal. The bottom panel of Figure 5 shows the bandwidth of the narrowband AKR emission computed by this technique. During the time intervals when there was only one spectral peak, this method produced minimum signal bandwidths of about 5 to 10 Hz with statistical errors (the standard deviation of the least-squares fit) of about 1 Hz. The gaps in the signal bandwidth correspond to times with multiple spectral peaks, and hence when the spectral shape model was invalid.

Even if the instantaneous bandwidths were actually zero, the minimum value obtainable for the instantaneous bandwidth of a signal drifting in frequency is approximately

$$\Delta f = T\, df/dt \qquad (4)$$

where T is the integration time and df/dt is the frequency drift rate. For a 400 Hz sec^{-1} drift rate (the approximate slope of the feature in Figure 5A) and the 0.014 sec integration time used in this analysis, this minimum value is about 5 Hz. In Figure 5 this minimum bandwidth occurs at the moment when the frequency drift rate was least, consistent with this interpretation and implying that the actual instantaneous bandwidth might have been even more narrow.

Discussion

On the assumption of a vertically-restricted cyclotron source in a dipole magnetic field, the vertical size of that source (y) would be given by

$$y = r\, df / 3\, f \qquad (5)$$

where r is the geocentric radius, f is the fre-

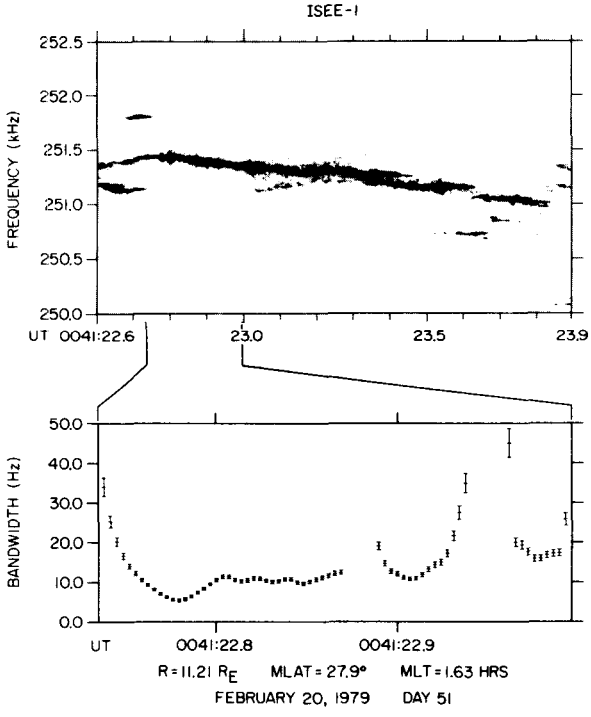

Fig. 5. (A) A spectrogram comparable to Figure 4, but reconstructed from the autocorrelation anaysis, along with (B) the apparent spectral bandwidth deduced from the best-fitting single Gaussian spectra having the same decrease of the autocorrelation for time lags up to 85.5 milliseconds. This figure illustrates apparent AKR spectral bandwidths as narrow as 5 Hz.

quency and df is the bandwidth. For the 5 Hz bandwidth determined above and a 250 kHz source at 1.85 earth radii, this gives about 80 meters, which is less than one-tenth of the approximately one-kilometer emitted wavelength.

At the outset, it is hard to imagine a natural wave source with a vertical thickness which is less than the emitted wavelength. However, even if that were possible, the horizontal size of the source (x) would then have to be limited by the so-called Sagitta formula

$$x = \sqrt{2 R y} \qquad (6)$$

where R is the pertinent radius of curvature (e.g., that of the constant cyclotron-frequency surfaces or that of wave refraction). Completely ignoring source wave refraction, this would give a source length of only about 40 km, which is less than the most optimistic lengths which are required to explain the observed AKR amplitudes by amplification alone [e.g., Omidi and Gurnett, 1984]. Moreover, if one more-realistically assumes that the source length is limited instead by source wave refraction, where the refraction radius of curvature may be as small as ten kilometers because of the very low source plasma densities [Calvert, 1982], the source length would then have to be only about one kilometer. Seeming to require a hundred decibels gain in that one kilometer to explain the AKR amplitudes, this would clearly rule out amplification.

There is, of course, no good reason to expect auroral structures with veritcal sizes as small as 80 meters, nor have any ever been observed.

The very narrow bandwidths reported here are considered conclusive evidence for radio lasing, since no other known mechanism could produce comparable monochromaticity. Although this one instance, of course, cannot prove that all of the AKR must be attributed to lasing, it clearly signifies that no other proposed mechanism could be the sole source of that radiation.

Conclusions

The AKR spectral bandwidth has been measured by two independent methods, conventional spectral analysis and lagged autocorrelation, both indicating bandwidths sometimes as narrow as 5 to 10 Hz. Implying apparent source thicknesses substantially less than the emitted wavelength, such narrow bandwidths are totally inconsistent with open-loop amplification or any other mechanism which must rely upon vertical source localization to explain the discreteness of the emissions. Instead, such narrow bandwidths are consistent only with radio lasing [Calvert, 1982].

Acknowledgments. This work being an outgrowth of Baumback's doctorial thesis, thanks are extended to his thesis advisors, S. D. Shawhan and D. A. Gurnett. It was supported by NASA contracts NAS5-26819 and NAS5-28701, and grants NAGW-256, NAG5-118, NGL-16-001-002, and NGL-16-001-043; and by the Office of Naval Research under grant N00014-85-K-0404.

References

Baumback, M. M., D. A. Gurnett, W. Calvert, and S. D. Shawhan, Satellite interferometric measurements of auroral kilometric radiation, Geophys. Res., Lett., 13, 1105-1108, 1986.

Calvert, W., The stimulation of auroral kilometric radiation by type III solar radio bursts, Geophys. Res. Lett., 8, 1091-1094, 1981.

Calvert, W., A feedback model for the source of auroral kilometric radiation, J. Geophys. Res., 87, 8199-8214, 1982.

Calvert, W., Auroral kilometric radiation triggered by type II solar radio bursts, Geophys. Res., Lett., 12, 337-380, 1985.

Calvert, W., An explanation for triggered auroral kilometric radiation, the auroral plasma cavity, and discrete auroral arcs, (abstract), EOS, Trans. Amer. Geophys. Union, 67, 1158, 1986.

Ellis, G. R. A., The decametric radio emissions of Jupiter, Radio Science, 69D, 1513-1530, 1965.

Gurnett, D. A., R. R. Anderson, F. L. Scarf, R. W. Fredricks, and E. J. Smith, Initial results from the ISEE-1 and -2 plasma wave investigation, Space Sci. Rev., 23, 103-122, 1979.

Gurnett, D. A., and R. R. Anderson, The kilometric radio emisson spectrum: Relationship to auroral acceleration processes, in Physics of Auroral Arc Formation, S.-I. Akasofu and J. R. Kan, eds., Geophys. Monogr. Ser., Vol. 25, Amer. Geophys. Union, Washington, DC, p. 341-350, 1981.

Melrose, D. B., An interpretation of Jupiter's decametric radiation and the terrestrial kilometric radiation as direct amplified gyroemission, Astrophys. J., 207, 651-662, 1976.

Omidi, N., and D. A. Gurnett, Path integrated growth of auroral kilometric radiation, J. Geophys. Res., 89, 10,801-10,812, 1984.

Weinreb, S., A Digital Spectral Analysis Technique and its Application to Radio Astronomy, M.I.T. Tech Rep. 412, Cambridge, MA, 1963.

Wu, C. S., and L. C. Lee, A theory of the terrestrial kilometric radiation, Astrophys. J., 230, 621-626, 1979.

(Received November 3, 1986;
revised December 18, 1986;
accepted December 30, 1986.)

NATURAL RADIO LASING AT JUPITER

W. Calvert

The University of Iowa

Y. Leblanc

Observatoire de Paris

G. R. A. Ellis

The University of Tasmania

Received 1987 October 1;

December 1987

Abstract. Like the comparable AKR radio emissions from the earth's magnetosphere, the well-known decametric radio S-bursts from Jupiter, observed in France and Australia at frequencies from 10 to 26 MHz, have been found to exhibit equally-spaced discrete spectral components which can be attributed to the adjacent longitudinal oscillation modes of natural radio lasers. Implying sizes of only a few kilometers for the individual radio lasers producing the S-bursts, the frequency spacing of these modes was roughly constant with frequency and about 30 to 50 kilohertz. Their corresponding temporal spacings, however, varied inversely proportional to the observing frequency, suggesting that the radio lasers producing the S-bursts were expanding uniformly at a rate of about four kilometers per second. Attributed to the projected motion of Io with respect to the planet, this expansion of the S-burst radio lasers would account for the downward frequency drifts of the S-bursts without the energetic electron bunches which have heretofore always been assumed to account for such behavior.

Subject headings: planets: Jupiter - planets: radio radiation - radiation mechanisms

INTRODUCTION

Planetary cyclotron radio emissions, like the earth's auroral kilometric radiation (AKR) and Jupiter's well-known decametric radio emissions (DAM), are widely attributed to the doppler-shifted cyclotron resonance instability of Ellis (1962, 1964, 1965), Melrose (1976), and Wu and Lee (1979). Also referred to as the 'maser' cyclotron or synchrotron instability (Melrose et al. 1982; Le Queau et al. 1985; Zarka et al. 1986; among others), this instability causes coherent wave growth near the electron cyclotron frequency, and at large angles to the source magnetic field, in low-density magnetized plasmas having suitable free energy in their electron velocity distributions. The underlying principle is that the waves are doppler-shifted into cyclotron resonance with energetic electons in the electron's moving frame of reference, where those waves can then efficiently pitch-angle scatter the electrons and thereby acquire part of the electron energy. For both the AKR at the Earth (Benson and Calvert 1979; Shawhan and Gurnett 1982; Calvert 1981a, 1985c; Mellott et al. 1984; Huff et al. 1987) and the DAM at Jupiter (Calvert, 1983), it has been verified that the waves originate near the cyclotron frequency and primarily in the extraordinary wave mode, just as they should for this wave instability.

An important question, however, still remains. Inspired by such emissions being externally triggerable by other radio waves from the

sun (Calvert 1981b, 1985a, 1985b), and based upon the same cyclotron wave instabilty, it has been proposed that these emissions must also involve natural radio lasing caused by the wave feedback which can occur between local irregularities of the source plasma density (Calvert 1982). Consisting of self-excited closed-loop wave feedback oscillations which proceed to saturation, this radio lasing is functionally equivalent to that which occurs inside man-made optical lasers, although at radio, rather than optical, wavelengths. The principal aspect of the laser model which distinguishes it from the previous open-loop wave amplification acting alone is therefore the occurrence of self-excited oscillations which saturate, and it is this saturation which causes the spatial and spectral quenching which are responsible for the laser's remarkable properties (see Verdeyen 1981).

Foremost among these remarkable laser properties are external emissions which are both coherent and virtually monochromatic, caused directly by the spatial and spectral quenching (see Calvert 1982). For the AKR, both of these expected emission properties have now been verified to degrees which would clearly eliminate the previous open-loop amplifier model (Baumback et al. 1986; Baumback and Calvert 1987). Moreover, it has also been shown that the AKR exhibits multiple discrete spectral components which can be attributed to a laser's adjacent longitudinal oscillation modes having a differing integral number of wavelengths around the wave feedback path (Gurnett and Anderson 1981; Calvert 1982). Besides further confirming the radio-laser emission hypothesis, these regularly-spaced laser modes can also be used to

measure the apparent laser length, W, between the laser's plasma mirrors, according to the equation

$$W = c / 2 n \Delta f \qquad (1)$$

where c is the speed of light, n is the source wave refractive index, and Δf is the frequency spacing between the adjacent modes (see Calvert 1982, Eqn. 35). In this equation, the major uncertainty in determining the laser length from the mode spacings is the unknown wave refractive index, which has to be less than unity for the extraordinary mode and is probably about one half, judging from the apparent AKR emission angles and certain models for a lasing source (Calvert 1981a, 1982).

Since the Jovian emissions presumably originate from the same basic cyclotron instability, it is reasonable to expect that they might also involve radio lasing. In particular, the well-known Jovian decametric radio S-bursts (see Carr et al. 1983) might be expected to result from lasing, since their spectrum is already known to be discrete and virtually monochromatic (Ellis 1982; among others). In order to confirm this possibility, a search was made for the corresponding longitudinal laser modes in the spectra of the S-bursts, and the purpose of this paper is to report the successful outcome of that search. As with the AKR from the Earth, this also permits measuring the apparent size of the individual radio-laser sources at Jupiter, as well as determining other properties of those sources.

Using S-burst radio observations which were recorded at Nancay, France, by the Paris Observatory, and at Hobart, Tasmania, in Australia,

by the University of Tasmania, it will be shown that the expected longitudinal laser modes can be distinguished from the more-or-less random occurrence of S-burst groups. It will also be shown that the temporal spacing of these modes varies inversely with the observing frequency, suggesting that the downward frequency drifts of the S-bursts can be attributed to an approximately uniform expansion of the S-burst radio lasers. Finally, it will be shown that the apparent velocity of this expansion is roughly equal the magnetically-projected surface velocity of the Jovian moon Io with respect to the planet, which raises the interesting possibility that this laser expansion can be attributed to the motion of Io through Jupiter's magnetic field.

The principal significance of these observations is to establish the occurrence of natural radio lasing at Jupiter. Besides also providing a second instance of true lasing in nature, this yields a better explanation for the S-bursts and their behavior, as well as a unified explanation for the discrete cyclotron emissions from two of the four radio planets at which it has thus far been observed. With possible application elsewhere, in similar natural magnetic structures at the Sun or elsewhere in the cosmos, this also provides an opportunity to study this remarkable natural laser emission phenomenon at close range and in sufficient detail to understand its properties.

Following a brief discussion of the S-bursts, the observations will be described and then used to determine the frequency dependence of the observed longitudinal mode spacings. Next, the new expanding-laser model to account for the S-bursts frequency drifts will be described, and the significance of these observations and the model discussed briefly.

S-BURSTS

From some of their earliest observations, by Kraus (1956) and Gallet (1961), the decametric radio emissions from Jupiter have been classified into two categories, depending upon their observed signal durations at a given frequency. The shortest of the Jovian radio bursts, lasting only a few milliseconds with receiver bandwidths of a few kilohertz, were designated S, for 'short'. The other longer bursts, which can last from less than a second to many seconds, were similarly designated L for 'long'. The S-bursts, which are also referred to as the 'millisecond' bursts, were subsequently found to consist of rapidly-drifting discrete spectral components (Gordon and Warwick 1967), whereas the L-bursts have been attributed to smoother emissions from Jupiter which are usually modulated by interplanetary scintillations (Douglas and Smith, 1961, 1967; Riihimaa 1977; Leblanc et al. 1980a; among others).

The widely-accepted explanation for these narrow, rapidly-drifting S-bursts is by cyclotron emission from rapidly-moving energetic electron bunches (Ellis 1965). Originally believed to originate in the Jovian magnetosphere perhaps somewhere near the position of Io, these electron bunches were at first expected to mirror in the Jovian magnetic field before they produced observable emissions, in order to account for the S-burst frequency drifts nearly always being downward. However, the predicted variation of the S-burst drift rate with

frequency did not materialize, and it has since been proposed that the energetic electrons causing the S-bursts must somehow be ejected upward from the Jovian ionosphere (Desch et al. 1978; Flagg and Desch 1979; Ellis 1980; Leblanc et al. 1980b). Except for a possible, but equally-unexplained, coherent phase modulation of these energetic electrons in the Jovian ionosphere which would develop into bunching as the electrons traveled upward (Staelin and Rosenkranz 1982; see also Ratner 1976), there has been no acceptable explanation for these electron bunches, nor any other measurements which would confirm their existence.

An important contribution of this paper is to provide an entirely new explanation for the S-burst frequency drifts which does not rely upon these always-assumed, but never confirmed, energetic electron bunches. In this connection, a similar new explanation for the S-burst frequency drifts has been proposed by Melrose (1986) which also involves feedback, but of a different sort that is comparable to that which is believed to account for VLF discrete emissions in the Earth's magnetosphere (Helliwell and Inan 1982). In this model, the feedback path is closed by particle motion rather than wave reflection and the resulting transient oscillations which could develop must move upward at approximately the electron velocity. Although possibly applicable to Jupiter, this model fails to account for the much slower AKR drifts, nor for the fact the AKR discrete spectral components sometimes reverse direction (Gurnett and Anderson 1981; Calvert 1982; Baumback and Calvert 1987). Moreover, just like the previous electron bunch hypothesis, this model still relies upon the electron velocity to account for the S-burst drifts, whereas the new laser expansion model would account for those drifts differently, by the lasers expanding at the Io flux tube velocity with respect to the planet.

OBSERVATIONS FROM TASMANIA

The S-burst observations from Tasmania were obtained with the 650-meter-square Llanherne Radio Telescope near Hobart, at 147°E, 43°S, consisting of an array of horizontal dipoles with closely-spaced reflectors for the frequency range from 2.5 to 17 MHz. Steerable only in declination, this system was used for transit observations of Jupiter from 1972 to 1977, recording for five-minute intervals as Jupiter crossed the antenna beam. During these intervals, the Jovian radio signals were converted to lower frequencies and recorded in 3 MHz segments, using an array of parallel video tape recorders. These data were subsequently spectrum analyzed with sampling bandwidths as narrow as 2 kHz, to produce numerous high-resolution radio spectrograms of the Jovian S-bursts extending down to as low as 3.2 MHz (Ellis 1982), many of which have now been published as an S-burst Atlas (Ellis 1979).

One example of these radio spectrograms is presented in Figure 1 (see Ellis 1982). This figure shows the S-burst signals as deflections of a horizontal raster in order to depict their time, frequency, and amplitude all on the same diagram. It shows a group of S-bursts with roughly equal spacings of approximately 30 kHz, drifting downward in frequency at approximately the same rate. It was this case, along with others published by Krausche et al. (1976), which first showed the regularly-spaced S-burst components which can be attributed to the adjacent longitudinal laser modes (see Calvert 1985d).

Sequences of S-bursts like those in Figure 1 were examined for periodic spacings. This was accomplished by measuring the time spacings between separate bursts at a constant frequency, and plotting them on statistical occurrence diagrams like that in Figure 2. This diagram shows the cumulative occurrence of different spacings on a logarithmic scale versus the spacing, so that a random sequence of spacings which followed Poisson statistics would produce a descending straight line. This figure, however, shows two different populations of spacings, one at the right corresponding to the random occurrence of S-burst groups, and another at the left corresponding to the periodic spacing of the S-bursts within those groups, with a period of about 5 milliseconds. Since approximately half of the spacing measurements in Figure 3 were random, the groups typically consisted of only a few members (Figure 1, for example, containing only three), and this explains why the periodic spacings are generally so hard to detect from casual examinations of the S-burst observations. On the other hand, the periodic spacings were approximately the same for the other half of the spacing measurements, and this implies that the different, randomly-occurring groups within the S-burst sequence all had approximately the same intercomponent spacings.

Another way of showing this same behavior is presented in Figure 3, which shows the statistical distribution of S-burst spacings for a different sequence of closely-spaced S-bursts at a lower frequency. Scaled from page 2 of the S-burst Atlas (Ellis 1979), this figure clearly shows the periodic spacing of the bursts as a prominent peak at about 8.3 milliseconds, having a standard deviation calculated separately for that peak, of about 1.6 msec.

Figure 3 also shows other spacings at approximate multiples of that period, near 17 and 25 milliseconds, which correspond to occasions when one or two of the intervening S-burst components happened to be missing. This behavior, moreover, did not seem to be attributable to those missing bursts having marginal amplitudes for detection, since all of the other neighboring bursts were quite strong and of seemingly similar amplitudes. In another case, up to fifteen consecutive and virtually identical bursts were found to occur in sequence (within a repetitive envelope which seemed to be dictated by other effects, like those observed by Krausche et al. (1976)), with only three of the expected equally-spaced components missing.

This peculiar behavior, in which some of the adjacent S-burst components are sometimes missing, could be explained by radio lasing, since not all of the adjacent lasers in the source would need to be active at the same time, and when such a laser is inactive, presumably by having too little gain or feedback to oscillate, it would disappear completely. Moreover, the difference which causes a laser to oscillate or not (i.e., which makes it 'lase') might be quite minor, since any loop gain which is even slightly greater than unity will cause oscillation, whereas anything even slightly less than unity would lead to oscillations which eventually die away. In this fashion, and also because of the possible quenching of one laser by its neighbors when they share the same electron free-energy reservoir, one or more of the lasers might easily be missing without much affecting those which remain.

Similar measurements of the S-burst spacings were carried out for four additional cases at frequencies of 12 to 15 MHz, selected from among the limited observations which had already been processed with the best spectral resolution. These cases consisted of the longest sequences of simple S-bursts which could be found, having similar frequency drifts and none of the irregular behavior which the S-bursts also sometimes exhibit (see Ellis 1979). They were analyzed by averaging their shortest temporal spacings, always with the same result that periodic spacings could be found, with periods of about four to seven milliseconds.

As will be discussed below in connection with Figure 7, the smaller temporal spacings tended to occur for the higher frequencies, thus filling in the trend which was already evident from Figures 1, 2, and 3, where the spacings progressively increased from about four to over eight milliseconds as the frequency decreased from about sixteen to less than ten megahertz. The spectral spacings, on the other hand, estimated from the temporal spacings and the frequency drifts, were roughly the same at the different frequencies and about thirty to fifty kilohertz (see also Krausche et al. 1976, Fig. 2). According to Equation 1, for a constant refractive index of about one-half, this would imply laser sources of roughly the same size at the different frequencies, with lengths of about six to ten kilometers.

OBSERVATIONS FROM FRANCE

The Nancay Radio Observatory in France, which is located about two hundred kilometers south of Paris, is equipped with an array of 144 conical-spiral receiving antennas for the frequencies from 10 to 120 MHz which can be phase-switched to follow Jupiter's motion across the sky. With up to 24 decibels of gain in both senses of circular polarization, this array has been providing excellent observations of the Sun and Jupiter since 1978. Normally used with a swept-frequency radio receiver for surveying the Solar and Jovian radio activity, it can also be used with a parallel array of radio receivers covering a one-megahertz segment of the spectrum in fifty twenty-kilohertz steps (Lecacheaux and Rosolen 1975). Providing simultaneous observations with adjacent nominal bandwiths of 20 kHz, this instrument was used to record the Jovian S-bursts during certain periods of 1979 and 1980, and it was these observations which were examined in the current study.

For periods when the S-bursts were being received, selected channels of the parallel receiver array were recorded and later played back, a few channels at a time, to produce pen recordings like those in Figure 4. This figure shows the logarithmic amplitude of the radio signals from Jupiter for four of the receiver channels near 22 MHz, equally-spaced and eighty kilohertz apart. The S-bursts in these records appear as brief pulses lasting from two to ten milliseconds and occurring at progressively later times on the lower frequencies. These progressive delays correspond

to the downward frequency drifts of the S-bursts, which in this case was about 15 MHz/sec and approximately typical of the S-burst drifts at the frequency of these observations (see Leblanc et al. 1980b).

First the spacings between the bursts were measured from such recordings, between the leading edges of adjacent pulses at an arbitrary but constant level for each of the S-burst sequences which were examined. These were also used to produce statistical occurrence diagrams like that in Figure 5, where the logarithmic cumulative occurrence of different spacings was plotted as a function of the spacing. Since the result in this case was approximately linear, with a slope that was correct for average occurrence rate of the bursts and Poisson statistics, it was concluded that these S-burst spacings were approximately random.

However, it was also noticed that many of the bursts seemed to have exactly the same size and shape, and that these similarly-shaped bursts were always among the narrowest that were observed and that they were almost identical from one S-burst noise storm to another. This was attributed to the individual S-bursts having bandwidths which were actually much less than that of the receiver and producing the observed pulses by drifting through the receiver's passband. On this basis, the shape of those minimum-length bursts would correspond to the receiver's selectivity curve, with its duration at different signal amplitudes being determined by the receiver bandwidth divided by the S-burst drift rate. The minimum-length bursts would then correspond to single S-bursts, and the longer bursts which are also observed, to S-bursts having more than one component.

In other words, it was concluded that the individual S-burst components, like those which were observed in Tasmania, could not be resolved by the Nancay instrument, but that they produced instead lengthened pulses whenever more than one of those components were simultaneously present. This, however, permits detecting the multiple S-burst components indirectly from the apparent S-burst durations in the Nancay records. This was accomplished by measuring the pulse durations always at the same constant fraction of their peak amplitudes, separately for each of the S-burst pulses of a sequence in order to minimize the effects of broader receiver bandwidths at larger signal amplitudes. This produced the distribution of durations shown in Figure 6. In this figure, the first peak corresponds to single S-bursts and to a bandpass-to-drift-rate ratio of approximately 2.5 milliseconds. Since the drift rate for this case was approximately 17 MHz/sec, this would correspond to an effective receiver bandwidth of about 40 kHz. Although this is somewhat larger than the quoted bandwidth of the Nancay receivers, this broader bandwidth would be consistent with their skirt bandwidths for signals which were as strong as the S-bursts usually are, of perhaps 30 decibels or more above the background noise level.

The other peaks in Figure 6, at equal intervals of about 2.2 milliseconds, would then correspond to S-bursts having progressively greater numbers of equally-spaced very narrow components, as is indicated by the labels in that figure. From these observations, integrating approximately under the separate peaks in Figure 6, it appears that about one-third of the S-bursts were single, about one-third were double, and

the remaining one-third consisted of three or more individual, equally-spaced S-burst components. From the drift rate for this case, and the 2.2 msec intercomponent spacing indicated by Figure 6, the corresponding spectral spacing between the S-burst components must have been about 37 kHz and hence approximately equal to that of the S-bursts observed in Tasmania at lower frequencies.

FREQUENCY VARIATION AND THE EXPANDING-LASER MODEL

Over a frequency range from about 10 to 26 MHz, the spectral spacings between the S-burst components were thus roughly the same and about 30 to 50 kHz, whereas the temporal spacings varied from about two to eight milliseconds. Since the S-burst drift rates, which should equal the ratio of these two spacings, are approximately proportional to the observing frequency (see Leblanc et al. 1980, Fig. 3; among others), this suggests that the temporal spacings between the S-burst components ought to vary inversely proportional to the frequency. This has been verified by plotting the observed temporal spacings as a function of the reciprocal frequency, as is shown in Figure 7. In this figure, error bars have been included for three of the cases which were examined, representing the standard deviation of the spacing measurements. Also indicated in that figure is the measurement from Nancay, at one of the highest frequencies for which data were available. The observed spacings in Figure 7 fit a straight line through the origin, confirming that the component spacings were indeed inversely proportional to the observing frequency, with the slope of that line implying a frequency-spacing product ($f \cdot \Delta t$ in the figure) of about 75,000.

This behavior can be understood if the proposed S-burst radio lasers were expanding during emission, since that would increase the wavelength for a given longitudinal oscillation mode, and thereby decrease its frequency. As a result, this would also force the lasers up to higher altitudes where the cyclotron frequency is less, since the oscillations

must still occur only quite close to the cyclotron frequency. For this to occur, of course, the laser's density mirrors would have to extend vertically, presumably in the direction of the source magnetic field (see Calvert 1982, Fig.11), and the expansion would have to occur primarily perpendicular to that direction. In other words, although an upward motion of the source is required in any even, to explain the downward S-burst drifts with emission at the cyclotron frequency, with radio lasing it can be attributed to an expansion of the source to neighboring field lines, rather than to electron bunching, and the resulting frequency drifts can be calculated as follows.

The condition which determines the frequency of a laser is

$$m \lambda = 2 W \qquad (2)$$

where

$$\lambda = c / n f \qquad (3)$$

is the wavelength inside the source, c is the speed of light, f is the frequency, n is the source wave refractive index, W is the laser length, and m is the longitudinal mode number, which should be an integer that differs by one between the adjacent S-burst components (see Calvert 1982, Eqn. 33). Provided the refractive index remains approximately constant, differentiating Equations 2 and 3 gives

$$df/dt = - (f/W)\ dW/dt \qquad (4)$$

for the frequency drift of an expanding radio laser. Since this is also

the ratio of the spectral and temporal spacings, $\Delta f/\Delta t$, with the former given by Equation 1:

$$\Delta t = c / (2 n f dW/dt) \qquad (5)$$

which shows that the temporal spacings between the adjacent modes should vary inversely proportional to the observing frequency, so long as n and dW/dt remain constant.

Depending upon the source wave refractive index, Equation 5 may also be used to determine the apparent laser expansion rate from the $f \cdot \Delta t$ product:

$$dW/dt = c / (2 n [f \cdot \Delta t]) \qquad (6)$$

For the $f \cdot \Delta t$ product from Figure 6, and an arbitrarily-assumed source refractive index of one-half, this expansion rate would be about four kilometers per second.

As is shown by Figure 8, Io revolves around Jupiter with an angular velocity of about 8.5 degrees/hour, whereas Jupiter itself rotates with an angular velocity of 36.3 deg/hr. This means that Io moves in the reverse direction with respect to Jupiter at an angular velocity of about 27.8 deg/hr. The corresponding velocity at the S-burst sources near Jupiter, which presumably occur at a Jovian latitude of about 65 degrees (for an L = 6 dipole field line), and at a Jovian longitude which is determined by Io and which follows Io around the planet, would thus be about four kilometers per second, and hence approximately equal to the apparent expansion velocity of the S-burst radio lasers.

It is therefore suggested that the relative motion of Io with respect to Jupiter might cause the laser expansion, and hence that it might be this motion which accounts for the S-burst's downward frequency drifts. Although the exact mechanism is not known, since it is still not certain how Io controls the DAM emissions, this might be pictured as the Io flux tube progressively laying down the S-burst laser sources as it moves across the planet, much as a moving dump truck lays down paving material when a road is being constructed. For instance, energetic particles, or else energy from Io in the form of Alfven waves or an electron current, might follow the magnetic field down to the planet and sporadically alter the plasma density where the S-bursts are produced, thereby creating one of the laser mirrors when the density change first occurs and another moving mirror for as long as the influence lasts. In this fashion, the Io flux tube (or its equivalent) would be capable of creating radio lasers which are always expanding and never contracting, just as the pile of paving material behind a moving dump truck always gets longer and never shorter. The significance of this analogy is that it would immediately account for the S-burst's frequency drifts always being downward.

The actual Io flux tube velocity should of course vary in a systematic way with the Jovian longitude, because of non-dipole distortions of the Jovian magnetic field, and this variation should be sought in future studies of the S-burst's temporal spacings in order to test the expanding-laser concept and perhaps also shed new light on the S-burst's actual source location and emission mechanism.

DISCUSSION

From the S-burst observations discussed above, it has been found that individual S-bursts, with intrinsic bandwidths which were still too small to be resolved even with the best available spectral resolution, tended to occur in groups with regular spacings of roughly 30 to 50 kHz (see also Krausche et al. 1976). Measured for a number of different S-burst events, the temporal spacings within these groups were found to decrease inversely proportional to the observing frequency, which for a constant spectral spacing is equivalent to the previous observation that the S-burst drift rates increase approximately proportional to the frequency (see Leblanc et al. 1980).

This is considered excellent evidence for the production of S-bursts by natural radio lasing, since it is hard to imagine any other source mechanism which could produce such remarkably regular spacings. On this basis, the very narrow spectral bandwidths of the individual bursts could then be attributed to the inherent monochromaticity of a laser, whereas the equal spacings within the S-burst groups could be attributed to the different longitudinal laser modes having a differing integral number of wavelengths around the wave feedback path (see Calvert 1982, Fig. 11). Moreover, the downward frequency drifts of the S-bursts can also be accommodated in this model, by laser expansion during emission at a uniform rate which is comparable to the projected surface velocity of Io flux tube with respect to the planet.

The roughly constant spectral spacing of the longitudinal laser modes, according to Equation 1, would imply source sizes of about eight kilometers which are approximately independent of the frequency. This dimension is presumably dictated by the optimum size that is required for lasing, which cannot be too small for the want of sufficient gain, nor too large because of increased diffraction losses. The corresponding transverse diameter of the lasing volume, according to straightforward laser theory (see Verdeyen 1981; or Calvert 1987, Eqn. 1) for a fundamental-mode laser and a source wavelength of 30 meters (i.e., at frequency of 20 MHz for n = 0.5), would be about 400 meters. The emission beamwidth, which is inversely proportional to the square root of laser length measured in wavelengths, would be about three degrees (ibid, Eqn. 2). The S-burst laser sources might thus appear as depicted in Figure 9.

Although it is difficult to estimate the absolute S-burst signal strengths from the measurements which are usually taken, one might assume approximately ten megawatts per steradian, since that would have produced an easily-detectable signal of a few microvolts per meter with the Nancay decametric array. Without allowing for the possible focusing by wave refraction as the waves escape, this would imply a total beam power of about thirty kilowatts for one of the S-burst radio lasers producing an individual S-burst component. Since the power associated with the Io flux tube, either in the form of an Alfven wave or an induced electrical current flowing along the magnetic field, might be as large as 10^{12} watts (see Acuna et al. 1983, p. 17), spread out over a magnetically-projected area which might be as small as only ten thousand square kilometers near the surface of Jupiter where the S-bursts are produced, the power which is

available for driving the lasers, each with a projected area of about three square kilometers perpendicular to the source magnetic field, might be as large as 300 megawatts. There should therefore be sufficient energy to power the proposed S-burst radio lasers, even if their overall conversion efficiency were as low as only 0.01 percent.

CONCLUSIONS

Regularly-spaced longitudinal laser modes, comparable to those which had previously been detected in the spectra of the AKR at the Earth (Calvert 1982), have now been identified in the spectra of the Jovian radio S-bursts observed in France and Tasmania. Observed as a statistically-distinct population of temporal S-burst spacings in the high-resolution radio spectrograms from Tasmania, these laser modes were not resolved by the instrument in France, although they were still detectable indirectly as quantized values for the apparent S-burst signal durations. As with the AKR at the Earth, these longitudinal laser modes are considered excellent evidence that the Jovian radio S-bursts must originate by natural radio lasing.

As a function of the observing frequency, the spectral spacing of these modes was found to be roughly constant and about thirty to fifty kilohertz. This would imply a laser length of about eight kilometers for the individual radio lasers producing the S-bursts (for an assumed source refractive index of 0.5), and that in turn would imply a source width of roughly 400 meters for the lasing volume at 20 MHz, and a beamwidth and power, uncorrected for the focusing which should occur as the waves escape, of three degrees and thirty kilowatts, respectively.

The temporal spacings, however, varied inversely with the observing frequency, from about 2.2 milliseconds at 26 MHz to 8.3 milliseconds at 9.7 MHz. This implies that the radio lasers were expanding uniformly at

the approximate surface velocity of the Io flux tube with respect to the planet, and this would account for the well-known downward frequency drifts of the S-bursts without the previously-assumed energetic electron bunches.

Acknowledgments. This research was conducted in part under the Jupiter and Uranus Data Analysis Programs of the National Aeronautics and Space Administration, supported by NASA grants NAGW-256, NAGW-1206, and NGL-16-001-043. The effort in France was also supported by the Observatoire de Paris and that in Tasmania by the University of Tasmania and the Australian Research Grants Committee.

REFERENCES

Acuña, M. H., K. W. Behannon, and J. E. P. Connerney, 1983, Physics of the Jovian Magnetosphere, ed. A. J. Dessler (Cambridge: Cambridge Univ. Press), p. 1.

Baumback, M. M., D. A. Gurnett, W. Calvert, and S. D. Shawhan, 1986, Geophys. Res. Lett., 13, 1105.

Baumback, M. M., and W. Calvert, 1987, Geophys. Res. Lett., 14, 119.

Benson, R. F., and W. Calvert, 1979, Geophys. Res. Lett., 6, 479.

Calvert, W., 1981a, J. Geophys. Res., 86, 76.

Calvert, W., 1981b, Geophys. Res. Lett., 86, 1091.

Calvert, W., 1982, J. Geophys. Res., 87, 8199.

Calvert, W., 1983, J. Geophys. Res., 88, 6165.

Calvert, W., 1985a, Geophys. Res. Lett., 12, 179.

Calvert, W., 1985b, Geophys. Res. Lett., 12, 377.

Calvert, W., 1985c, Geophys. Res. Lett., 12, 381.

Calvert, W., 1985d, EOS Trans. AGU, 66, 1048.

Calvert, W., 1987, J. Geophys. Res. 92, 8792.

Carr, T. D., M. D. Desch, and J. K. Alexander, 1983, in Physics of the Jovian Magnetosphere, ed. A. J. Dessler (Cambridge: Cambridge Univ. Press), p. 226.

Desch, M. D., R. S. Flagg, and J. Mag, 1978, Nature, 272, 38.

Douglas, J. N., and H. J. Smith, 1961, Nature, 192, 741.

Douglas, J. N., and H. J. Smith, 1967, Astrophys. J., 148, 885.

Ellis, G. R. A., 1962, Aust. J. Phys., 13, 344.

Ellis, G. R. A., 1964, Aust. J. Phys., 17, 63.

Ellis, G. R. A., 1965, Radio Science, 69D, 1513.

Ellis, G. R. A., 1979, An Atlas of Selected Spectra of the Jupiter S-bursts (report) (Hobart, Tas., Aust.: University of Tasmania).

Ellis, G. R. A., 1980, Nature, 283, 48.

Ellis, G. R. A., 1982, Aust. J. Phys., 35, 165.

Flagg, R. S., 1976, Icarus, 29, 477.

Flagg, R. S., and M. D. Desch, 1979, J. Geophys. Res., 84, 4238.

Gallet, R. M., 1961, Ch. 14 of Planets and Satellites, eds. G. P. Kuiper and B. M. Middlehurst (Chicago: Univ. Chicago Press), p. 500.

Gordon, M. A., and J. W. Warwick, 1967, Astrophys. J., 148, 511.

Gurnett, D. A., and R. R. Anderson, 1981, in Physics of Auroral Arc Formation, Vol. 25, eds. S.-I. Akasofu and J. R. Kan (Washington, DC: Amer. Geophys. Union, Geophys. Monogr. Ser.), 161.

Helliwell, R. A., and U. S. Inan, 1982, J. Geophys. Res., 87, 3537.

Huff, R. L., W. Calvert, J. D. Craven, L. A. Frank, and D. A. Gurnett, 1987, J. Geophys. Res., Submitted.

Kraus, J. D., 1956, Astrophys. J., 61, 182.

Krausche, D. S., R. S. Flagg, G. B. Lebo, and A. G. Smith, 1976, Icarus, 29, 463.

Leblanc, Y., F. Genova, and J. de la Noe, 1980a, Astron. Astrophys., 86, 362.

Leblanc, Y., M. G. Aubier, C. Rosolen, F. Genova, and J. de la Noe, 1980b, Astron. Astrophys., 86, 349.

Lecacheaux, A., and C. Rosolen, 1975, Astron. Astrophys., 41, 223.

Le Queau, D., R. Pellat, and A. Roux, 1985, Annales Geophysicae, 3, 273.

Mellott, M. M., W. Calvert, R. L. Huff, D. A. Gurnett, and S. D. Shawhan, 1984, Geophys. Res. Lett., 11, 1188.

Melrose, D. B., 1976, Astrophys. J., 207, 651.

Melrose, D. B., 1986, J. Geophys. Res., 91, 7970.

Melrose, D. B., K. G. Ronnmark, and R. G. Hewitt, 1982, J. Geophys. Res., 87, 5140.

Ratner, M. J., 1976, Astrophys. J., 209, 945.

Riijimaa, J. J., 1977, Astrophys. and Space Sci., 51, 363.

Shawhan, S. D., and D. A. Gurnett, 1982, Geophys. Res. Lett., 9, 913.

Staelin, D. H., and P. W. Rosenkranz, 1982, J. Geophys. Res., 87, 10,401.

Verdeyen, J. T., 1981, Laser Electronics, (Englewood Cliffs, New Jersey: Prentice-Hall).

Wu, C. S., and L. C. Lee, 1979, Astrophys. J., 230, 621.

Zarka, P., D. Le Queau, and F. Genova, 1986, J. Geophys. Res., 91, 13,542.

CAPTIONS

Fig. 1. A high-resolution spectrogram of the Jovian radio S-bursts showing multiple discrete components which can be attributed to the longitudinal oscillation modes of natural radio lasers (observed near Hobart, Tasmania, see Ellis (1982), Fig. 2). The roughly-equal thirty-kilohertz spectral spacings between the S-burst components in this case, according to Equation 1, would imply lasers with a length of about ten kilometers, whereas their temporal spacings of about four milliseconds, according to Equation 6, would imply that those radio lasers were expanding at a rate of approximately five kilometers per second.

Fig. 2. The logarithmic cumulative occurrence of S-burst spacings for a sequence of S-bursts observed in Tasmania at 14.5 MHz on 14 August 1975, showing the separate populations of spacings which are attributed to the longitudinal laser modes and to the random occurrence of S-burst groups.

Fig. 3. S-burst spacings measured from the spectrogram on page 2 of the S-burst Atlas (Ellis 1979), showing periodic spacings of 8.3 ± 1.6 milliseconds, plus other spacings which were multiples of that amount. These spacings are attributed to the longitudinal modes of radio lasers, with the multiple spacings corresponding to occasions when some of the intermediate lasers were inoperative, presumably for the lack of sufficient wave gain or feedback.

Fig. 4. S-bursts observed at Nancay, France, by the Paris Observatory at four fixed frequencies near 22 MHz, shown with logarithmic amplitude scales as a function of the time, and with the time scale indicated by the timing waveform at the bottom. The progressive delays at the lower frequencies represent the rapid downward frequency drifts of these bursts, with that of the single narrow burst near the center of the figure indicating a drift rate of about 14.9 MHz/sec. The duration of such bursts is attributed to the finite receiver bandwidth, and the sometimes longer durations which are also observed, to the occurrence of multiple discrete components which could not be resolved by the Nancay receivers.

Fig. 5. The cumulative percentage occurrence of S-burst spacings measured from Nancay observations like those in Figure 4, showing a linear variation which is consistent with Poisson statistics and hence with the random occurrence of S-bursts groups.

Fig. 6. Apparent durations of S-bursts measured from Nancay observations like those in Figure 4, showing the quantized durations which indicate unresolved discrete spectral components with equal spacings of about 2.2 milliseconds.

Fig. 7. Variation of the S-burst temporal mode spacings between about 10 and 26 MHz, measured from Figures 1, 2, 3, and 6 and four other cases, shown with an inverted frequency scale to emphasize its reciprocal dependence on the observing frequency. The slope of the straight line

drawn through the measured points and the origin indicates a frequency-spacing product of $f \cdot \Delta t = 75{,}000$, which according to Equation 6, implies a uniform laser expansion velocity of about four kilometers per second.

Fig. 8. The geometry of Jupiter's moon Io with respect to Jupiter, showing its magnetically-projected relative surface velocity near where the S-burst presumably originate of about 5.3 - 1.3 = 4 kilometers per second. Since this approximately equals the apparent expansion velocity of the propsed S-burst radio lasers, it is suggested that this motion accounts for the laser expansion, and hence also for the S-burst's downward frequency drifts.

Fig. 9. An idealized illustration of the proposed S-burst radio lasers, showing the approximate dimensions of their oscillating wave fields and their emitted beams at 20 MHz, for a source refractive index of 0.5 (not to scale, see Calvert 1987, Fig. 1). The density mirrors presumably result from abrupt changes of the source plasma density, and the wave growth which drives the laser oscillations from the doppler-shifted cyclotron resonance instability, both of these being optimum for extraordinary-mode waves near the electron cyclotron frequency in low-density energized plasmas.

W. Calvert, Department of Physics and Astronomy, 612 Van Allen Hall, The University of Iowa, Iowa City, Iowa 52242, USA

G. R. A. Ellis, Department of Physics, University of Tasmania, GPO Box 252C, Hobart, Tasmania, 7001, Australia

Y. Leblanc, Section d'Astrophysique, Observatoire de Paris, 5 Place Jules Janssen, 92195 Meudon Principal Cedex, France

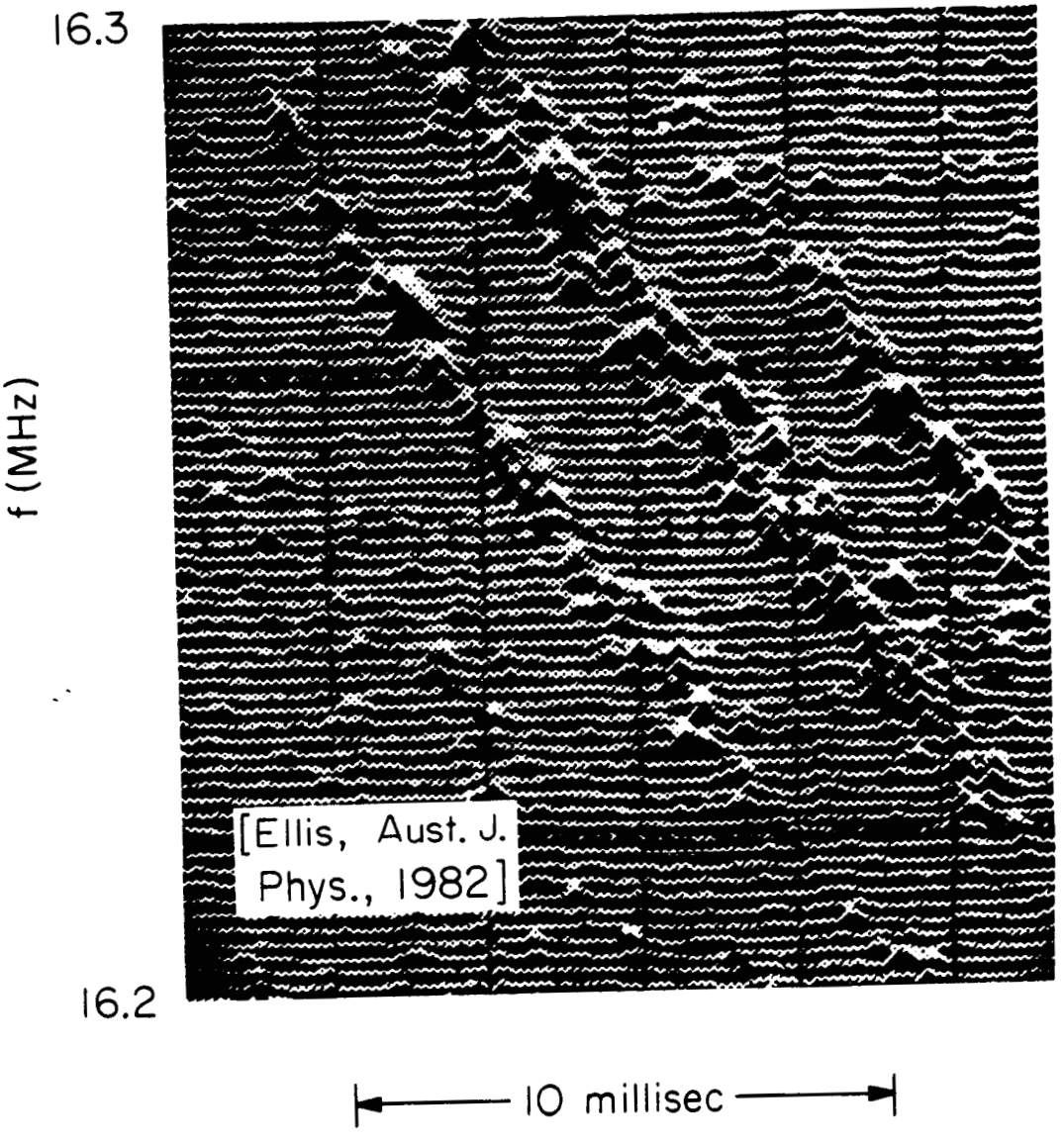

Figure 1

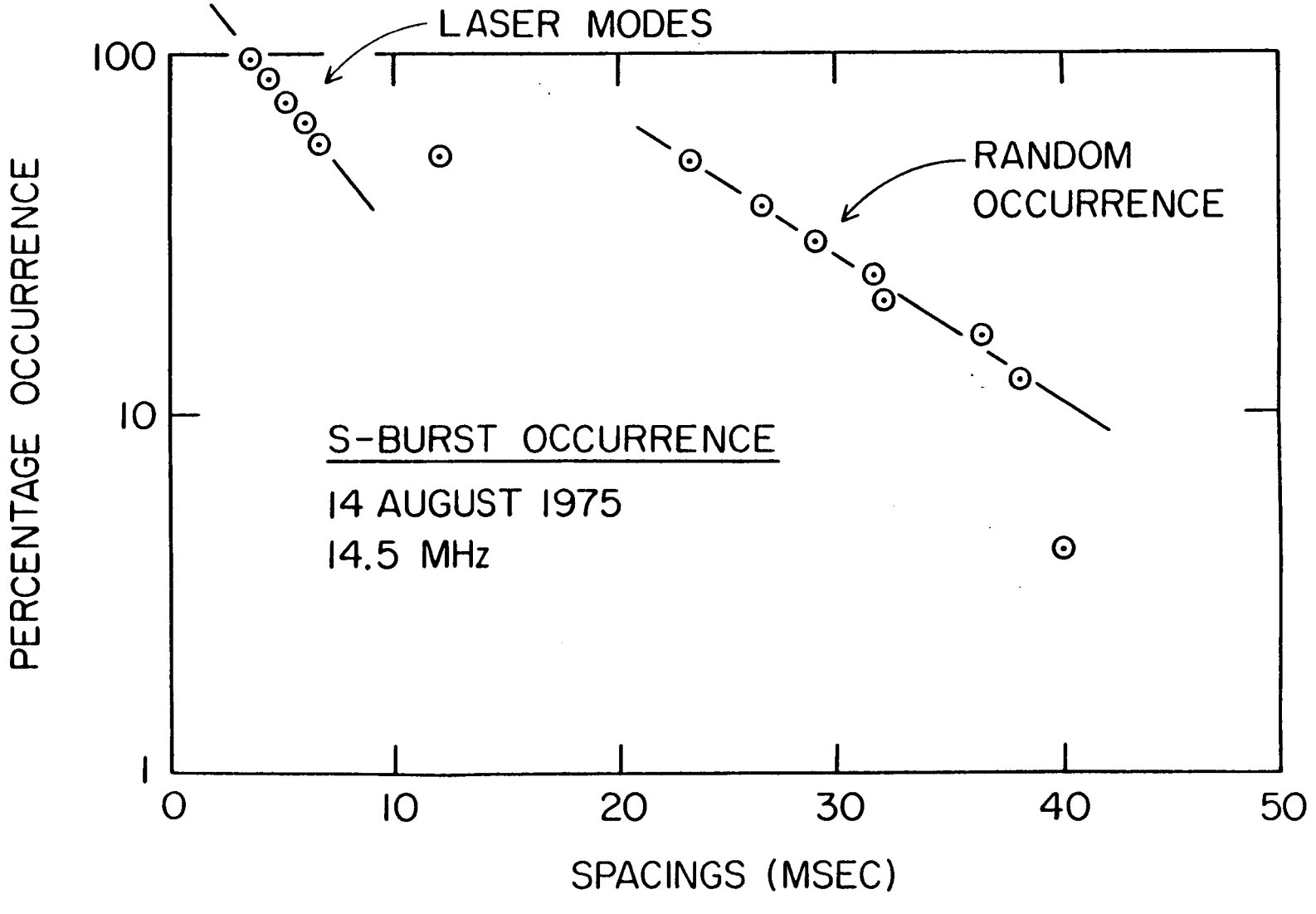
LASER MODES
RANDOM
OCCURRENCE
S-BURST OCCURRENCE
14 AUGUST 1975
14.5 MHz
PERCENTAGE OCCURRENCE
100
10
1
0
10
20
30
40
50
SPACINGS (MSEC)

Figure 2

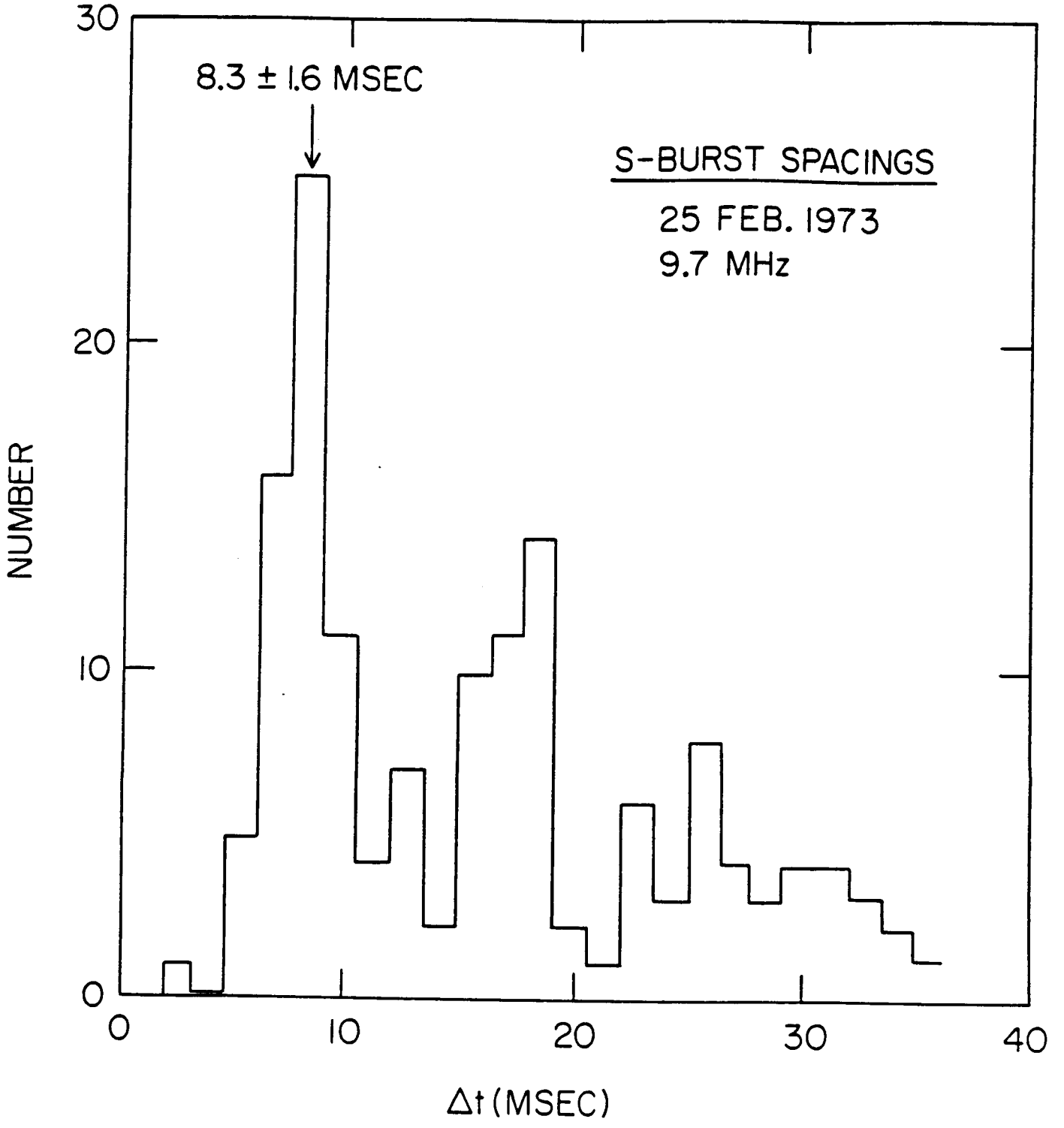
30
20
10
0
8.3 ± 1.6 MSEC
S-BURST SPACINGS
25 FEB. 1973
9.7 MHz
NUMBER
0
10
20
30
40
Δt (MSEC)

Figure 3

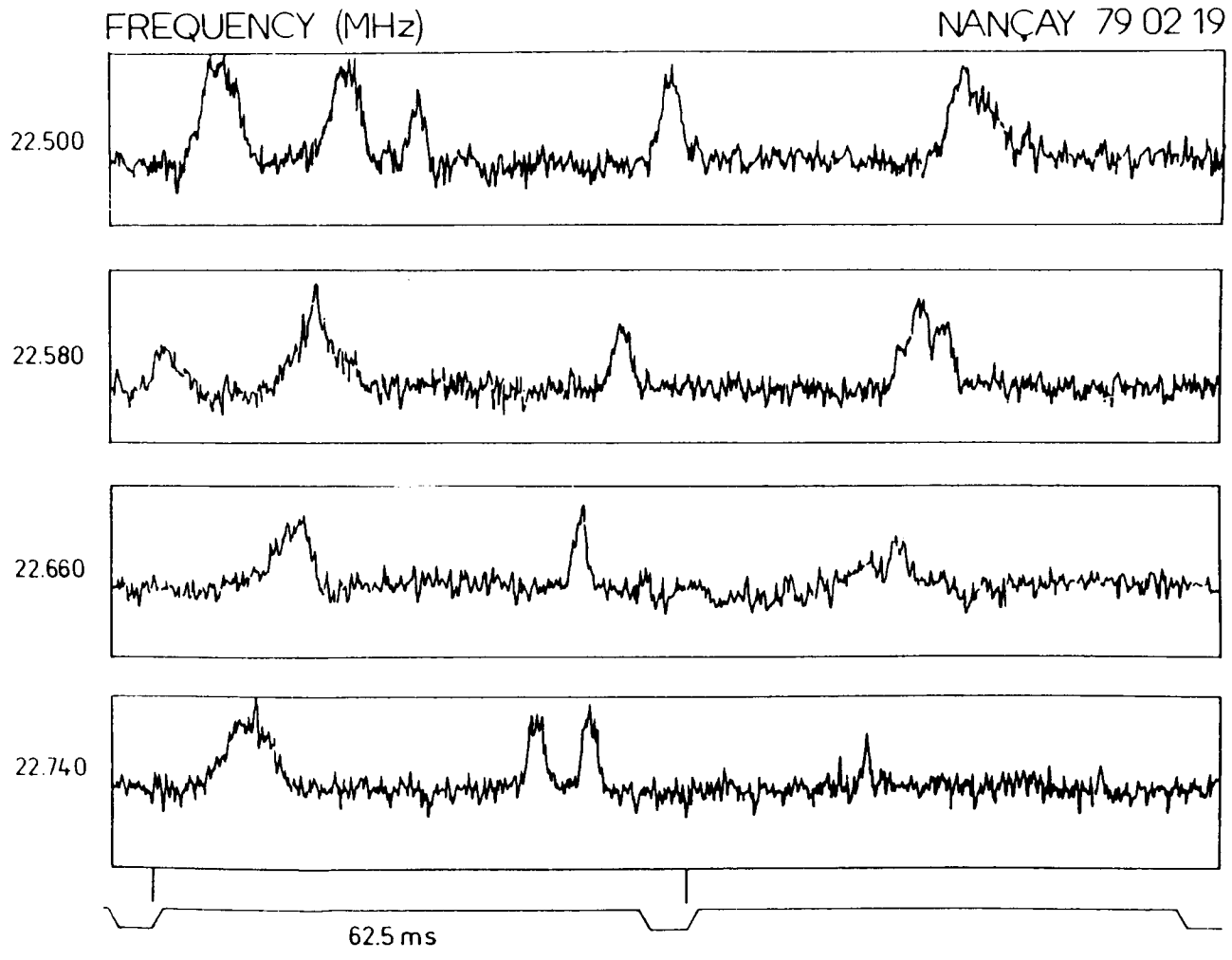

Figure 4

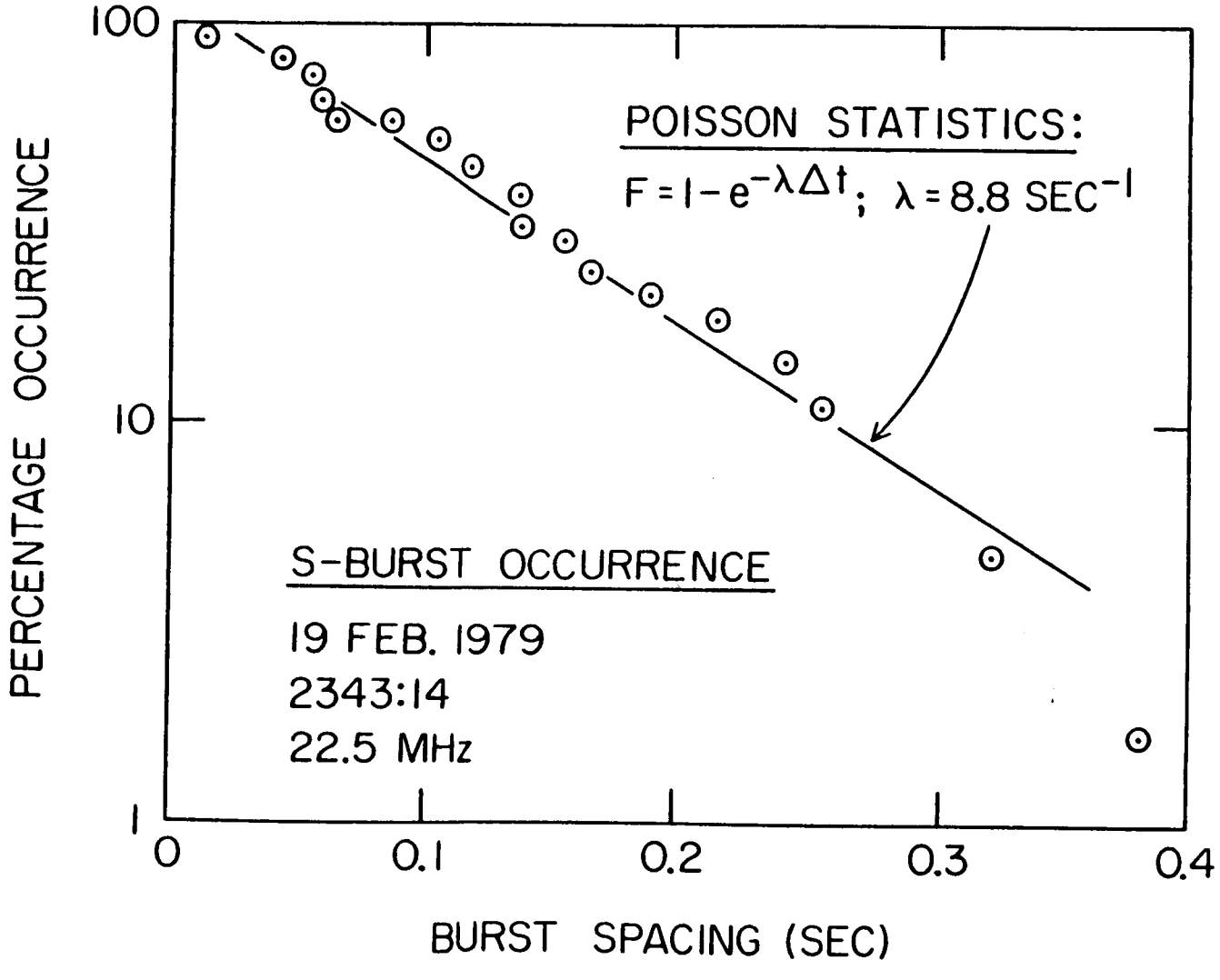
100
10
1
PERCENTAGE OCCURRENCE
POISSON STATISTICS:
$F = 1 - e^{-\lambda \Delta t}$; $\lambda = 8.8\ SEC^{-1}$
S-BURST OCCURRENCE
19 FEB. 1979
2343:14
22.5 MHz
0
0.1
0.2
0.3
0.4
BURST SPACING (SEC)

Figure 5

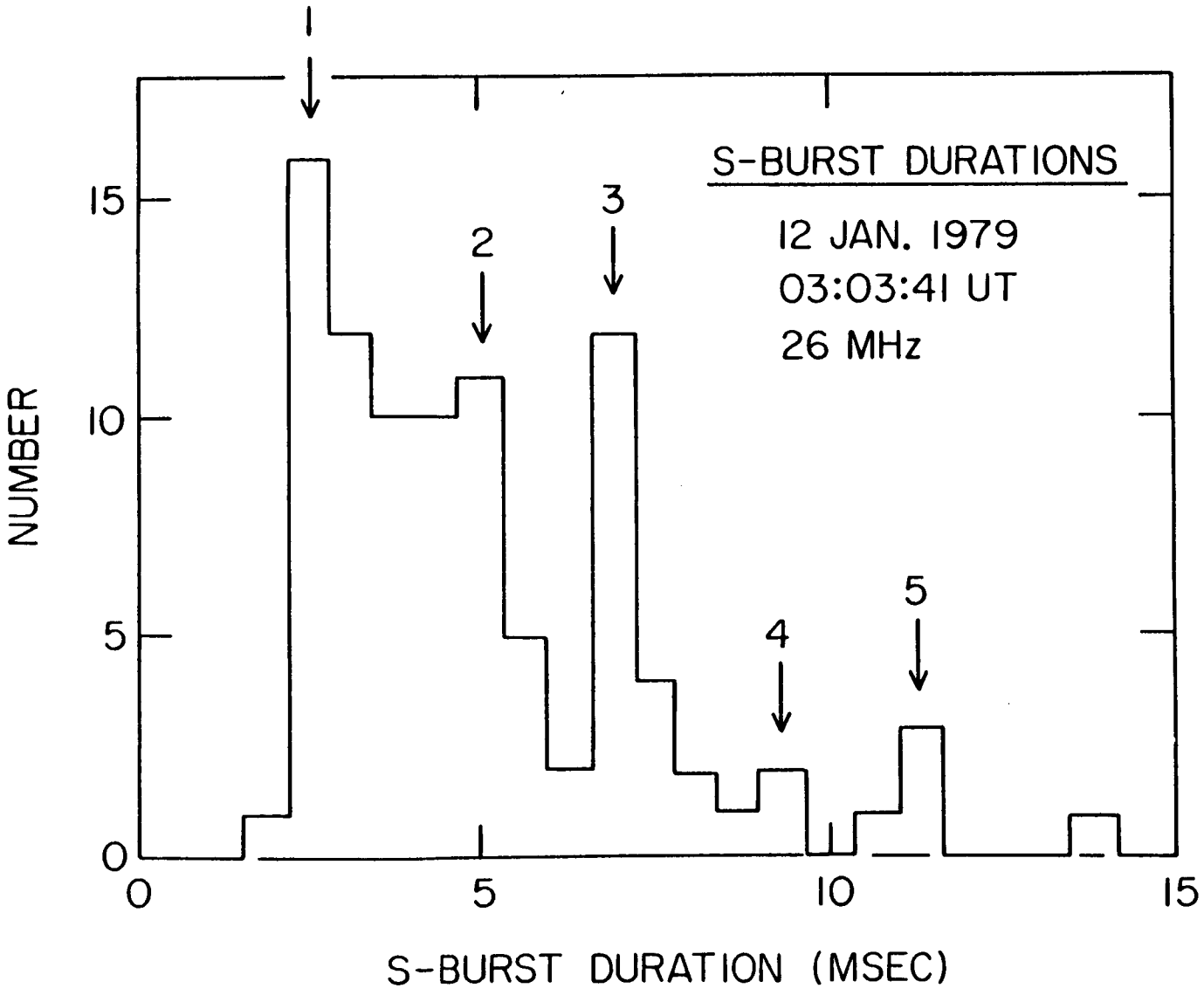
S-BURST DURATIONS
12 JAN. 1979
03:03:41 UT
26 MHz
1
2
3
4
5
NUMBER
0
5
10
15
0
5
10
15
S-BURST DURATION (MSEC)

Figure 6

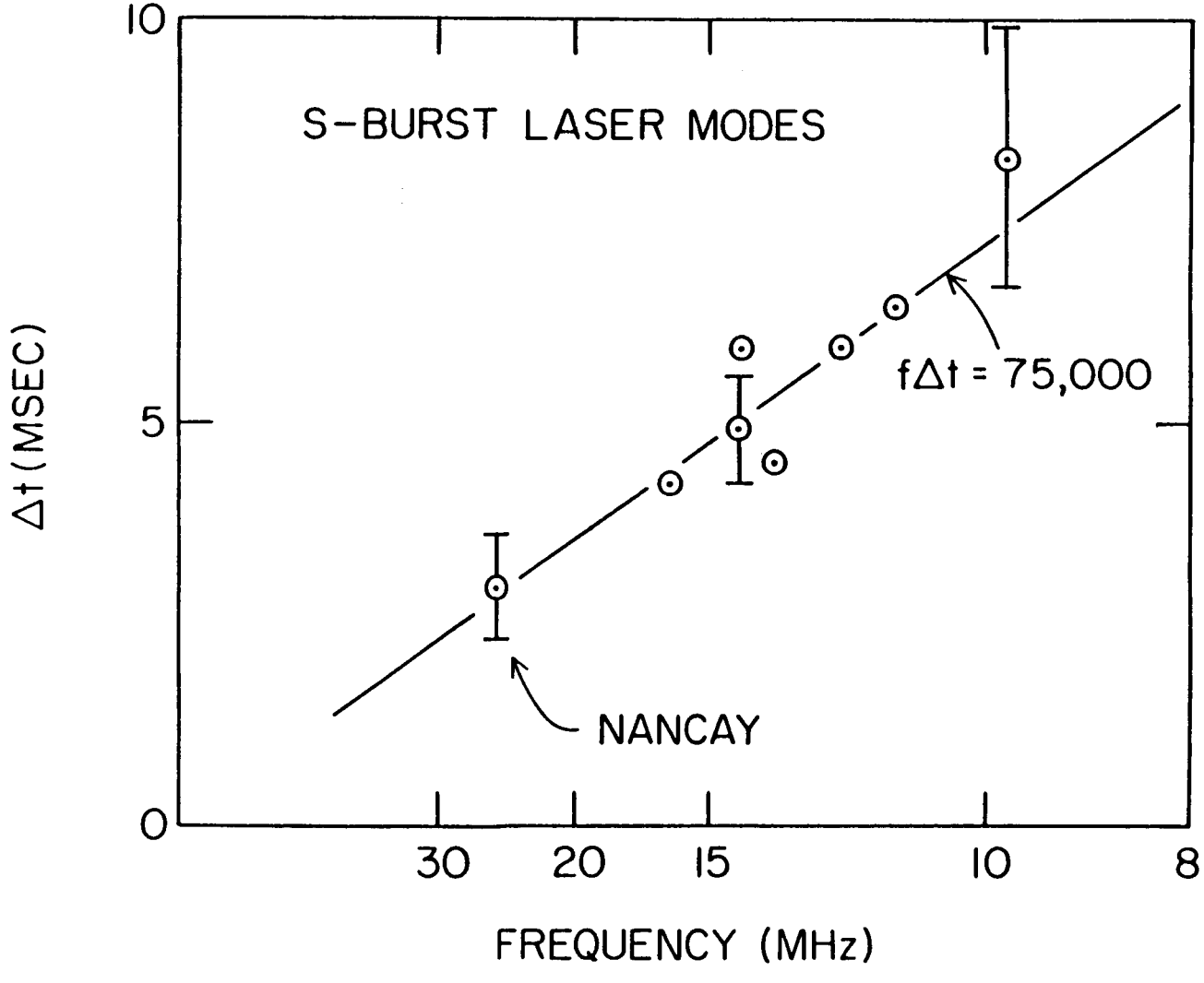
S-BURST LASER MODES
fΔt = 75,000
NANCAY
Δt (MSEC)
10
5
0
30
20
15
10
8
FREQUENCY (MHz)

Figure 7

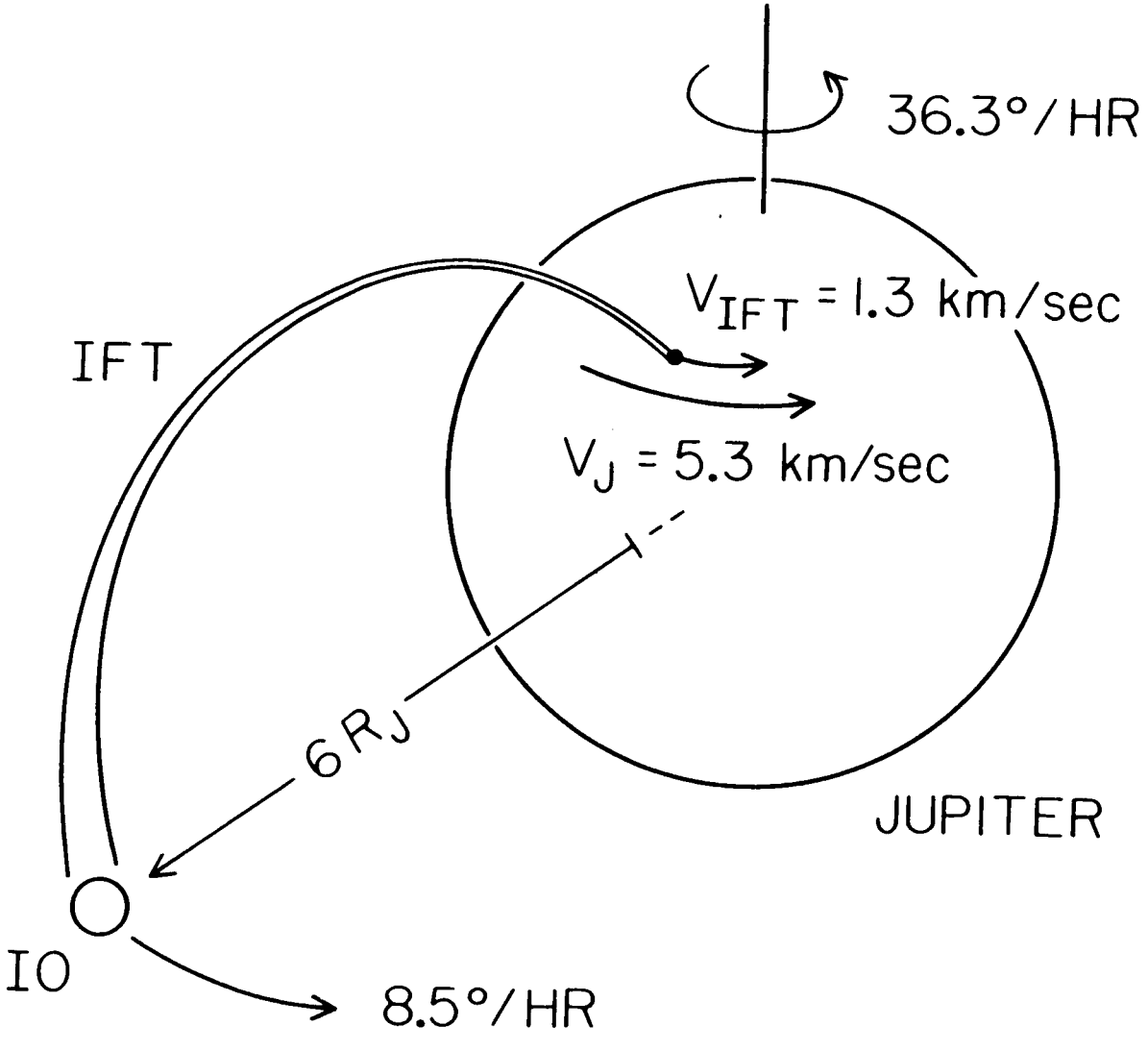

Figure 8

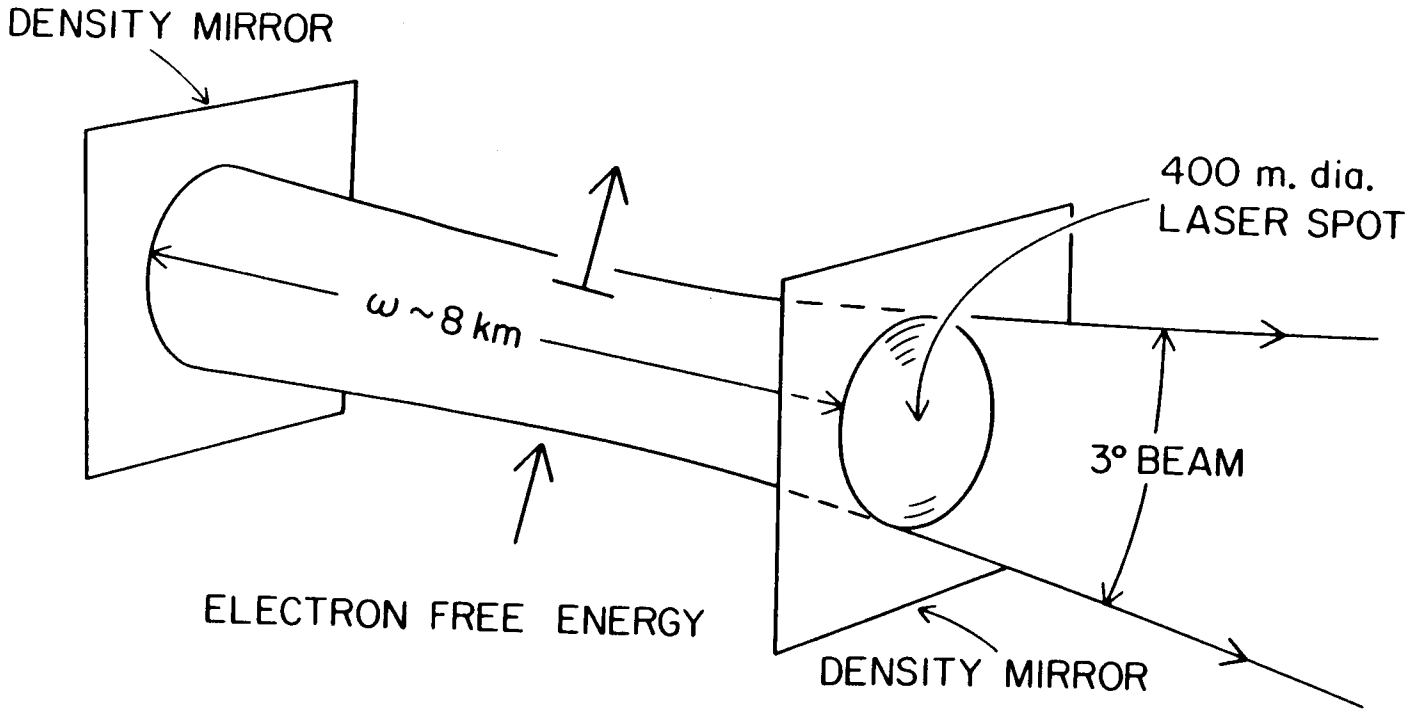
DENSITY MIRROR
400 m. dia.
LASER SPOT
ω ~ 8 km
3° BEAM
ELECTRON FREE ENERGY
DENSITY MIRROR

Figure 9

PLANETARY RADIO LASING

by

W. Calvert

The University of Iowa
Iowa City, Iowa 52242 USA

Abstract. Both the Earth's auroral kilometric radiation (AKR) and Jupiter's decametric radio S-bursts are attributed to natural radio lasing. Presumably consisting of self-excited, closed-loop wave feedback oscillations between local irregularities of the source plasma density, this radio lasing is comparable to that which occurs in man-made optical lasers, although at radio, rather than optical wavelengths. As a result, it should produce a multiple discrete emission spectrum and intense, coherent beams. Recent observations of the AKR's discreteness and coherence have clearly ruled out the previous open-loop amplifier model for such emissions, and recent observations of the jovian S-bursts have shown the expected, regularly-spaced, longitudinal laser modes. These new observations thus confirm the proposed planetary cyclotron radio lasing at both planets.

INTRODUCTION

Intense, nonthermal radio emissions from Jupiter at decametric wavelengths were discoverd by Burke and Franklin in 1955 [Burke and Franklin, 1955; Carr et al., 1983]. Since then, with numerous earth satellites and the Voyager missions to the outer planets, similar nonthermal radio emissions have also been found to originate from the Earth, where they are called the auroral kilometric radiation (AKR), as well as also from Saturn and from Uranus [Benediktov et al., 1965; Dunckel et al., 1970; Gurnett 1974; Kaiser et al., 1980; Warwick et al., 1986]. It thus seems that such emissions are a common feature of planetary magnetospheres, and the challenge, for more than thirty years, has been to explain their origin and behavior.

Although other mechanisms have been proposed [e.g., Oya and Morioka, 1983], these emissions are now most widely attributed to the electron-cyclotron wave instability of Carr [Smith and Carr, 1964], Ellis [1962, 1964, 1965], Melrose [1976], Wu and Lee [1979], Grabbe [1981, 1982], Melrose et al. [1982] Dusenbery and Lyons [1982], Hewitt et al. [1982], and Le Queau et al. [1985], Zarka et al. [1986], among others. This instability is also known as the doppler-shifted cyclotron resonance instability because of the doppler shift which is needed, in the electron's moving frame of reference, to produce cyclotron resonance between gyrating energetic electons and the waves. It occurs primarily for the right-hand-polarized extraordinary wave mode, quite near the electron cyclotron frequency and at large angles to the source magnetic field, in low-density, magnetized plasmas having suitable free energy in their electron velocity distributions.

The basic predictions of this instability are now quite well verified, since the emissions clearly originate from near the cyclotron frequency and primarily in the extraordinary wave mode [Kaiser et al., 1978; Benson and Calvert, 1979; Calvert,

1981, 1983, 1985; Shawhan and Gurnett, 1982; Bahnsen et al., 1987]. This is further demonstrated by Figure 1, which shows the results of a new radio direction-finding technique based upon the phase change which occurs as DE-1's rotating electric dipole antenna sweeps past the direction of the source [Calvert, 1985; Huff et al., 1987]. In this figure, the top panel is a DE-1 radio spectrogram showing the AKR at its highest frequencies, well above the local cyclotron frequency (fce) at the satellite. Immediately below that panel are the simultaneous polarization sense measurements indicating a right-handed polarization with respect to the source magnetic field. From these same observations, at a constant frequency of 218 kHz, the wave source directions were calculated and these directions were projected down to the altitude for cyclotron resonance and thence along the magnetic field down to the altitudes for generation of the aurora. The resulting source field lines were then overlaid upon images of the aurora, also produced with DE-1, as is shown in the bottom six panels of the figure. The excellent agreement which this produces with the brightest features of the aurora, in this case with a bright arc at the expanding poleward edge of the aurora during a substorm, clearly confirms both production at the local cyclotron frequency and the very close association of the AKR with the aurora [Gurnett, 1974; Voots et al., 1977].

Although such observations clearly confirm the basic cyclotron emission process, other measurements of the emitted wave spectra are in serious disagreement, since they tend to show discrete spectral components rather than the smooth emissions which would be expected for the cyclotron instability operating at different altitudes in the planetary auroral zones, and hence over a continuous range of cyclotron frequencies [Gurnett and Anderson, 1981; Baumback and Calvert, 1987; Ellis, 1982]. Moreover, they also cannot readily account for the multiple discrete emission components which are frequently observed [Krausche et

al., 1976; Calvert 1982; Calvert et al., 1987], nor can such open-loop amplification of the presumably incoherent incoming cosmic radio noise produce the recently-observed phase coherence of the AKR in different directions [Baumback et al., 1986].

Instead, such aspects require what I have called 'radio lasing', which consists of the same wave instability operating between local, reflecting irregularities of the source plasma density to produce self-excited, closed-loop wave feedback oscillations [Calvert, 1982]. Functionally identical to the oscillations which occur in man-made optical lasers, this radio lasing would immediately produce the required discreteness, multiplicity, and coherence. Moreover, this lasing constitutes a quite significant modification of the previous open-loop amplifier concept, since it forces saturation upon the amplifier, thereby increasing both its intensity and its efficiency, as well as also necessarily altering the energetic electron velocity distributions and possibly causing the aurora [Calvert, 1987].

The purpose of this paper is to review these recent observations which require radio lasing and to clarify how the lasing produces such properties.

MONOCHROMATICITY

One of the most difficult aspects to explain by open-loop amplification acting alone is the observed spectral discreteness, or monochromaticity, of the emitted wave signals. For the AKR at the Earth, the emission spectra are invariably discrete [Gurnett and Anderson, 1981], except for rare instances when they are modulated by ion oscillations [R. R. Anderson, private communication, see also Grabbe, 1982]. The decametric emissions from Jupiter, on the other hand, are sometimes discrete, with durations of only a few milliseconds at a single frequency and consequently designated the 'S-bursts', with 'S' for 'short'; whereas at other times they are smoother, modulated instead by longer-period interplanetary scintillations, and known as the 'L-bursts', with 'L' for 'long' [Gallet, 1961].

As stated previously [Calvert, 1982] and discussed further below, laser emissions must always be discrete because of the unavoidable spectral quenching of adjacent frequencies. On this basis, each of the discrete spectral components of the AKR or the S-bursts can be attributed to an individual active laser at the source. The jovian L-bursts, on the other hand, might be attributed either to laser emissions which are too numerous to be resolved, or else to the corresponding open-loop amplification acting alone.

The previous, and currently the most widely accepted explanation for the observed discreteness, is by cyclotron emission from vertically-confined sources. For Jupiter, this confinement is generally attributed to localized electron bunches ejected upward from the jovian ionosphere [Ellis, 1965; Desch et al., 1978; Staelin and Rosenkranz, 1982]. Another possibility, which assumes a variant of the proposed radio lasing to produce its discreteness, is for transient feedback to occur by the phase bunching of energetic electrons and the subsequent reemission

of waves for further amplification, like presumably occurs also for triggered whistler-mode emissions in the Earth's magnetosphere [Melrose, 1986; Helliwell and Inan, 1982].

Both of these would require a vertical motion of the source, at the pertinent energetic electron velocity, and this was considered to account for the ubiquitous downward spectral drifts of the S-bursts [Gordon and Warwick, 1967; Ellis, 1965, 1979, 1982; Leblanc et al., 1980]. For the AKR at the Earth, however, this explanation does not work, since the observed drifts are always very much slower, and they occasionally also reverse direction, which should be impossible for either of the electron bunch or transient feedback proposals. Instead, Gurnett and Anderson [1981] have suggested that the AKR spectral drifts might be attributed to some other disturbance of unknown origin, traveling primarily downward at the ion-acoustic velocity. Again, this proposal does not account for the observed drift reversals. Lasing, on the other hand, can account for both the drifts and their reversals, by changes or not of the effective laser length, as will be discussed further below.

A new observation by Baumback and myself [1987] addressed directly this problem of source monochromaticity. In this study, we examined the most narrow spectral bandwiths which we could find in the ISEE-1 and ISEE-2 "wideband" radio observations of the AKR. As shown in Figure 2, this bandwidth can sometimes be as narrow as only five Hertz. Although the more-typical AKR bandwidths of about one kilohertz might be accounted for by source localization (requiring a vertical source thickness of about 15 km in a dipole magnetic field), a bandwidth of only five Hertz cannot, since that would require a thickness of only eighty meters, which is substantially less than even the one-kilometer emitted wavelength. Moreover, even if the cyclotron instability could be so limited in altitude, this would give an estimated pathlength through the source, from the Sagitta formula for the chord of an arc, considering wave refraction, of

only about one kilometer, which is far too short to account for the observed AKR amplitudes.

A similar argument can also be applied to the S-burst observations of the finest spectral resolution, like those of Ellis [1982] shown in Figure 3. Such observations frequently show bandwidths of less than five kilohertz at 16 MHz, with often little or no spectral spreading for more than 150 milliseconds. For the S-bursts in Figure 3, with their bandwidths of about 5 kHz and their spectral drifts of 8.1 MHz/sec, the electron bunch hypothesis would require 600-microsecond pulses of energetic electrons, with a parallel energy of about 700 electron volts. However, in order to account for the apparent lack of spectral spreading, it would also require an energy spread of less than one percent, as well as, for electrons near the loss cone, a pitch-angle spread of less than one degree. Although electron bunches with such stringent requirements might conceivably occur, they are not considered very likely.

Another possible explanation for the observed discreteness was suggested to me independently by P. Zarka and C. S. Wu, to wit: Since the cyclotron instability is strongly angle-dependent, the different frequencies should be emitted in somewhat different directions, and when this is sampled in a single direction by a satellite, only a narrow band of frequencies might be detected. However, for this to account for the observed five-Hertz bandwidth in Figure 2, the emitted angular beamwidth for a five-Hertz segment of the spectrum would have to have been comparable to the angle which is subtended by an eighty-meter source at the distance of the ISEE satellites, or only about 10<exp -4> degrees. On this basis, the two satellites, with their angular separation of about three degrees during Figure 2, should not have intercepted the same frequencies. However, they did, and generally do, as is demonstrated by the coherence measurements in the next section, and that eliminates this as a possible explanation for the observed spectral discreteness.

COHERENCE

One of the remarkable properties of a laser beam is its phase coherence in different directions. Because of the spatial quenching which occurs inside a laser, its oscillation pattern is synchronized at every location inside, and as a result, the phase of its emitted radiation field is a constant function of direction.

Although a truly monochromatic signal is automatically coherent, coherence can also arise from a random source which is sufficiently small so that the phase differences for each of its spectral components from different parts of the source are negligible, and this is the principle for measuring the size of an incoherent source by correlation measurements. This was the original basis for a correlation study of the AKR using the ISEE-1 and ISEE-2 satellites, which were flown in similar orbits with different separations [Baumback et al., 1986]. The basic idea was to measure the presumably auroral-zone size of the AKR source from the decrease of correlation which should occur for the largest spacecraft separations. In this study, the same discrete components of the AKR, observed simultaneously by both of the satellites, were isolated and their cross-correlations calculated, using one-bit correlation techniques. The result, which is illustrated by Figures 4 and 5, indicated nearly perfect correlation for all spacecraft separations.

Unless the AKR sources were extremely small, and less than about ten kilometers across and again too small to account for the observed AKR amplitudes by open-loop amplification, these measurements indicate that the AKR is phase coherent.

It was also noted in this study that the same spectral components could generally be detected at the same time by both of the satellites, and this is interpreted as the AKR beamwidths being broader than the few-degree maximum spacecraft separations.

LONGITUDINAL MODES

Another important consequence of lasing is that the oscillations must always correspond to inphase feedback, which for lasers which are long compared to their widths (as is generally the case), is equivalent to requiring a half-integral number of wavelengths between the mirrors [see Verdeyen, 1981; Calvert, 1982]. In any laser, even at optical wavelengths, oscillations can occur only in one of these so-called longitudinal laser modes, and it is this which actually determines the exact oscillation frequency, according to the equation

$$f = m c / 2 n W \qquad (1)$$

where m is an integer known as the longitudinal mode number, c is the speed of light, n is the source wave refractive index, and W is the laser length [see Calvert, 1982, Eqn. 34]. An important aspect in the original development the radio laser concept was the detection of these regularly-spaced longitudinal laser modes in the AKR emission spectrum [ibid., Fig. 4].

If the jovian radio S-bursts are also to be attributed to radio lasing, it was expected that they, too, might exhibit these regularly-spaced longitudinal laser modes, and in order to confirm this, a search was made for them in the ground-based radio observations from France and Tasmania [Calvert et al., 1987]. In this study, as illustrated by Figure 6, it was found that regular temporal spacings, much like those previously reported by Krausche et al. [1976], could be statistically distinguished from the more-or-less random occurrence of S-burst groups. It was also found that the temporal spacings within the groups varied inversely with the observing frequency, from about two milliseconds at 26 MHz to over eight milliseconds at 10 MHz, as is shown by Figure 7. Since the S-burst frequency drifts are

approximately proportional to the frequency, with rates of about 0.4 to 0.8 of the frequency per second [see Leblanc et al. 1980, among others], this implies that the frequency spacings between the adjacent members of a group (like those in Figure 3) are approximately independent of the frequency, and about 30 to 50 kHz. This in turn implies a constant laser length of about eight kilometers, according to Equation 1 (for an arbitrarily-assumed wave refractive index of about one-half).

This result also suggested that the frequency drifts of the S-bursts can be attributed to a laser expansion during emission, at an approximately-constant velocity of about four kilometers per second [see Calvert et al., 1987, Eqn. 6]. Since this equals the approximate surface velocity of the Io magnetic flux tube with respect to Jupiter, it further suggests that the S-burst lasers are progressively laid down by some aspect of that moving Io flux tube, and that this could account for the apparent laser expansion. Although the details aren't certain, this new model for the S-burst drifts would also automatically explain why the observed drifts are always downward, since such progressive creation should produce lasers which are always expanding and never contracting.

The principal results of this study, however, are independent of this interesting new explanation for the S-burst drifts. Those results show that the discrete S-bursts are often equally spaced, with frequency spacings that are approximately independent of the frequency. Unless one is to contemplate multiple electron bursts with the same stringent requirements mentioned above, in addition to a temporal periodicity which somehow increases proportional to the cube root of the joviocentric altitude, this behavior is quite hard to account for without radio lasing.

LASING

In the previous three sections I have presented the principal evidence for radio lasing at the Earth and Jupiter, consisting of the AKR and jovian S-burst observations showing their monochromaticity, their phase coherence in different directions (for the AKR only), and the occurrence of their regularly-spaced longitudinal laser modes. However, in order to fully appreciate the significance of these observations, it is first necessary to understand the functioning of a laser. In this and the following section, I shall therefore discuss the concept of lasing and show how it applies to these planetary radio emissions.

First of all, as the term 'laser' is most commonly used, it actually implies a laser oscillator, consisting of a medium which is capable of stimulated emission, plus mirrors to form a closed-loop wave feedback path. Whenever such a system oscillates, with the consequent emission of an intense coherent beam, it is said to 'lase', and such systems are generally used as primary sources of radiation, whereas a laser amplifier (or a 'maser', at radio wavelengths) is built without feedback and it is generally used to amplify wave signals produced elsewhere. The behavior of a laser is therefore that of a self-excited, closed-loop wave feedback oscillator, and it is primarily this which produces all of its remarkable properties.

It must be emphasized that lasing is not necessarily a quantum-mechanical effect, not is it simply a scheme to increase the total wave growth by repeated reflections. Although in most optical lasers the stimulated emission results from quantized atomic or molecular energy levels, this is actually incidental to their functioning as lasers. For instance, in the so-called free-electron lasers there are no such quantized levels, and yet they still produce comparable laser behavior. What is important is that such systems are self-excited oscillators, providing their own input signals rather than amplifying waves produced elsewhere.

Lasing occurs whenever the stimulated wave growth and the feedback of a laser are sufficient to replenish its wave signal. This, however, generally produces growing waves which would continue to grow indefinitely, were it not for the eventual gain saturation of the stimulated emission, either by depleting its excited population or by otherwise destroying the free energy which is available for wave growth. The wave signals within a laser therefore always grow to the point of gain saturation, and this is what limits their amplitude, at least over the short term, before the free energy decreases substantially. Moreover, since the saturation presumably reduces the wave gain more for larger amplitudes, this limiting amplitude is usually stable. Under such conditions, the oscillating wave signal within a laser exactly replicates itself after its round trip transit between the mirrors. This means that the wave pattern within a laser must be one of its so-called 'self-reproducing' diffraction patterns and that the wave signal at every location must be exactly repetitive, at a submultiple of the two-way transit time between the mirrors, and perfectly synchronized. In other words, lasers always saturate, and that causes them to oscillate in a single coherent mode at a single frequency (that frequency being one of those given by Equation 1).

Another way of viewing this is to imagine a laser just starting up, with some initial random excitation. For all of its possible wave modes and frequencies, some will have enough wave gain and feedback to grow, while others will not, and those others will eventually die away. However, once saturation is reached, by any one of the growing modes and frequencies, the wave gain will be reduced, not only for it, but presumably also for all of the others. Because of this, still more of the possible modes and frequencies will have insufficient gain to replenish themselves, and they, too, will eventually die away. The ultimate outcome of this process, which is known as 'quenching' is the survival of a single oscillation mode at a

single frequency, since there can be only one mode and frequency with just exactly the right saturated gain and feedback to exactly replicate itself. It is as if all of the modes and frequencies within a laser competed with one another to be the final one which saturates the gain and thereby extinguishes all of the others.

The self-reproducing oscillation patterns of a laser are almost, but not quite, the normal modes of its equivalent Fabry-Perot optical resonator. The frequencies are also almost, but not quite, its resonant frequencies; the difference being that the modes and frequencies of the optical resonator are altered slightly by its losses, and in the equivalent laser, those losses are canceled out by the stimulated emission. An actual laser, with its losses to absorption and radiation, is therefore equivalent to a slightly-modifed, perfectly loss-less resonantor. The effective 'Q' of a laser is consequently always infinite, and its spectral bandwidth is always precisely zero, except for perturbations caused by noise or by variations of its parameters.

The simplest self-reproducing pattern (in a laser with plane parallel mirrors), involves an inphase gaussian spot in the plane of its mirrors, since that produces a gaussian diffraction patten at the opposite mirror. Equating the size of this spot to that of its diffraction pattern yields

$$a_o = [2 \lambda W / \pi]^{1/2} \qquad (2)$$

for the size of the spot and

$$\alpha_o = [2 \lambda W / \pi]^{1/2} \qquad (3)$$

for the width of its beam, both measured to their respective 1/e power points, where λ is the wavelength and W is the distance between the mirrors. This wave distribution is known as the fundamental transverse mode, and it can occur for each of the frequencies given by Equation (1).

The other, higher-order transverse modes of a laser correspond to multiple spots of somewhat smaller size, with their spacings given approximately by Equation 2, and to multilobe beams with their lobe spacings given approximately by Equation 3. For an exact description of these higher-order modes, see Verdeyen's [1981] Equation 3-22.

A laser therefore consists of a self-excited closed-loop wave feedback oscillator in which the quenching which is brought on by gain saturation produces a single, synchronized oscillation mode at a single frequency, with the possible frequencies given by Equation 1, the width of the lasing volume (or else its periodic spacings) given by Equation 2, and the width or scale of its emitted beam given by Equation 3. Also because of this quenching, the emission spectrum is virtually monochromatic, except for perturbations caused by parametric variations or noise, and phase coherent in different directions. Moreover, all of these properties are direct consequences of lasers' being self-excited oscillators rather than just open-loop amplifiers.

NATURAL RADIO LASING

The term which I have adopted for the proposed natural lasing at the Earth and Jupiter, with frequencies ranging from a few ten's of kilohertz to a few ten's of megahertz, is 'radio lasing'. Although taking obvious liberties with the original acronym (which would imply light amplification for what is actually radio oscillation), this term describes best how the phenomenon occurs and ought to behave, including the emission of intense, coherent, and virtually monochromatic beams. Moreover, it is also consistent with the names for other extensions of the laser concept, to the infrared, to the ultraviolet, and even to X-ray wavelengths.

This concept relies upon the same doppler-shifted cyclotron resonance instability as the previous open-loop amplifier model, but operating instead between local irregularities of the source plasma density. These irregularities, which presumably extend along the magnetic field in altitude, and probably also for the AKR in longitude along the electron drift L-shells [see Calvert, 1987], would provide the wave feedback which is needed to turn the previous amplifier into self-excited lasers. Since the instability occurs primarily across the magnetic field, in the extraordinary mode, and near its cutoff, where the wave refractive index is a sensitive function of the density, such density irregularities should provide efficient mirrors for that mode at the appropriate frequencies.

These radio lasers (for the AKR) are pictured as shown in Figure 8. They are oriented perpendicular to the assumed density mirrors, and hence almost horizontal and aligned with magnetic meridian (except for possible local distortions caused by auroral electric fields). Its length for the AKR, of about 25 km, was determined from the observed spectral spacings of its longitudinal laser modes, according to Equation 1, for an

assumed refractive index of one-half. This yields a fundamental-mode laser spot size of about 4 km, and a corresponding emission beamwidth of about nine degrees, according to Equations 2 and 3, for a wavelength of one kilometer. The corresponding dimensions for the jovian S-burst lasers [see Calvert et al., 1987, Fig. 9] would be a length of about 8 km (as mentioned above), a spot size of about 400 meters, for a source wavelength of 30 meters, and a beamwidth of about three degrees.

For the S-burst lasers, the source of electron free energy is uncertain, but for the AKR it is most likely the energetic electron loss cone, as proposed by Wu and Lee [1979]. This, plus the fact that a laser must at least partially destroy its own free energy by gain saturation, would imply that, for resonant kilovolt electrons coming upward from the ionosphere, the cumulative electric field which they enounter during their transit of the laser must be some fraction of a kilovolt, in order for those electrons to be pitch-angle scattered sufficiently to affect the wave growth. This implies a wave electric field of something less than 1000/4 volts per kilometer, or 250 millivolts per meter, and this agrees reasonably well with that originally predicted from estimates of the available loss-cone free energy, of 20 to 200 millivolts per meter [Calvert, 1982], as well as also with that calculated from estimates of the AKR laser power, of about five kilowatts, or 400 microwatts per square meter (or 0.4 V/m) over the exit area of the laser spot [Calvert, 1987]. Applying this same arguement in reverse for the S-burst lasers, with their estimated power of about thirty kilowatts [Calvert et al., 1987], and their exit area of 13,000 square meters, the source field strengths could be as much as ten volts per meter, and the requisite electron energy, about four kilovolts.

Such lasers would thus account for the observed monochromaticity, coherence, and longitudinal laser modes, by the gain saturation and quenching discussed in the previous section.

Although the apparent laser source sizes are smaller than might have been expected to produce such intense radio emissions, they are nonetheless consistent with the observed power fluxes and the expected electron energies, primarily because of their relatively narrow emission beamwidths and saturation amplitudes.

Although possibly produced as by-products, because of the large fundamental, extraordinary-mode amplitudes at the source, separate harmonic and ordinary-mode laser emissions are not expected to occur, for the want of suitable mirrors to provide wave feedback. Although this is consistent with some of the reported harmonic and ordinary-mode observations of the AKR [Mellott et al., 1984, 1986; Calvert, 1985], it is inconsistent with others [Benson, 1982, 1985; Bahnsen et al., 1987], and such matters require further study.

There is also a need for better laser models, including calculations of the saturated wave gain and full-wave solutions for the oscillating wave fields in different possible source density structures. Although the original enhancement source model was sufficient to show that stable lasing was possible, other considerations would now suggest lasing within density depletions, despite their apparent lack of feedback closure [Calvert, 1982, 1987], and this matter also requires further study.

Another interesting prediction of the laser model is that satellites flying directly through the AKR source region, like ISIS-1, DE-1, or Viking, should generally miss the actual sources, since they are so small relative to their spacings. Moreover, in the rare instances when they are observed, they should consist of extremely intense localized wave signals, like those recently observed by Bahnsen et al. [1987] in their Figure 2 at 1157 UT, having a size of about 60 km and a field strength of roughly 60 mV/m, and a further study of such cases would also be beneficial.

SUMMARY

In this paper I have reviewed the principal new evidence for the production of planetary cyclotron radio emissions, like the Earth's AKR or the S-bursts from Jupiter, by natural radio lasing. This evidence consists of observations of their monochromaticity, their phase coherence in different directions, and their regularly-spaced longitudinal laser modes, none of which can be accounted for by the previous open-loop amplifier model.

I have also described how these properties are produced by the proposed radio lasers: The monochromaticity resulting directly from the spectral quenching caused by gain saturation (just as it is in any other kind of oscillator), and the phase coherence being produced by the comparable spatial quenching of all but a single, synchronized oscillation mode. The regularly-spaced longitudinal laser modes are also produced by this same quenching and the resulting need for inphase feedback having a half-integral number of wavelengths between the laser mirrors.

Finally, I have also discussed the apparent size and power of the radio lasers at the Earth and Jupiter, their connection to the electron energies causing wave growth, and a few of the current uncertainties requiring further study.

Acknowledgments. This work was supported by NASA grants NGL-16-001-043, NAG5-310, NAGW-256, and NAGW-1206. I also thank my many friends and colleagues who have helped in this effort, including M. M. Baumback, Y. Leblanc, G. R. A. Ellis, and R. L. Huff.

REFERENCES

Bahnsen, A., M. Jespersen, E. Ungstrup, and I. B. Iverson, Auroral hiss and kilometric radiation measured from the Viking satellite, Geophys. Res. Lett., 14, 471-474, 1987.

Baumback, M. M., D. A. Gurnett, W. Calvert, and S. D. Shawhan, Satellite interferometric measurements of auroral kilometric radiation, Geophys. Res. Lett., 13, 1105-1108, 1986.

Baumback, M. M., and W. Calvert, The minimum bandwidths of auroral kilometric radiation, Geophys. Res. Lett., 14, 119-122, 1987.

Benediktov, E. A., G. G. Getmantsev, Y. A. Sazonov, and A. F. Tarasov, Preliminary results of measurement of the intensity of distributed extraterrestrial radio-frequency emission at 725 and 1525 kHz frequencies by the satellite Elektron-2, Cosmic Res., 3, 492-494 (Translation: Kosm. Issled., 3, 614-617), 1965.

Benson, R. F., Harmonic auroral kilometric radiation of natural origin, Geophys. Res. Lett., 9, 479-482, 1982.

Benson, R. F., Auroral kilometric radiation: Wave modes, harmonics, and source region electron density structures, J. Geophys. Res., 90, 2753-2784, 1985.

Benson, R. F., and W. Calvert, ISIS-1 observations at the source of auroral kilometric radiation, Geophys. Res. Lett., 6, 479-482, 1979.

Burke, B. F., and K. L. Franklin, Observations of a variable radio source associated with the planet Jupiter, J. Geophys. Res., 60, 213-217, 1955.

Calvert, W., The signature of auroral kilometric radiation on ISIS-1 ionograms, J. Geophys. Res., 86, 76-82, 1981.

Calvert, W., A feedback model for the source of auroral kilometric radiation, J. Geophys. Res., 87, 8199-8214, 1982.

Calvert, W., The source location of certain jovian decametric radio emissions, J. Geophys. Res., 88, 6165-6170, 1983.

Calvert, W., DE-1 measurements of AKR wave directions, Geophys. Res. Lett., 12, 381-384, 1985.

Calvert, W., Auroral precipitation caused by auroral kilometric radiation, J. Geophys. Res., 92, 8792-8794, 1987.

Calvert, W., Y. Leblanc, and G. R. A. Ellis, Natural radio lasing at Jupiter, Astrophys. J., submitted, 1987.

Carr, T. D., M. D. Desch, and J. K. Alexander, Phenomenology of magnetospheric radio emissions, in Physics of the Jovain Magnetosphere, A. J. Dessler, ed., Cambridge Univ. Press, Cambridge, England, 226-284, 1983.

Desch, M. D., R. S. Flagg, and J. May, Jovian S-burst observations at 32 MHz, Nature, 272, 38-40, 1978.

Dunckel, N., B. Ficklin, L. Rorden, and R. A. Helliwell, Low-frequency noise observed in the distant magnetosphere, J. Geophys. Res., 75, 1854-1862, 1970.

Dusenbery, P. B., and L. R. Lyons, General concepts on the generation of auroral kilometric radiation, J. Geophys. Res., 87, 7467-7481, 1982.

Ellis, G. R. A., Cyclotron radiation from Jupiter, Austr. J. Phys., 13, 344-353, 1962.

Ellis, G. R. A., On external radio emission from the Earth's outer atmosphere, Austr. J. Phys., 17, 63-74, 1964.

Ellis, G. R. A., The decametric radio emissions from Jupiter, Radio Sci., 69D, 1513-1530, 1965.

Ellis, G. R. A., An Atlas of Selected Spectra of the Jupiter S-Bursts (report), Univ. of Tasmania, Hobart, Tas., Australia, 1979.

Ellis, G. R. A., Observations of the Jupiter S-bursts between 3.2 and 32 MHz, Austr. J. Phys., 35, 165-175, 1982.

Gallet, R. M., Radio observations of Jupiter, Ch. 14 of Planets and Satellites, G. P. Kuiper and B. M. Middlehurst, eds., Univ. of Chicago Press, Chicago, Illinois, 500-533, 1961.

Gordon, M. A., and J. W. Warwick, High time-resolution studies of Jupiter's radio bursts, Astrophys. J., 148, 511-533, 1967.

Grabbe, C. L., Auroral kilometric radiation: A theoretical Review, Rev. Geophys. Space Phys., 19, 627-633, 1981.

Grabbe, C. L., Theory of the fine structure of the auroral kilometric radiation, Geophys. Res. Lett., 9, 155-158, 1982.

Gurnett, D. A., The earth as a radio source: Terrestrial kilometric radiation, J. Geophys. Res., 79, 4227-4238, 1974.

Gurnett, D. A., and R. R. Anderson, The kilmetric radio emission spectrum: Relationship to auroral acceleration processes, in Physics of Auroral Arc Formation, Geophys. Monogr. Ser., 25, S. -I. Akasofu and J. R. Kan, eds., American Geophysical Union, Washington, D. C., 341-350, 1981.

Helliwell, R. A., and U. S. Inan, VLF wave growth and discrete emission triggering in the magnetosphere: A feedback model, J. Geophys. Res., 87, 3537-3550, 1982.

Hewitt, R. G., D. B. Melrose, and K. G. Rönnmark, The loss-cone-driven electron-cyclotron maser, Austr. J. Phys., 35, 447-471, 1982.

Huff, R. L., W. Calvert, J. D. Craven, L. A. Frank, and D. A. Gurnett, Mapping of auroral kilometric radiation sources to the aurora, J. Geophys. Res., submitted, 1987.

Kaiser, M. L., J. K. Alexander, A. C. Riddle, J. B. Pearce, and J. W. Warwick, Direct measurements by Voyagers 1 and 2 of the terrestrial kilometric radiation, Geophys. Res. Lett., 5, 857-860, 1978.

Kaiser, M. L., M. D. Desch, J. W. Warwick, and J. B. Pearce, Voyager detection of nonthermal radio emission from Saturn, Science, 209, 1238-1240, 1980.

Krausche, D. S., R. S. Flagg, G. B. Lebo, and A. G. Smith, High resolution spectra of the Jovian decametric radiation. I. Burst morphology and drift rates, Icarus, 29, 463-475, 1976.

Leblanc, Y., M. G. Aubier, C. Rosolen, F. Genova, and J. De la Noe, The jovian S-bursts: Frequency drift measurements at different frequencies throughout several storms, Astron. Astrophys., 86, 349-354, 1980.

Le Queau, D., R. Pellat, and A. Roux, The maser synchrotron instability in an inhomogeneous medium: Application to the generation of the auroral kilometric radiation, Annales Geophys., 3, 273-292, 1985.

Mellott, M. M., W. Calvert, R. L. Huff, D. A. Gurnett, and S. D. Shawhan, DE-1 observations of auroral kilometric radiation in the ordinary and extraordinary wave modes, Geophys. Res. Lett., 11, 1188-1161, 1984.

Mellott, M. M., R. L. Huff, and D. A. Gurnett, DE-1 observations of harmonic AKR, J. Geophys. Res., 91, 13,732-13,738, 1986.

Melrose, D. B., An interpretation of Jupiter's decametric radiation and the terrestrial kilometric radiation as direct amplified gyro-emission, Astrophys. J., 207, 651-662, 1976.

Melrose, D. B., A phase-bunching mechanism for fine structures in auroral kilometric radiation and jovian decametric radiation, J. Geophys. Res., 91, 7970-7980, 1986.

Melrose, D. B., K. G. Rönnmark, R. G. Hewitt, Terrestrial kilometric radiation: The cyclotron theory, J. Geophys. Res., 87, 5140-5150, 1982.

Oya, H., and A. Morioka, Observational evidence of Z and L-O mode waves at the origin of auroral kilometric radiation from the Jikiken (EXOS-B) satellite, J. Geophys. Res., 88, 6189-6203, 1983.

Shawhan, S. D., and D. A. Gurnett, Polarization measurements of auroral kilometric radiation by Dynamics Explorer 1, Geophys. Res. Lett., 9, 913-916, 1982.

Smith, A. G., and T. D. Carr, Radio Exploration of the Planetary System, Van Nostrand, Princton, New Jersey, 1964.

Staelin, D. H., and P. W. Rosenkranz, Formation of Jovian decametric S-bursts by modulated electron streams, J. Geophys. Res., 87, 10,401-10,406, 1982.

Verdeyen, J. T., Laser Electronics, Prentice-Hall, Englewood Cliffs, New Jersey, 1981.

Voots, G. D., D. A. Gurnett, and S.-I. Akasofu, Auroral kilometric radiation as an indicator of auroral magnetic disturbances, J. Geophys. Res., 82, 2259-2266, 1977.

Warwick, J. W., D. R. Evans, J. H. Romig, C. B. Sawyer, M. D. Desch, M. L. Kaiser, J. K. Alexander, T. D. Carr, D. H. Staelin, S. Gulkis, R. L. Poynter, M. Aubier, A. Boischot, Y. Leblanc, A. Lecacheux, B. M. Peterson, and P. Zarka, Voyager 2 radio observations of Uranus, Science, 233, 102-106, 1986.

Wu, C. S., and L. C. Lee, A theory of the terrestrial kilometric radiation, Astrophys. J., 230, 621-626, 1979.

Zarka, P., D. Le Queau, and F. Genova, The maser synchrotron instability in an inhomogeneous medium: Determination of the spectral intensity of auroral kilometric radiation, J. Geophys. Res., 91, 13,542-13,558, 1986.

CAPTIONS

Fig. 1. DE-1 observations of the auroral kilometric radiation from above the northern polar cap on 4 January 1982, showing in the top panel, at its highest frequencies, the AKR spectral flux density, and in the panel just below, the measured wave electric vector rotation sense, with red indicating a right-handed rotation with respect to the downward-directed source magnetic field. For a constant frequency of 218 kHz (±10%), and at the times indicated for each of the six bottom panels (±2.5 min), the AKR source directions were determined from the variation of signal phase versus antenna rotation [Calvert, 1985] and projected down to the altitudes for cyclotron resonance. The field lines from these presumed source locations down to auroral altitudes were then calculated and superimposed upon the corresponding DE-1 UV auroral images [see Huff et al., 1987]. The excellent agreement which this invariably produces with the brightest features of the aurora, in this case with a discrete arc at the expanding poleward edge of the aurora during a substorm, conclusively confirms that the AKR is generated at the cyclotron frequency on auroral field lines, in this case to a precision of about ten percent in frequency or 400 kilometers in position.

Fig. 2. A single discrete spctral component of the AKR reconstructed from an autocorrelation analysis of the ISEE-1 radio observations [Baumback and Calvert, 1987], showing in the bottom panel, for gaussian fits to its spectral shape, its minimum bandwidths of only five Hertz.

Fig. 3. High-resolution observations of the jovian S-bursts, recorded at Hobart, Tasmania, by Ellis [1982], showing their downward spectral drifts of about 8.1 MHz/sec, their bandwidths of 5 kHz, and the approximately equal spacings between components, of about 4.3 milliseconds in time or 32 kHz in frequency.

Fig. 4. Simultaneous observations of the AKR with ISEE-1 and ISEE-2, showing their nearly-perfect phase coherence by the large correlation excursions in the bottom panel which occurred as the receiver frequencies and positions slowly changed. The bottom panel also shows, for an angular satellite separation of about two degrees, that the AKR was observed at the same frequencies at both satellites, to within about eight Hertz.

Fig. 5. Observed correlations of the AKR received by ISEE-1 and ISEE-2 versus their projected separations, for a number of AKR correlation measurements at each separation, showing that the expected decrease for an incoherent source larger than about nine kilometers did not occur [Baumback et al., 1986]. Such measurements indicate that the AKR is phase coherent.

Fig. 6. Cumulative percentage occurrence of the observed S-burst's temporal spacings, plotted on a logarithmic scale so that a Poisson (or random) distribution would produce a descending straight line [Calvert et al., 1987]. Whereas the larger spacings seemed to be randomly distributed, the separate population of smaller spacings implies a periodic spacing of approximately four milliseconds within S-burst groups.

Fig. 7. Variation of the S-burst's temporal spacing with frequency, including the case in Figure 2 , previously published by Ellis [1982, Fig. 2], one measurement from the observations of Y. Leblanc, of the Observatoire de Paris at Meudon, France, and others from the further observations of Ellis [1979]. These observations show that the S-burst's temporal spacings decreased inversly proportional to the frequency, implying that the radio lasers which produced them were expanding at a uniform velocity of about four kilometers per second.

Fig. 8. A schematic illustration of the proposed radio lasers [Calvert, 1982, 1987], showing for the AKR their approximate dimensions and emitted beamwiths, and suggesting how they might be powered by the upcoming energetic electron loss cone.

NOTE TO THE TYPESETTER

Certain symbols which are not available with my word processor were represented using the angle brackets "‹" and "›", as follows:

SYMBOL	MEANING
‹alpha›	the greek letter "alpha"
‹lambda›	the greek letter "lambda"
‹pi›	the greek letter "pi"
‹sub o›	a subscript "o"
‹exp 1/2›	an exponent of 1/2 or the square root
‹exp -4›	an exponent of -4

Equations 2 and 3 should thus appear as:

$$a_o = [2 \lambda W \pi]^{1/2} \qquad (2)$$

$$\alpha_o = [2 \lambda W \pi]^{1/2} \qquad (3)$$

and the quantity on page 7, sixth line from the end as: 10^{-4}.

JANUARY 4 1982 ORBIT 540

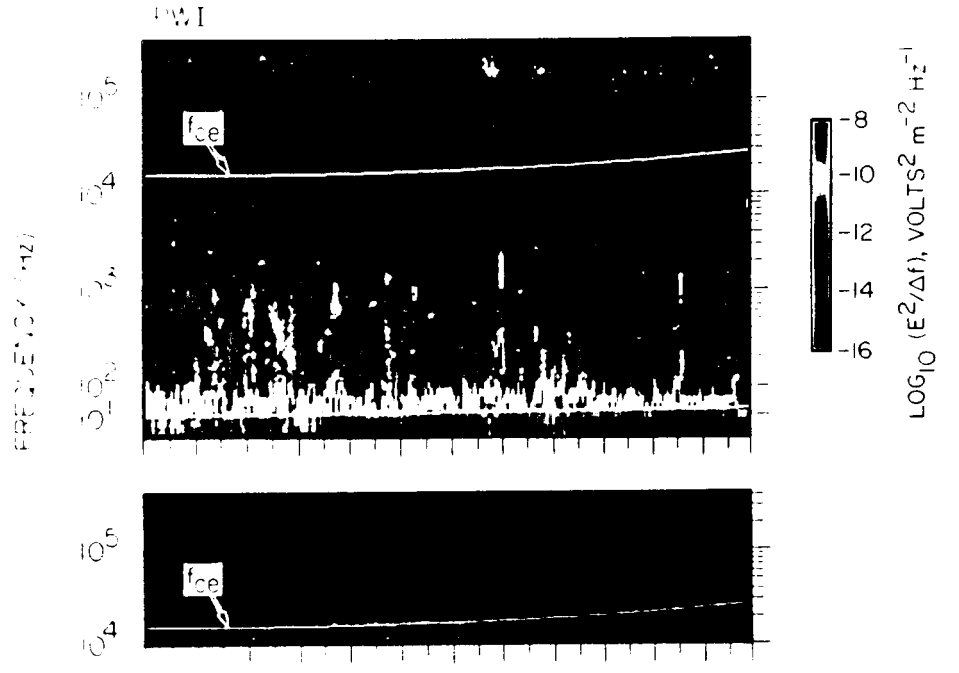

	0820	0840	0900	0920	0940	1000	1020
	4.58	4.65	4.65	4.60	4.47	4.29	4.03
	13.0	17.3	24.0	35.2	58.4	118	352
	4.08	3.99	3.85	3.62	3.22	2.45	0.43
	53.9	59.1	64.3	69.2	74.3	79.2	83.6

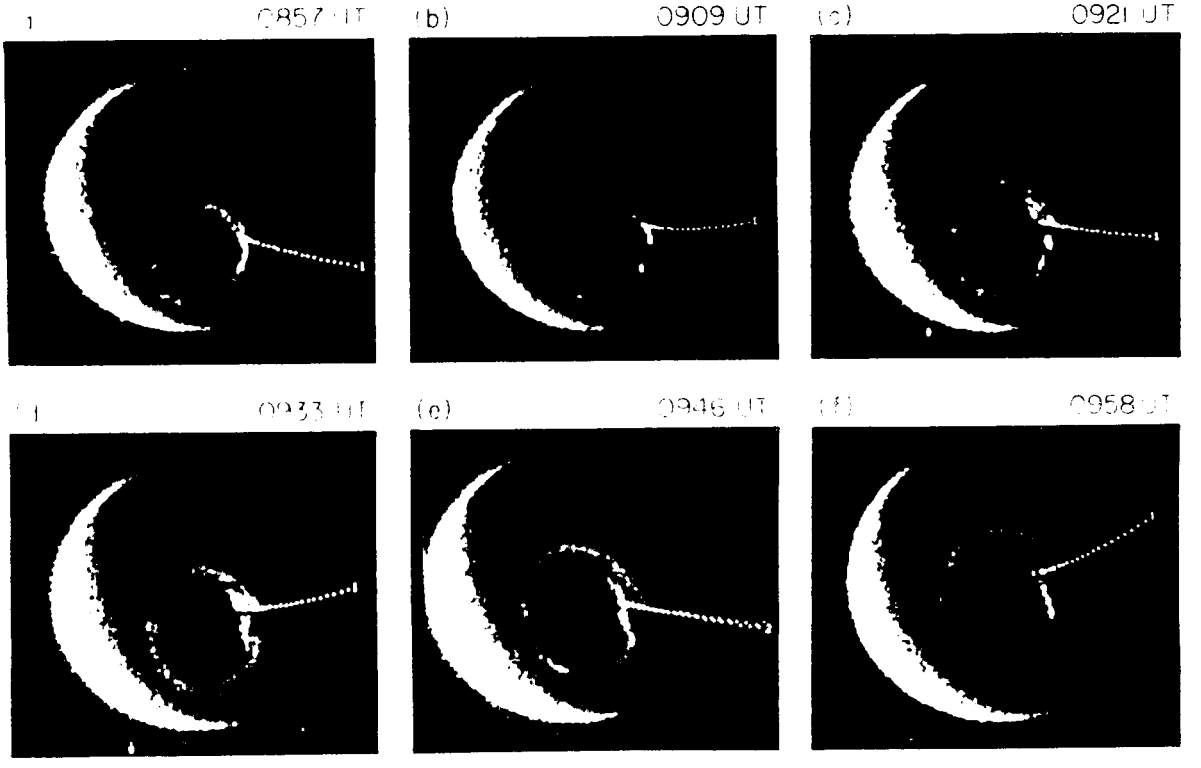

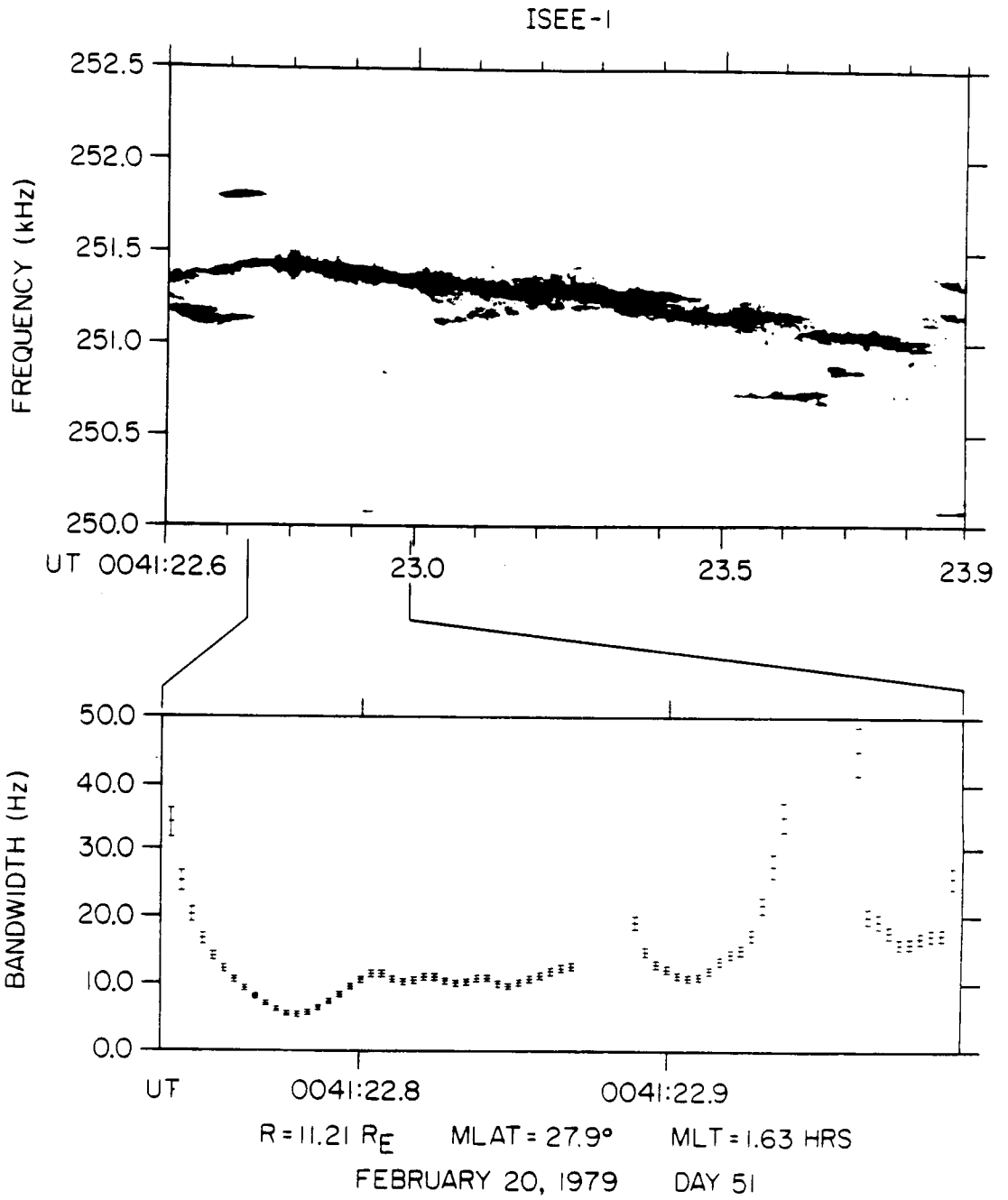
ISEE-1
252.5
252.0
251.5
251.0
250.5
250.0
FREQUENCY (kHz)
UT 0041:22.6
23.0
23.5
23.9
50.0
40.0
30.0
20.0
10.0
0.0
BANDWIDTH (Hz)
UT
0041:22.8
0041:22.9
R = 11.21 R_E
MLAT = 27.9°
MLT = 1.63 HRS
FEBRUARY 20, 1979
DAY 51

Fig. 2

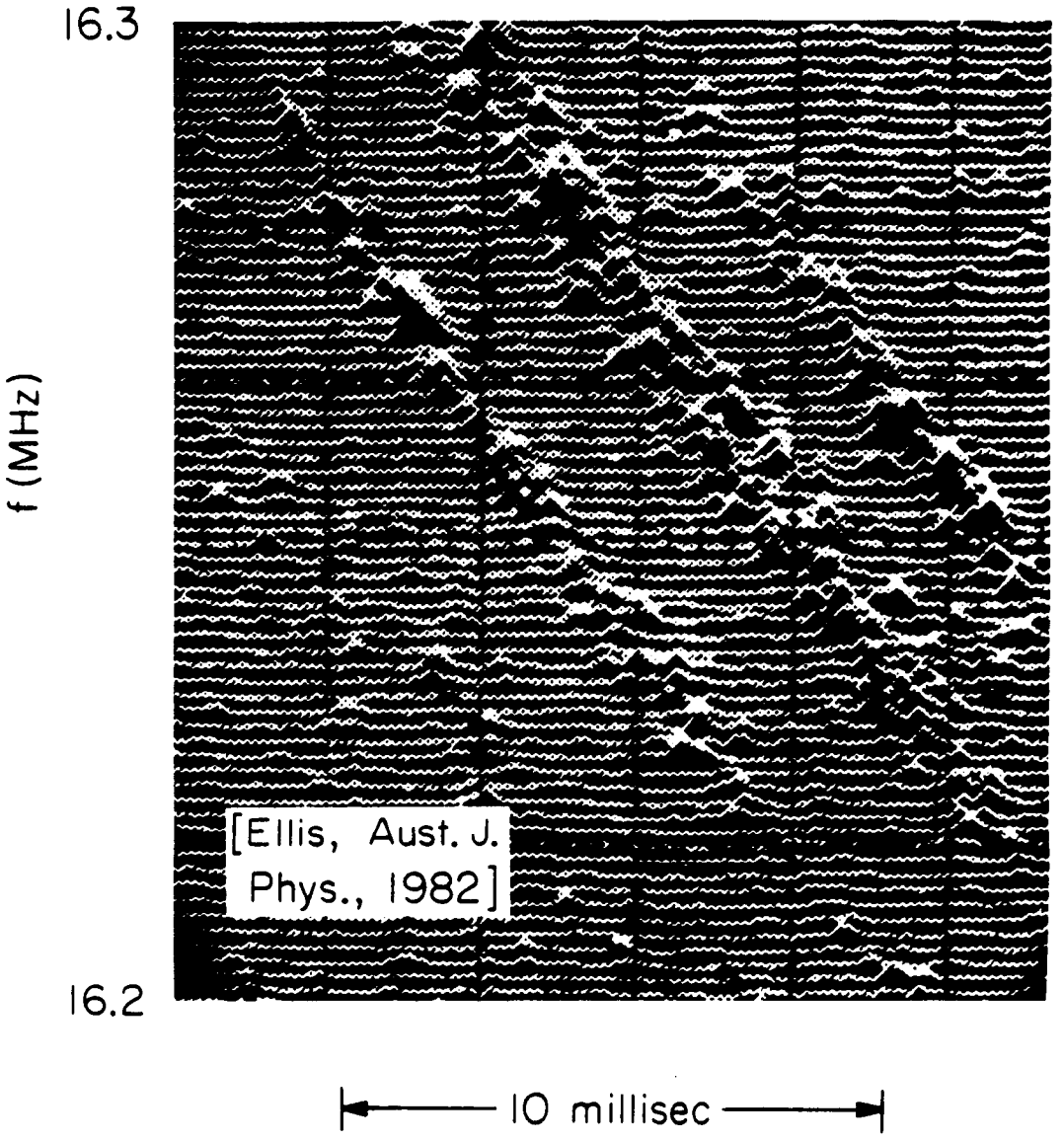

FIG. 3

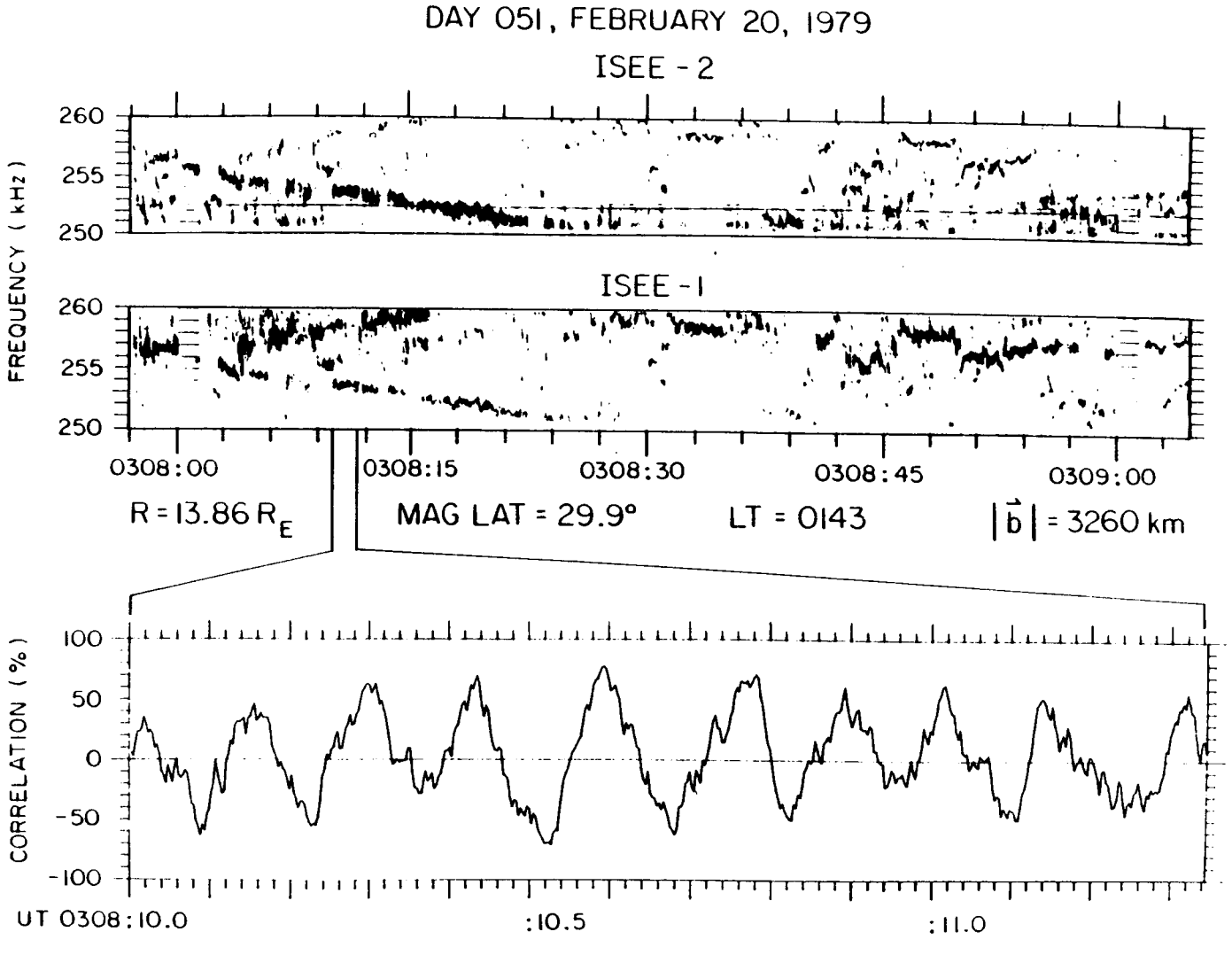
DAY 051, FEBRUARY 20, 1979
ISEE - 2
ISEE - 1
FREQUENCY (kHz)
260
255
250
0308:00
0308:15
0308:30
0308:45
0309:00
R = 13.86 R_E
MAG LAT = 29.9°
LT = 0143
|b| = 3260 km
CORRELATION (%)
100
50
0
-50
-100
UT 0308:10.0
:10.5
:11.0

Fig. 4

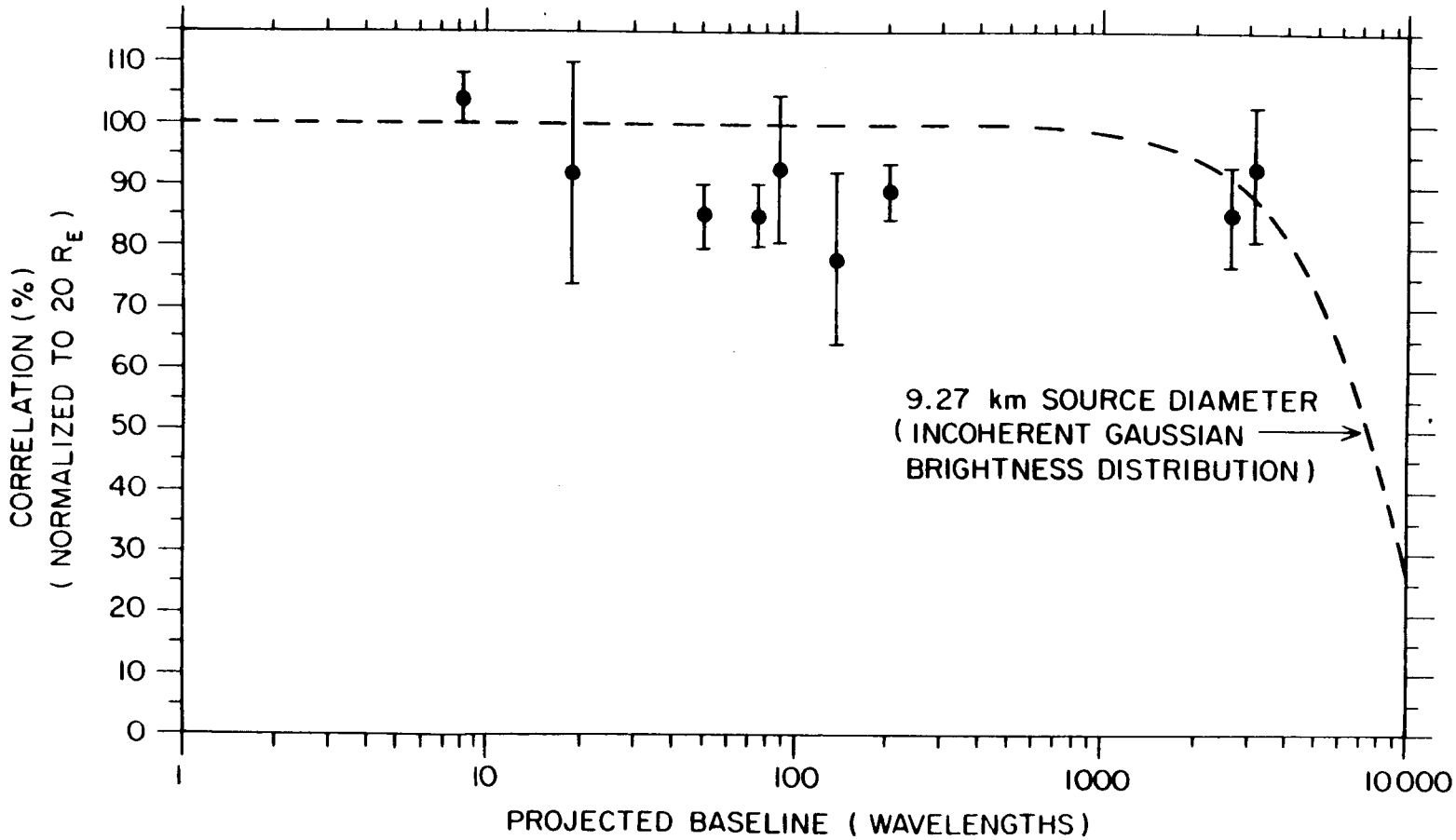
CORRELATION (%)
(NORMALIZED TO 20 R_E)
110
100
90
80
70
60
50
40
30
20
10
0
1
10
100
1000
10000
PROJECTED BASELINE (WAVELENGTHS)
9.27 km SOURCE DIAMETER
(INCOHERENT GAUSSIAN
BRIGHTNESS DISTRIBUTION)

Fig. 5

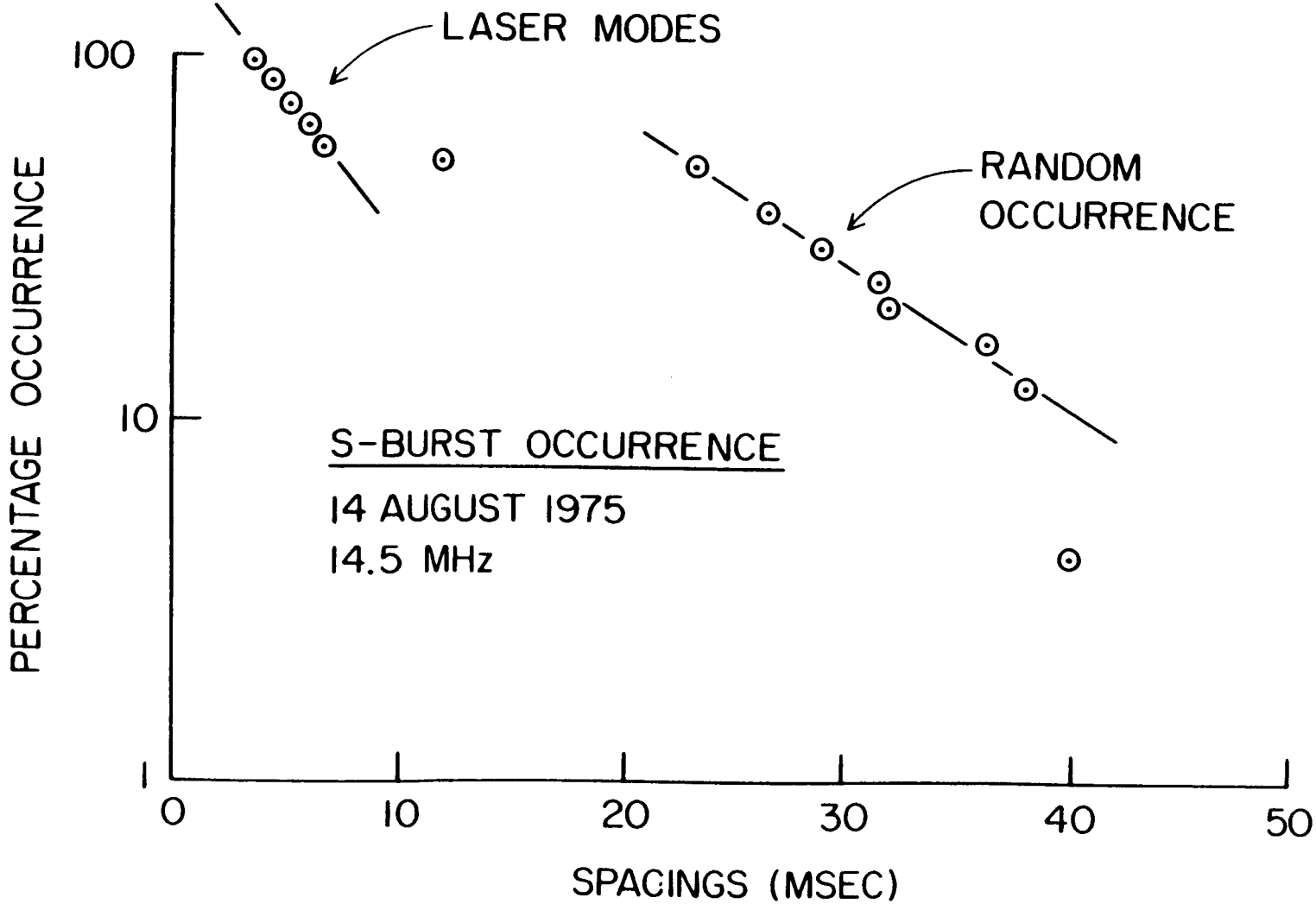
LASER MODES
RANDOM
OCCURRENCE
100
10
1
PERCENTAGE OCCURRENCE
S-BURST OCCURRENCE
14 AUGUST 1975
14.5 MHz
0
10
20
30
40
50
SPACINGS (MSEC)

Fig. 6

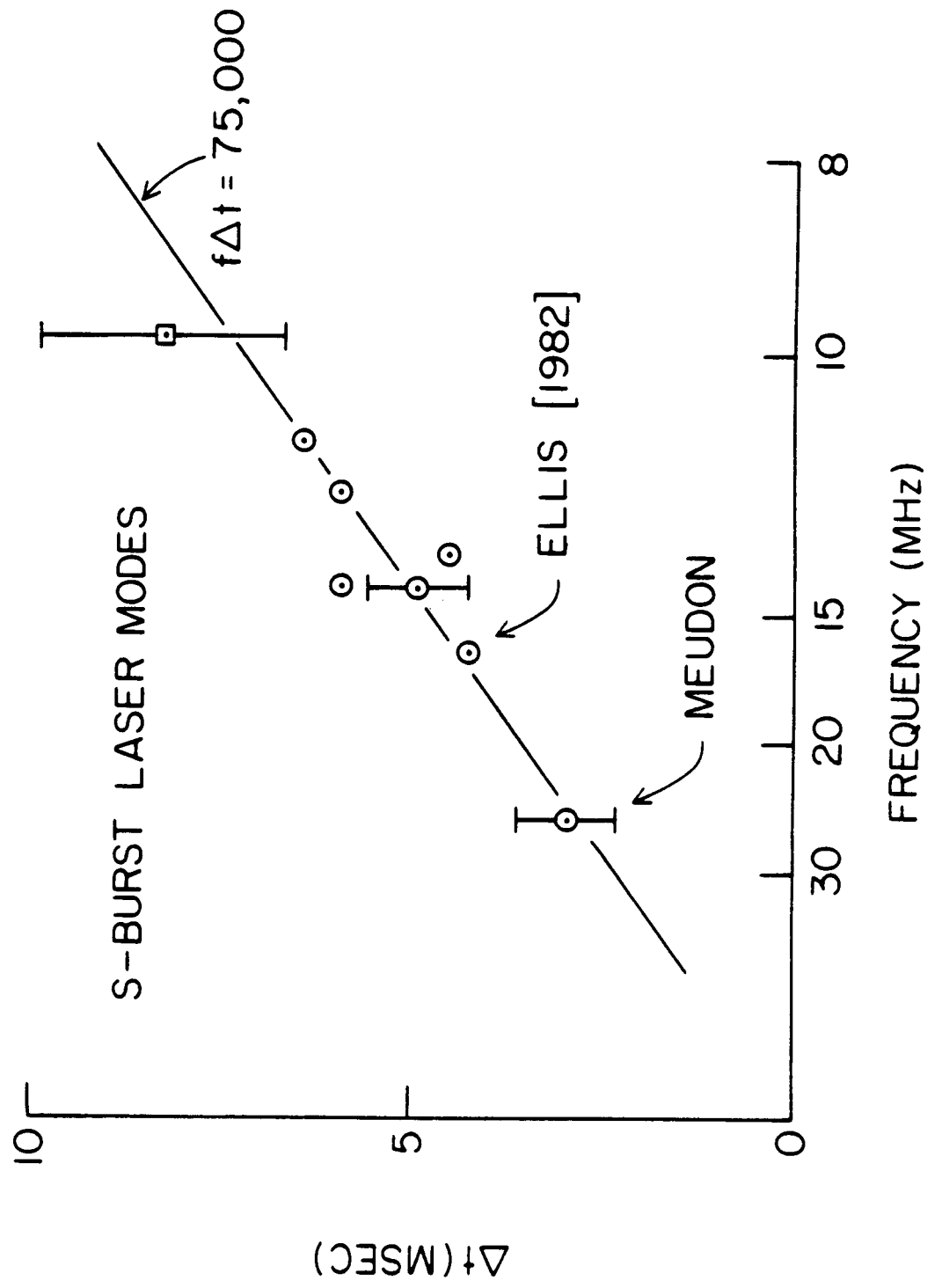
S-BURST LASER MODES
fΔt = 75,000
ELLIS [1982]
MEUDON
10
5
0
Δt (MSEC)
0
10
15
20
30
8
FREQUENCY (MHz)

Fig. 7

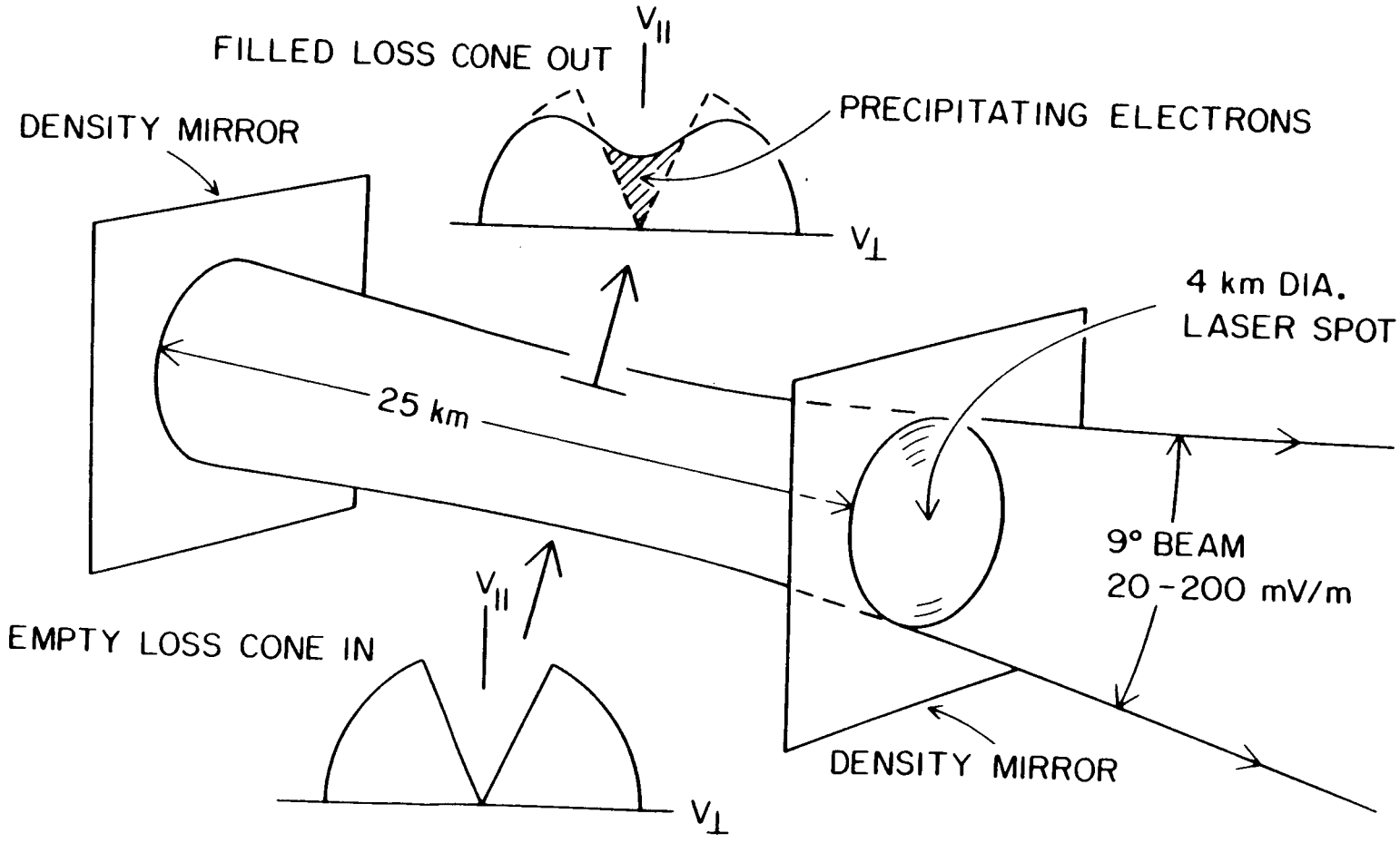
FILLED LOSS CONE OUT
V_{II}
PRECIPITATING ELECTRONS
DENSITY MIRROR
$V_{\perp}$
4 km DIA.
LASER SPOT
25 km
9° BEAM
20 - 200 mV/m
V_{II}
EMPTY LOSS CONE IN
DENSITY MIRROR
$V_{\perp}$

Fig. 8

JOURNAL OF GEOPHYSICAL RESEARCH, VOL. 92, NO. A8, PAGES 8792–8794, AUGUST 1, 1987

Auroral Precipitation Caused by Auroral Kilometric Radiation

W. CALVERT

Department of Physics and Astronomy, University of Iowa, Iowa City

If the auroral kilometric radiation were generated by loss cone lasing on closed field lines, as has been proposed, then it should cause substantial auroral precipitation by the pitch angle scattering of energetic electrons into the loss cone. A rough estimate for this precipitation, based upon the observed auroral kilometric radiation (AKR) amplitudes, would imply a flux of at least 2×10^8 el/cm^2 s over the projected ionospheric footprint of an individual laser and, if most of the AKR radio lasers occupied the same electron drift an L shell, an arc of 8 km width with a minimum average flux of roughly 10^9 el/cm^2 s. It is believed that this will account for auroral arcs and other aspects of auroral electron precipitation.

It has been proposed that the auroral kilometric radiation (AKR) originates from natural radio lasing [*Calvert*, 1982]. It has also been proposed that the free energy for the instability driving those lasers comes from the energetic electron loss cone [*Wu and Lee*, 1979]. If these are so, and the pertinent auroral field lines are closed to the conjugate hemisphere, then the generation of the AKR must cause auroral electron precipitation, since loss cone lasing should cause the pitch angle scattering of energetic electrons into the loss cone, where those electrons would automatically have to precipitate. In this paper I shall estimate the precipitation which should occur based upon the apparent size and power of the observed AKR radio lasers.

The apparent length of the AKR radio lasers (W) has already been determined from the observed spectral spacing of their longitudinal modes [*Calvert*, 1982], and it was found to be approximately 25 km (depending upon the assumed source refractive index). According to straightforward laser theory [*Verdeyen*, 1981], the width of the wave field inside a lasing laser depends primarily only upon this dimension. For the fundamental transverse mode, where the internal wave field and the emitted beam are both of Gaussian shape, this width is given by

$$a_0 = (2\lambda W/\pi)^{1/2} \tag{1}$$

where a_0 is measured to the $1/e$ power points and λ is the wavelength. For a 1-km wavelength this would give a laser such as that illustrated in Figure 1, having an exit spot width of about 4 km.

The corresponding angular beam width, also measured to the $1/e$ power points, is given by

$$\alpha_0 = (2\lambda/W\pi)^{1/2} \tag{2}$$

This would give a 9° beam width, and upon correcting for compression of the beam by wave refraction as it escapes, an emission solid angle of about 0.005 sr. Multiplying this by the peak AKR power flux of 1 MW/sr deduced from the IMP 6 observations of *Gurnett* [1974], this gives a total beam power of about 5 kW [*Calvert*, 1984]. For a total average power of 40 MW [see *Gallagher and Gurnett*, 1979], the AKR must consist of about 8000 such laser beams, all at different frequencies and altitudes throughout the AKR source region.

(Equations (1) and (2) can be derived by equating the size of a Gaussian illumination pattern to that of its own diffraction pattern at the opposite end of the laser, since the wave field within a laser must reproduce itself. Otherwise, it can be deduced directly from *Verdeyen*'s [1981, p. 60] equation 3-22.)

Since the AKR lasers are presumably oriented perpendicular to the source magnetic field, the loss cone free energy which is driving them would come either from below, as is illustrated in Figure 1, or from the conjugate hemisphere. As a result of the lasing (and also causing it) the incoming loss cone should emerge from the laser at least partially filled by pitch angle scattering, and it is this filling which causes the proposed auroral precipitation. Occurring over an area of 100 km^2, such pitch angle scattering into the loss cone would have to contribute approximately 50 W/km^2 to the emitted beam, since it is this scattering into the loss cone which actually provides the emitted AKR energy.

To the extent that the lasers are powered by the loss cone, therefore, this would cause flux of electrons into the loss cone of

$$\Phi = 50/E\eta \quad \text{el/km}^2 \tag{3}$$

where E is the electron energy in joules and η is the fraction of the electron energy which is given up to the wave. Since η cannot be greater than 1, the precipitation flux for kilovolt electrons would then have to be greater than 3×10^7 el/cm^2 s measured at the laser. Projected into the ionosphere, where the magnetic field is about 6 times stronger, this would imply a flux of at least 2×10^8 el/cm^2 s over the projected area of a laser.

If one further assumes that the AKR radio lasers are oriented perpendicular to and distributed along an electron drift L shell, as certain of the AKR observations would seem to suggest [*Calvert*, 1987], then that would produce an arc of precipitation having a width W determined by the laser length. For a 2000-km evening sector arc spanning the region where the AKR seems to originate, this would imply a projected width of 8 km and an average of perhaps eight overlapping lasers at each longitude, since the projected footprint of an individual laser would then be approximately 8 km in latitude by 2 km in longitude. Counting both hemispheres, this would give a minimum average precipitation flux of about 10^9 el/cm^2 s.

Paper number 6A8852.
0148-0227/87/006A-8852$02.00

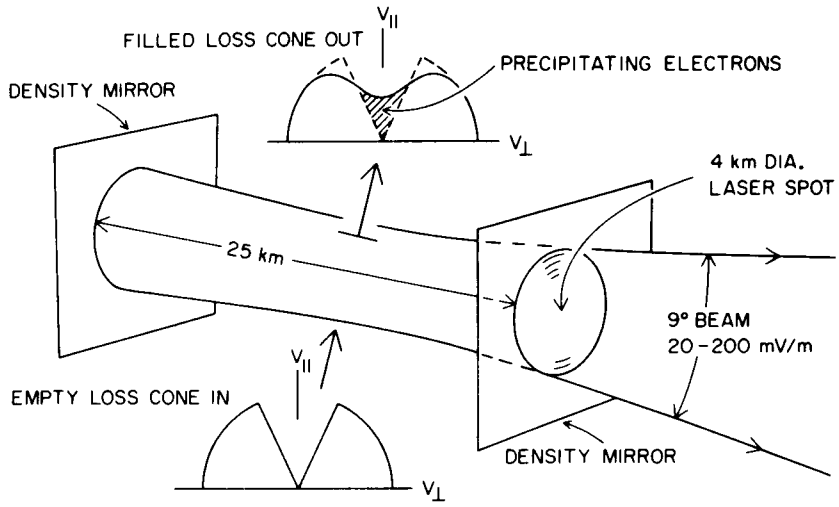

Fig. 1. AKR radio laser causing electron pitch angle scattering into the loss cone.

To recapitulate: If the AKR is attributed to loss cone lasing on closed field lines, with the lasers powered by kilovolt electrons, producing 5 kW, and having a length of 25 km, then that should cause a laser-induced precipitation flux of at least 2×10^8 el/cm^2 s over the 8 km $\times$ 2 km ionospheric footprint of an individual laser. Moreover, if most of the apparently 8000 lasers producing the AKR occupied the same electron drift L shell, then that could supply an evening sector arc of electron precipitation having a width of about 8 km and a minimum average flux of about 10^9 el/cm^2 s.

As stated elsewhere [*Calvert*, 1986], the above precipitation should also reduce the source plasma density, since it presumably represents an unreplenished loss to the source. Provided the source contains mostly energetic electrons with a total column content of around 10^{10} el/cm^2 (based on an initial density of roughly 2 el/cm^3 and a field line length of eight earth radii), this density decrease should occur within approximately $10^{10}/3 \times 10^7 = 300$ s or 5 min for an individual laser, and for the precipitation arc which I have postulated, within only about 1 min. Moreover, because of the expected energy spread of the electrons being precipitated, this density decrease should spread itself along electron drift L shells to create a thin sheet of reduced density, within which, because of the increased wave gain and feedback which this would cause, one would expect the lasing to promulgate itself. It is therefore proposed that the AKR radio lasers occur preferentially along the same electron drift L shells by mutually reducing their own source plasma density, and that they would preferentially orient themselves across these shells for the same reason, by creating their own L-shell-aligned density mirrors.

Although still requiring a plasma which is energized by some other means, this raises the possibility that the emission of the AKR by radio lasing actually causes the discrete auroral arcs with which it is associated [*Gurnett*, 1974; *Voots et al.*, 1977]. If this were so, as is illustrated schematically in Figure 2, the width of an arc would be attributed to the optimum size which is required for lasing (which cannot be too large because of diffraction losses, nor too small for the want of sufficient gain), whereas its extension in longitude would be attributed to a longitudinal spread of the resulting density depletion along electron drift L shells.

It must be emphasized that the above estimates represent an extreme lower limit for the precipitation which should occur, based upon the emission of AKR with 100% efficiency. Since the actual emission efficiency could obviously be much less than this, the actual precipitation could be much greater, and the time scales for forming an organized arc, correspondingly shorter. For instance, if the actual emission efficiency (with respect to the precipitating electrons) were as small as 1% or less, as the apparent ratio of the AKR and auroral energies would suggest [*Gurnett*, 1974], then the expected precipitation could be 100 times greater. This means that the precipitation flux of a single laser could be as large as 10^{10} el/cm^2 s, and the average for an arc, over 10^{11} el/cm^2 s. In view of the uncertainties and variabilities of both the aurora and the AKR, this certainly represents adequate agreement with the observed auroral electron fluxes [*Hultqvist*, 1973].

Since the pitch angle scattering should occur regardless, as long as the AKR is powered by the loss cone, the overall auroral electron precipitation might have been accounted for on this basis without the concept of lasing. This, however, would not give the localized precipitation which occurs in the aurora, nor would it give the very intense wave electric fields (of 20–200 mV/m, according to previous estimates [*Calvert*, 1982]) which would be required to scatter an electron significantly during a single pass through the thin source region depicted in Figure 1. (Lasing, on the other

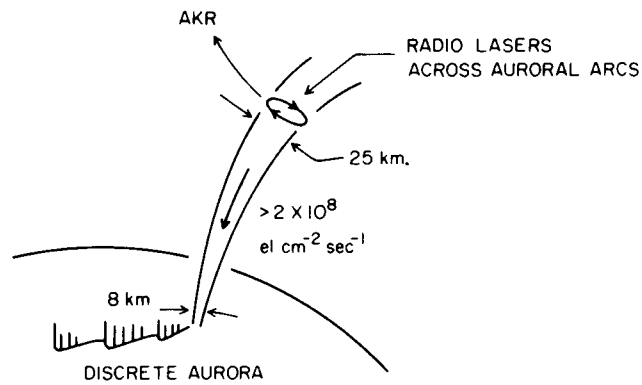

Fig. 2. Illustration of how the AKR radio lasers might cause discrete auroral arcs.

hand, guarantees this automatically because of the inevitable gain saturation which must occur, since that immediately implies that a laser must produce wave amplitudes which are sufficient to deplete the available free energy.) Moreover, it is suspected that the emission efficiency for linear amplification would be far less than even the 1% previously mentioned, in which case the predicted overall electron precipitation would be vastly greater than that which is observed. I would therefore expect that the inherent high efficiency of lasing would be required so as not to exceed the observed auroral precipitation, and hence that this could become yet another argument in favor of the lasing hypothesis.

Be that as it may, I consider that there is already ample evidence that the AKR must be generated by lasing, from its discrete multiple spectrum [*Gurnett and Anderson*, 1981; *Calvert*, 1982], its angular coherence [*Baumback et al.*, 1986], and its monochromaticity [*Baumback and Calvert*, 1987]. Besides, for the purposes of this paper the laser hypothesis is not at question. It was introduced as a premise, and the results are cast as a consequence of that premise, in the belief that this was the nature of the AKR emitters as they exist, according to their radio signature. Although the argument could be applied in either direction, the resulting explanation for auroral arcs which has been presented here is simply that, an explanation for the arcs, and not offered primarily as further evidence for the lasing.

The deduction of an auroral arc width of approximately 8 km is a specific prediction of the laser precipitation model. Also predicted by that model would be finer structure along the arc of roughly 2 km thickness corresponding to the transverse dimension of a fundamental-mode laser, as well as even finer periodic structures with similar spacings corresponding to the higher-order transverse modes which can also occur. What I have just described would correspond to a homogeneous arc, an auroral ray, and a rayed band, as described by *Omholt* [1973]. The radio laser precipitation model could thus account for various phenomenological aspects of the aurora which have hitherto lacked concrete explanation, and it could do so with the correct order of magnitude for their dimensions.

What one should see in an auroral arc, viewed with sufficiently fine spatial and temporal resolution, is an overlapping pattern of rays, presumably varying and moving on time scales comparable to those of the AKR discrete emissions (of seconds to a few minutes), with each ray elongated perpendicular to the arc by ratios of 4:1 or more, depending upon which of the transverse laser modes are excited. What one actually does see, in the excellent auroral images of *Ono et al.* [1987] and M. Ejiri and T. Hirasawa (private communication, April 1987), is precisely that, although I am not at liberty to reproduce their results.

If the concept of laser-induced auroral precipitation proves correct, as I am certain it will for reasons beyond those presented here, it should clearly revolutionize auroral research, since it constitutes a radical departure from the conventional wisdom which would attribute auroral precipitation to externally imposed field-aligned currents and localized electron acceleration. Its principal impact will be to separate the phenomenon of precipitation from that of electron energization and to remove the need for the latter to account for the detailed pattern of electron deposition. It will also open many new concerns about auroral electrodynamics and many new questions about the auroral observations which have heretofore been interpreted differently.

Acknowledgments. This work was supported by NASA contract NGL-16-001-043 and developed from the author's analysis of the AKR radio observations over the past nine years, with ISIS 1, Hawkeye, IMP 6, ISEE 1, and DE 1, partly under NASA contracts NAG5-310 and NAS5-28701 and NASA grant NAGW-256. R. L. Huff is thanked for his encouragement.

The Editor thanks M. L. Kaiser and another referee for their assistance in evaluating this paper.

REFERENCES

Baumback, M. M., and W. Calvert, The minimum bandwidths of auroral kilometric radiation, *Geophys. Res. Lett.*, *14*, 119–122, 1987.

Baumback, M. M., D. A. Gurnett, W. Calvert, and S. D. Shawhan, Satellite interferometric measurements of auroral kilometric radiation, *Geophys. Res. Lett.*, *13*, 1105–1108, 1986.

Calvert, W., A feedback model for the source of auroral kilometric radiation, *J. Geophys. Res.*, *87*, 8199–8214, 1982.

Calvert, W., New evidence for the production of AKR by radio lasers, paper presented at General Assembly, Union Radio Sci. Int., Florence, Italy, 1984.

Calvert, W., An explanation for triggered auroral kilometric radiation, the auroral plasma cavity, and discrete auroral arcs (abstract), *Eos Trans. AGU*, *67*, 1158, 1986.

Calvert, W., Hollowness of the observed auroral kilometric radiation pattern, *J. Geophys. Res.*, *92*, 1267–1270, 1987.

Gallagher, D. L., and D. A. Gurnett, Auroral kilometric radiation: Time-averaged source location, *J. Geophys. Res.*, *84*, 6501–6509, 1979.

Gurnett, D. A., The earth as a radio source: Terrestrial kilometric radiation, *J. Geophys. Res.*, *79*, 4227–4238, 1974.

Gurnett, D. A., and R. R. Anderson, The kilometric radio emission spectrum: Relationship to auroral acceleration process, in *Physics of Auroral Arc Formation*, *Geophys. Monogr. Ser.*, vol. 25, edited by S.-I. Akasofu and J. R. Kan, pp. 341–350, AGU, Washington, D. C., 1981.

Hultqvist, B., Auroral particles, in *Cosmical Geophysics*, edited by A. Egeland, O. Holter, and A. Omholt, pp. 161–179, Universitetsforlaget, Oslo, 1973.

Omholt, A., Auroral morphology, in *Cosmical Geophysics*, edited by A. Egeland, O. Holter, and A. Omholt, pp. 203–210, Universitetsforlaget, Oslo, 1973.

Ono, T., M. Ejiri, and T. Hirasawa, Monochromatic auroral images observed at Syowa Station in Antarctica, *J. Geomagn. Geoelectr.*, *39*, 65–95, 1987.

Verdeyen, J. T., *Laser Electronics*, Prentice-Hall, Englewood Cliffs, N. J., 1981.

Voots, G., D. A. Gurnett, and S.-I. Akasofu, Auroral kilometric radiation as an indicator of auroral magnetic disturbances, *J. Geophys. Res.*, *82*, 2259–2266, 1977.

Wu, C. S., and L. C. Lee, A theory of the terrestrial kilometric radiation, *Astrophys. J.*, *230*, 621–626, 1979.

W. Calvert, Department of Physics and Astronomy, University of Iowa, Iowa City, IA 52242.

(Received December 1, 1986;
revised May 19, 1987;
accepted May, 22, 1987.)